THE UNIVERSITY OF MANITOBA

"THE RESPONSE OF A HOT-WIRE OF FINITE LENGTH TO FINE-SCALE STRUCTURE IN A TURBULENT FLOW"

by

ROBERT W. DERKSEN

A THESIS

SUBMITTED TO THE FACULTY OF

GRADUATE STUDIES IN PARTIAL FULFILLMENT

OF THE REQUIREMENTS FOR THE DEGREE OF

MASTER OF SCIENCE IN ENGINEERING

DEPARTMENT OF MECHANICAL ENGINEERING

WINNIPEG, MANITOBA

August, 1981

THE RESPONSE OF A HOT-WIRE OF FINITE LENGTH TO FINE-SCALE STRUCTURE IN A TURBULENT FLOW

BY

ROBERT W. DERKSEN

A thesis submitted to the Faculty of Graduate Studies of the University of Manitoba in partial fulfillment of the requirements of the degree of

MASTER OF SCIENCE

ABSTRACT

A set of measurements of the one-dimensional u velocity spectrum were made, at $y+ = 150$ in a boundary layer growing inside a pipe, with 14 different hot-wire probes. The Reynolds number was 36,500 based on non-turbulent velocity and boundary layer thickness. The probes fit into two groups 5 μm and 2.5 μm diameters, with an asortment of lengths from 0.33 mm to 2.81 mm in length.

The spectra varied in magnitude, at the highest wave numbers, by a factor of 3. When the spectra were normalized by the dissipation measured with that particular wire the variation was reduced.

The measurements tended to confirm the validity of Wyngaard's (1968) correction. The correction of dissipation proposed by Skramstad (1937) and developed by Frenkiel (1949) was tested and found to work very well.

The optimum wire geometry indicated from these measurements was 5 μm diameter and 1.1 mm length.

ACKNOWLEDGEMENTS

The author would like to thank: Dr. R.S. Azad for his guidance, encouragement, and extremely helpful assistance, Dr. J. Tinkler for reading this thesis, Mrs. P. Giardino for typing the manuscript, and Mr. K. Tart for his assistance.

The National Sciences and Engineering Research Council is greatly appreciated for providing financial assistance for the author and experimental budget. Additionally the financial assistance of the University of Manitoba Graduate Fellowship is gratefully appreciated.

TABLE OF CONTENTS

LIST OF FIGURES

LIST OF TABLES

NOMENCLATURE

A	Relative attenuation with respect to the shortest wire
C_f	Friction coefficient $C_f = 2(u_*/U_\infty)^2$
d	Diameter of the hot-wire
D_w	Thermal Diffusivity of the wire
e	Fluctuating output from the hot-wire anemometer
ENB	Equivalent noise bandwidth
f	Frequency
f_o	Center frequency of a bandpass filter
f_1, f_2	3 db down points for a filter
$F(\ )$	Flatness factor of ( )
$\underline{\ell}$	Vector parallel to sensor with the same length
ℓ	The length of the hot-wire
$R(s)$	Correlation coefficient at separation s
Ra	Hot-wire resistance at ambient temperature
R_{op}	Operating resistance of the hot-wire
$Re_{\delta 99}$	Reynolds number based on $\delta 99$, U_∞, and ν
$Re_{\delta 1}$	Reynolds number based on $\delta 1$, U_∞, and ν
$Re_{\delta 2}$	Reynolds number based on $\delta 2$, U_∞, and ν
Re_λ	Reynolds Number Based on λ, u', and ν
$S(\ )$	Skewness factor of ( )
S	Spatial Separation for correction
t	Time
U	Local mean velocity

$\bar{U}$	Mean velocity
u_+	Non-dimensional velocity (U/u_*)
U_∞	Free stream or centerline velocity
u	Fluctuating velocity
u'	RMS Fluctuating velocity
u_*	Friction velocity
u_i, u_j	Fluctuating velocity at i or j
X	Distance in streamwise direction
Y	Distance from a wall or distance between two sensors
Y_+	Non-dimensional wall distance (Yu_*/ν)
Z	Distance parallel to the sensor
Z_i, Z_j	Z position at i or j

Greek Symbols

α_1	One-dimensional Kolmogoroff spectrum constant
δ	Boundary layer thickness
$\delta 99$	Boundary layer thickness based on 0.99 U_∞
δ_1	Displacement thickness
δ_2	Momentum thickness
ΔP_c	Contraction cone pressure drop
$\bar{\varepsilon}$	Mean dissipation
η	Kolmogorov microscale
$\varepsilon_{k\ell m}$	Antisymmetrical tensor
κ_1	Wave number X component

κ_2	Wave number Y component
κ_3	Wave number Z component
λ_g	Taylor microscale
ν	Kinematic viscosity
ρ	Density
σ	Standard deviation
ϕ_1	One-dimensional spectrum
ϕ_{ij}	One-dimensional spectral tensor
$\underline{\chi}$	Wave number vector
ω_i	Vorticity in i direction (same as κ_i)

Other Symbols

$( )_{avg}$	Average
$( )_{meas}$	Measured
$( )^{meas}$	Measured, when ( ) is a subscripted variable
$( )'$	RMS of ( )
$\overline{( )}$	Time average of ( )

I INTRODUCTION

Turbulent flow is a highly irregular nonlinear phenomenon. It is generally characterized by extremely high rates of exchange, which, in the case of momentum, can result in dramatic increases in drag due to the wall shear stress or conversely dramatic reductions in drag due to separation.

To date there is no single theory or prediction scheme that can predict flow characteristics, such as mean velocity, shear stress, or transport rates, for all flows. In an effort to formulate a theory, equations for two-point velocity correlations are used (developed from the Navier-Stokes equations). This is done in recognition of the observation that the flow is not solely a function of local variables. Mathematically one must recognize that the Fourier transform of the velocity correlation (or Lag functions) is what is called the power spectrum. This new function is the density (i.e. per unit wave number) of the correlation at a wave number. If the spectrum were integrated with respect to wave number it would give the net energy.

This gives important information about how energy is distributed among various frequencies or wave numbers. As well information on how to correct measuring instruments for reduced sensitivity at higher frequencies may be obtained.

If the study of turbulence is to advance it is important to know how the spectra behave at high wave numbers. For, it is at these wave numbers that the energy the turbulence absorbs from the mean flow is dissipated as heat. If one wishes to have an accurate model of the flow one must know how energy is converted from pressure energy (mean flow) to the kinetic energy of the fluctuations, and ultimately to heat. It is for this reason that the spectra must be known accurately. A very well developed model for homogeneous isotropic turbulence has been developed based on these ideas, see Batchelor (1967), Hinze (1975) or Monin and Yaglom (1975).

The u spectrum can be measured by taking the output of a hot-wire anemometer and passing the signal through a bandpass filter. Then the mean square of the output of the filter divided by the bandwidth is taken as the spectral density at the center frequency. Generally filters with fixed bandwith to center frequency are used.

Unfortunately the spectral density is not as easy to measure as it sounds. Its accuracy is high dependent on four factors. The frequency response of the measuring system, the bandwidth of the filter, the amount of data used (measuring time X bandwidth), and the spatial resolution of the probe.

For most modern hot-wire systems the high frequency cutoff is much larger than is required. Hence this is no longer a major

difficulty. And, as shown later, the measurement is not as sensitive to bandwidth as one might think. The error in the spectra due to insufficient data can, within limits, be overcome by using more data.

The more difficult problem to solve experimentally is how does the finite sensor size affect the measurement. Practically this is only important if the sensor is larger than the smallest turbulence length scale.

Kolmogorov's theory of local isotropy, for flows with sufficiently high Reynolds numbers, gives the scales associated with the finest structure. He postulated that almost all the dissipation ($\bar{\varepsilon}$) occurred at the highest frequencies, and that viscosity (ν) was the dominant mechanism of dissipation. Dimensional arguments result in the following relationship for the smallest (Kolmogorov) length scale (η):

$$\eta = \left(\frac{\nu^3}{\bar{\varepsilon}}\right)^{\frac{1}{4}} \quad .$$

This length is assumed to be the smallest length to be significant in a turbulent flow. In most experimental flows it is of the order of 0.10 mm. We can recognize that in order to obtain a reasonable indication of a quantitys local value the measuring device should be much smaller than the smallest scale.

This requires that the hot-wire length (ℓ) be much smaller than η . But this is not possible. In order to maintain a fairly uniform

temperature distribution along the wire ℓ/d (d-wire diameter) should be greater than, say, 160. Using this criterion the wire would have to be smaller than 0.5 μm in diameter. It is quite impractical to work with such a fine wire. Most commercially available hot-wire probes have a 5 μm diameter.

The first work done on this effect was done by Skramstad (Dryden, Schubauer, Mock, and Skramstad) in 1937[†]. This work is based on the Taylor microscale (λ) and was used to correct for the magnitude of the intensity. Frenkiel (1949, 1954) developed the findings of Skramstad to obtain (for ℓ/λ small)

$$\left(\frac{u'_{meas}}{u'}\right)^2 = 1 - \frac{\ell^2}{6\lambda^2} \quad . \tag{1}$$

Hinze (1975) summarized this work and included a correction for the Taylor microscale

$$\frac{\lambda}{\lambda_{meas}} = 1 - \frac{\ell}{3\lambda_{meas}} - \quad . \tag{2}$$

Again for ℓ/λ small. Corrsin (1963) shows for a long wire in a non-uniform velocity fluctuation field that

[†]This was before Kolmogorov developed his theory of local isotropy and the relation for η.

$$\frac{D_w}{\nu} \ll \frac{1}{2} R_\lambda^{\frac{1}{2}} \frac{\bar{U}}{u'} \quad , \; D_w\text{-thermal diffusivity} \qquad (3)$$

for the correction previously discussed to be adequate to account for imperfect spatial resolution. For most hot-wires D_w/ν is between 1 and 5. The term $R_\lambda^{\frac{1}{2}} \bar{U}/2u'$ is in the order of 50.

Later Uberoi and Kovasznay (1953) developed a theory to predict how a probe of finite length maps the true spectrum of a random vector field into the measured vector field. Wyngaard (1968) developed this theory assuming Pao's spectrum for isotropic turbulence. From this he obtained several curves of the attenuation of the one-dimensional spectra versus $\kappa_1 \ell$ (κ_1 is the X direction wave number).

Roberts (1973) attempted to extend the work of Uberoi and Kovasznay, and Wyngaard for the anisotropic case. Unfortunately he assumed small values of $\kappa_2 \ell$ (κ_2 wave number in the direction parallel to the wire axis) in his analysis. This is not possible as the maximum values of κ_2 are proportional to η^{-1}, and that implies that ℓ/η must be small. If this were true no correction would be required.

Serag (1978) carried out spectral measurements with an extensive assortment of hot-wires with different lengths and diameters. There was no quantitative check on any of the existing correction techniques.

The objective of the following work was to obtain data on the spectra with several wires of different lengths and diameters for the

same flow conditions. This data was used to check on the validity of the corrections of Skramstad*(1937), Frenkiel (1949, 1954), and Wyngaard (1968). As well, data on the boundary layer growing inside a pipe was desired.

*The reference to Skramstad may be found in the paper by Dryden, Schubauer, Mock, and Skramstad (1937).

II THEORETICAL BACKGROUND

This section will be brief and is intended to indicate where information on the theory is available.

Blackman and Tukey (1958) is the definitive reference on the various aspects of the measurement of power spectra. But this is a very difficult book to read. Bradshaw (1971) presents a much more readable and easy (although basic) to understand section on the measurement. Intermediate to these sources is Lumley and Panofsky (1964).

Various references such as: Landau and Lifshitz (1959), Schlichting (1979), Monin and Yaglom (1971), and Goldstein (1965) to name a few contain a great wealth of information on basic fluid mechanics, and boundary layer information.

A good reference for turbulence measurements is contained in Hinze (1975) and Bradshaw (1971). The theory of turbulence is covered in Batchelor (1967), Lumley and Panofsky (1964), Hinze (1975), Bradshaw (1971, 1978), Townsend (1976), Tennekes and Lumley (1972), and Monin and Yaglom (1971, 1975). It would be best for the interested reader to use these references for any questions concerning theory.

Unfortunately a relation for the skewness of du/dt is not generally available. It is given in Appendix A. The corrections

for dissipation (Taylor microscale) and spectra are developed below.

Skramstad (1937) developed a correction for the measured intensity e'_{meas} and two point correlation $R(Y)_{meas}$, based on a series model of the response of the wire. The response is assumed to be

$$e_{meas} = K \int_0^{\ell} u_i \, dZ_i \tag{4}$$

where e_{meas} is instantaneous voltage, K is the sensitivity, u_i is instantaneous velocity at the point i and dZi is an element of length parallel to the wire.

Thus

$$e^2_{meas} = K^2 \int_0^{\ell} u_j \, dZ_j \int_0^{\ell} u_i \, dZ_i$$

$$= K^2 \int_0^{\ell} \int_0^{\ell} u_j u_i \, dZ_j \, dZ_i \quad . \tag{5}$$

Introducing the correlation function

$$R(Z_i - Z_j) = \frac{\overline{u_i u_j}}{u'} \quad . \tag{6}$$

The mean square of e can be determined

$$\overline{e^2_{meas}} = K^2(u')^2 \int_0^{\ell} \int_0^{\ell} R(Z_i - Z_j)\, dZ_j\, dZ_i$$

but

$$\overline{e^2} = K^2(u')^2\, \ell^2 \quad .$$

Thus

$$\frac{\overline{e^2_{meas}}}{\overline{e^2}} = \frac{1}{\ell^2} \int_0^{\ell} \int_0^{\ell} R(Z_i - Z_j)\, dZ_j\, dZ_i \tag{7}$$

and by a transformation of coordinates $S = Z_i - Z_j$, (7) can be reduced to

$$\frac{\overline{e^2_{meas}}}{\overline{e^2}} = \frac{2}{\ell^2} \int_0^{\ell} (\ell - Z)\, R(Z)\, dZ \quad . \tag{8}$$

By similar arguments Skramstad showed that

$$R(Y)_{meas} = \frac{\int_0^{\ell} (\ell - Z)\, R(\sqrt{Z^2 + Y^2}\, dZ}{\int_0^{\ell} (\ell - Z)\, R(Z)\, d(Z)} \quad . \tag{9}$$

These equations (8 and 9) were also found by Frenkiel (1954) and Uberoi and Kovansnay (1953). Relations (8) and (9) can be reduced to equations (1) and (2), for (ℓ/λ) small see Hinze (1975).

Uberoi and Kovasnay (1953) developed a relation for the spectrum that is measured from a sensor of finite length. Wyngaard (1968) extended this work to give the following correction

$$\phi_1(\kappa_1) = \int_{-\infty}^{\infty}\int_{-\infty}^{\infty} \phi_{ij}(\underline{\chi})\, d\kappa_2\, d\kappa_3 \tag{10}$$

$$\phi_1^{meas}(\kappa_1,\underline{\ell}) = \int_{-\infty}^{\infty}\int_{-\infty}^{\infty} \phi_{ij} \left(\frac{\sin(\underline{\chi}\cdot\underline{\ell}/2)}{(\underline{\chi}\cdot\underline{\ell}/2)}\right)^2 d\kappa_2\, d\kappa_3$$

$$= \int_{-\infty}^{\infty}\int_{-\infty}^{\infty} \phi_{ij} \frac{\sin^2(\kappa_2\ell/2)}{(\kappa_2\ell/2)^2}\, d\kappa_2\, d\kappa_3 \tag{11}$$

where ϕ_1 is the one-dimensional spectral density, $\underline{\chi}$ is the wave number vector, $\underline{\ell}$ is a vector parallel to the wire and of the same length and ϕ_{ij} is the spectral density tensor. By assuming isotropy and Pao's (1965) spectrum Wyngaard numerically calculated the response ϕ_1^{meas}/ϕ_1 which he gives as a figure in his paper.

III EXPERIMENTAL EQUIPMENT

The wind tunnel used was previously described by Burhanudin (1980), and Serag (1978). Basically it is composed of a wooden inlet cone, four stages of axial fans, a Woods type silencer, wooden diffuser and turning sections, a settling section, a wooden contraction cone (ratio 16:1), and a brass pipe discharging into the laboratory.

The brass pipe is 267 cm long and 27.1 cm in diameter. It was honed smooth on the inside, and had a number 4 grit sand paper trip (1 diameter long) installed immediately after the contraction cone.

All measurements were taken 15.25 cm upstream of the outlet. The wind tunnel was calibrated for centerline velocity using the contraction cone pressure drop, measured with an Airflow Developments Ltd. inclined manometer (maximum pressure of 0.5 in H_2O and graduated in 0.002 in H_2O increments). For all other pressure measurements a Combust micro-manometer was used. A Hero and a Betz Micromanometer were also used, but the Combust was found to be most consistant.

The anemometer used was a DISA 55 M01 with a standard bridge. For the boundary layer measurements a 55P01 DISA boundary layer type probe was used ($d = 5\mu m$, $\ell = 1.1$ mm). Using a sine-wave test it was found that the 3 db down point was about 200 kHz at 14 m/s. This compared quite favorably to Fremuth and Fingerson's (1977) relation based on the square wave test response. The bridge was balanced

maximal flat (see Fremuth, 1974) in order to minimize problems with non-linearity.

Linearization was performed with a DISA 55D10 linearizer for the initial measurements of $\bar{U}$ and u'. It was found to behave poorly when the linearization range was more than 1 octave ($U_{min} < \frac{1}{2} U_{max}$). All subsequent hot-wire measurements were performed using a DISA 55M25 type linearizer, which was accurate to within 1% from 2 m/s to 14 m/s.

Processing was done using a Tri-met turbulence processer TM377. For some measurements, a DISA 52B25 turbulence processor was used as a check. No significant differences were noticeable.

A pair of Khron-Hite 3550 adjustable filters were tested in band-pass mode. The amplitude attenuation and power attenuation were plotted against frequency. As Figures 1 and 2 show, the response closely followed the ideal response. This was done for two bandwidths (ENB $\simeq$ 0.5 and ENB $\simeq$ 0.6). There was some concern as to which filter bandwidth was optimum for the spectral measurements. So at $Y_+ \simeq 150$ the spectrum of the fluctuating voltage was measured for both relative bandwidths. No significant variation in the spectrum was apparent from these measurements. Hence the filter that was easiest to use (ENB = 0.5, $f_1 = f_2 = f_o$) was used.

Except for the spectrum, all of the measurements used a 30-second or longer (some instruments did not average at 30 seconds) integration

time that gave a stable output. For the spectra a 100-second integration time had to be used at low frequency (order 1-100 Hz).

Other equipment used were: a Techtronics 466 storage scope with a DM43 Digital Volt Meter, a DISA 55D31 Digital Volt Meter, a DISA 55D35 RMS Meter, and a DISA True Integrator. Differentiation of the signal was performed using a spectral differentiator based on the design of Wyngaard and Lumley (1967).

Pressure measurements were made using United Sensor Probes a flattened boundary layer impact tube, and a boundary layer type static tube.

For the spectrum measurements, fourteen wires of different length and diameter were used. The dimensions of the probes were obtained by photographing the wires in an ISI Mini-Sem Electron Microscope, with large sample holding stage. This technique also gave valuable information about the condition of the wires. Photos of the wires are given at the back of the thesis, Figure 3. The hot-wire geometry is given in Table 1. These probes were specially ordered from DISA based on the 55P01 with nominal diameters of 2.5 and 5μm.

IV EXPERIMENTAL PROCEDURE

Initially the wind tunnel was calibrated using the static and total pressure on the centerline of the brass pipe, 15.24 cm upstream of the outlet. Then the velocity distribution at this section (for three free-stream or centerline velocities $\bar{U}_\infty$; 4 m/s, 8 m/s, and 12 m/s) was measured, with a Pitot tube. From this data the friction velocity u_* was calculated, using the cross-plot method (see Burhandudin 1980) and by calculating slope at the wall.

Following this,hot-wire measurements of $\bar{U}$, u', $\overline{u^3}$, and $\overline{u^4}$ were made for the same velocities. This was done in three sets of y ranges; 0-2 mm by 0.1 mm increments, 1-20 mm by 1 mm increments, and 5-55 mm in 5 mm increments. The smallest distance from the wall that could be obtained was 0.15 mm. The mean velocity was corrected for the wall effect by measuring the voltage across the bridge with no flow, at a point, and subtracting this voltage from the voltage across the bridge with the flow.

Next the measurements of $\bar{U}$, u' $(\partial u/\partial t)'$, $\overline{(\partial u/\partial t)^3}$, and $\overline{(\partial u/\partial t)^4}$ were made. This time only in the 1-20 mm and 5-55 mm ranges, but for all three velocities.

The reasoning for repeating so many of the measurements is to have some means to check on the quality of the measurements. If the mean velocity distribution for the hot-wire matches the Pitot-tube

results, then the linearization is alright. If the rms of the velocities match then the u and du/dt data should match.

Finally the spectra were measured at Y+ = 150 (Y $\simeq$ 5 mm) and U_∞ = 12 m/s. A low pass filter, set at the Kolmogorov frequency ($\bar{U}/2\pi\eta \simeq$ 12 kHz), was used before the adjustable bandpass filter to eliminate noise. The center frequency of the bandpass filter was tuned to a distribution of values logarithmically distributed from 2.1 Hz to 12 kHz, 8 measurements per decade.

V RESULTS AND DISCUSSION

Calibration

From 0.010 in H_2O to 0.350 in H_2O of contraction cone pressure drop both the static and total pressure were linear on cone pressure. From this data U_∞ was calculated and plotted against $\sqrt{\Delta P_c/\rho}$. On this curve a straight line was drawn through the data points. From this line the ΔP_c values for linearizing the hot-wire and setting the tunnel were taken. This resulted in a ΔP_c = 0.027 in H_2O @ U_∞ = 4 m/s, ΔP_c = 0.107 in H_2O @ U_∞ = 8 m/s, and ΔP_c = 0.239 in H_2O @ U_∞ = 12 m/s. These data are shown in Figures 4, 5 and 6.

Boundary Layer Distributions

The mean velocity ($\bar{U}$) distributions for both the hot-wire and Pitot-tube data are in agreement. Burhanudin (1980) has measurements in the same tunnel, and his values of friction velocities are the same, for similar calculation techniques as the results listed in Table 2.

The velocity distributions, from Pitot tube measurements, are plotted in Figures 7, 8 and 9. These measurements have a universal nature when the velocity is normalized with the free stream velocity and the distance is scaled by the boundary layer thickness ($\delta 99$). This is to be expected and is shown in Figure 10. Plots of the displacement thickness weighting ($1-U/U_\infty$) and momentum thickness weighting

$U(1-U/U_\infty)/U_\infty$ are given in Figures 11 and 12 respectively. These plots also have a universal shape. This indicates that δ_{99}, the displacement thickness, δ_1, and the momentum thickness δ_2 have values independent of U_∞. This is most certainly true to within experimental error. The boundary layer thickness δ_{99} was found to be within 4.0 cm to 4.9 cm, corresponding to an error of about 10%. This is not unreasonable. The displacement thickness δ_1 was calculated to be 7.38 mm, and the momentum thickness δ_2 was 5.52 mm. For the same free-stream velocities these parameters are essentially identical to those of Purtell, Klebanoff, and Buckly (1981).

Using the cross-plot method the friction velocities u_* are: $u_* = 0.48$ m/s @ $U_\infty = 12.0$ m/s, $u_* = 0.33$ m/s @ $U_\infty = 8.0$ m/s, and $u_* = 0.18$ m/s @ $U_\infty = 4.0$ m/s. This corresponds to Friction Coefficients ($C_f = 2\ (u_*/U_\infty)^2$) of 3.2×10^{-3}, 3.4×10^{-3}, and 4.3×10^{-3} respectively. The boundary layer parameters are summarized in Table 2.

Table 3 lists near wall laws due to two sources Van Driest (1956), and Kader and Yaglom (1978). Figure 13 is a comparative plot of these Laws' gradients plus the theoretical gradient due to Von Karman. From this graph it appears that there is not much difference in the applicable ranges.

The above gradients were integrated and are shown in Figure 14 along with hot-wire measurements. The corrected measurements have had the u_* values adjusted to fit the log-law. Within experimental

error both "laws" are the same. Thus Kader and Yaglom's equation is the best to use due to its simpler mathematical form. These velocity distributions are shown in Figure 15 without experimental data.

Figure 16 is a plot of the velocity distribution in the first two millimeters from the wall: it shows that the hot-wire and Pitot-tube results roughly correspond. This data was used to calculate dU/dY at the wall and hence u_*. This set of u_* values (see Table 2) is generally lower than that for the cross-plot method. This is also shown by Burhanudin (1980). The cross-log u_* is used throughout.

Figure 17 is a plot of U_+ versus Y_+ using the friction velocities from both cross-plot and wall derivative methods in estimating u_*. From it the error is roughly bounded by $\pm$ 1.0, which is similar to that shown by the plots of Kline, Reynolds, Schraub, and Runstadler (1967). Figures 18 and 19 are plots of U_+ adjusted to fit in the logarithmic region and linear region respectively. They indicate that errors in calculating u_* can contribute significant errors in non-dimensionalized plots.

Figure 20 shows the distribution of u' (RMS fluctuating velocity) scaled by friction velocity. Considering the error band this set of data corresponds to that due to Laufer (1954), Klebanoff (1955), Ueda and Hinze (1975), Hussain and Reynolds (1975), Kline, Reynolds, Schraub and Runstadler (1967), and Purtell, Klebanoff, and Buckley

(1981). Figures 21 and 22 show the distribution of u' scaled by the local mean velocity U. These distributions compare favourably with data due to Klebanoff (1954) (see Hinze 1975).

The skewness of u is given in Figures 23 and 24. This plot agrees fairly well with the results of Ueda and Hinze (1975), except for $Y_+ > 15$ where Ueda and Hinze report a skewness of -0.4 and the present study gives -0.15. It should be noted that the triple correlation is very small in this range and hence the error is large.

Figures 25 and 26 give distribution of the flattening factor of u. This is in tolerably good agreement with Ueda and Hinze (1975), although Klebanoff (1955) lists a higher value in the range $0 < Y/\delta < 0.6$ and a lower maximum value.

The skewness of $\partial u/\partial t$ (Figure 27) has a constant region where $S(\partial u/\partial t) \simeq 0.3\text{-}0.35$. Ueda and Hinze also have a constant range but with $S(\partial u/\partial t) = 0.4$. Considering the measurement errors involved this difference is small.

Plots of the flatness of $\partial u/\partial t$ also have a constant region. This is shown in Figure 28. The value of $F(\partial u/\partial t)$ in this region is given as 5 in present study, 5.5 in Ueda and Hinze (1975), and 6 in Frenkiel and Klebanoff (1975).

Other calculated data was: the turbulence Reynolds number Re_λ

($= u'\lambda/\nu$) shown in Figure 29, the Taylor microscale λ shown in Figure 30, the Kolmogorov length scale η, shown in Figure 31, and dissipation $\bar{\epsilon}$ shown in Figure 32 (as $\delta\bar{\epsilon}/u_*^3$). The dissipation is about 30% low of that reported by Klebanoff (1955). This is probably due to an error in calculating the time constant of the differentiator.

The Spectra

Table 4 lists the uncorrected measured one-dimensional spectra ϕ_1, as well as second and fourth moments. Table 5 gives values of the above spectra and moments when non-dimensionalized by dissipation (from $(\partial u/\partial t)'$), the constant α_1 for the -5/3 law as well as the relative attenuation A when compared to the shortest wire. Table 6 is a list of relative attenuations for the above case calculated from Wyngaard's correction (1968).

Figures 33 and 34 show the distribution of spectral energy, and Figures 35 and 36 are the corresponding non-dimensional forms. The spectra shows no functional dependence on d the wire diameter. This is most likely due to the limited range that the wire diameters cover (2.5 to 5 μm). Thus the frequency response is nearly the same.

On the basis of the length ℓ there is a variation of the magnitude of the spectra at the largest κ_1 values of about ½ an order of magnitude (~ 5% of the range on a logarithmic plot of 8 orders of

magnitude). This variation disappears when the spectra are normalized with the dissipation scales calculated from measurements from the particular wire. A - 1/7 power law appears to hold for about 1/3 of a decade at the highest wave number range. The -5/3 power law holds for roughly 1/2 of a decade. These power laws are separated by a decade.

The fact that the non-dimensionalized spectra collapse seems to indicate that if one only wishes have information about the approximate shape of the spectra, no correction is needed. This is quite reasonable in light of the fact that most filters can only be tuned to within 5 or 10% of the frequency. A difference of 1/2 of an order of magnitude can be explained by an offset in true center frequency of 10%, for the -1/7 region.

It is true that the shorter the wire the larger the spectral density large wave numbers. But, this could be masked if different filters are used. In the present study the same filter was used for all of the different wires.

The dimensional second moment spectra is plotted in a semi-log form in Figures 37 and 38 and in a fully logarithmic form in Figures 39 and 40. These plots accentuate the difference between the longest wire's ($\ell \sim 2.5$-2.8 mm) and all of the rest. But the other wires' second moments appear to fall within experimental error of each other.

Figures 41, 42, 43 and 44 are plots of the fourth moments, in various forms. As with the second moment the apparent variation of all but the longest wires is small.

The values of the non-dimensional second and fourth moments agree with those of Wyngaard and Pao (1971) and Champagne (1971) when corrected for the error in the differentiator time constant and wire length.

The α_1 values calculated using the (uncorrected) dissipation measured with the differentiator and are given in Figures 45 and 46. Thus they are too large by a factor of about 1.3. Correcting for this reduces the average maximum α_1 from 0.7 - 0.8 to 0.5 - 0.6. This is in line with typically value of 0.5, see Townsend (1976).

Azad, Arora, and Reichert (1978) give a value of α_1 of 0.6 ± 0.1 for developing pipe flow. This value is corroborated by Paquin and Pond (1971) in an atmospheric boundary layer. But Monin and Yaglom (1975) give a value of roughly 1. This is an unexplained contradiction.

In order to compare the results with the theory of Wyngaard (1968), the attenuation (A) in the spectra was calculated using the shortest wire (ℓ = 0.3 mm) as a standard. A least squares method was used for interpolation.

Then the attenuation predicted for Wyngaard's correction was calculated (see Table 6). This attenuation for the wires with $\eta/\ell = 0.05$, $\eta/\ell = 0.08$, and $\eta/\ell = 0.10$ are virtually identical for both the measured and predicted values. For $\eta/\ell = 0.16$ the attenuation was significantly larger. For the theoretical values, Figure 47 is a plot of A versus $\ell\kappa_1$, for $\eta/\ell = 0.16$. From it, the experimental data can be seen to follow Wyngaard's prediction. This is also true for $\eta/\ell = 0.10$ Figure 48 (includes $\eta/\ell = 0.08$) and $\eta/\ell = 0.05$ (Figure 49). But the scatter is so large $\pm$ 0.1 that all the data may be said to collapse.

Although the data does not refute Wyngaard's correction it also does not confirm its validity.

The reason that the long wires diverge from the other wires, for the dimensional spectra, and its moments, is due to the fact that the maximum attenuation it experiences is 0.3 at $\ell\kappa_1 \simeq 20$. All the rest have a maximum attenuation of 0.7 - 0.8.

Dissipation and the Moments

Dissipation for each wire was calculated two different ways: by using local isotropy and $(\partial u/\partial t)'$

$$\bar{\varepsilon} = 15\,\nu\,\frac{1}{U^2}\left[\left(\frac{\partial u}{\partial t}\right)'\right]^2 \quad , \tag{13}$$

and local isotropy and the measured spectrum ϕ_1

$$\bar{\varepsilon} = 15\,\nu \int_0^\infty \kappa_1^2\,\phi_1\,d\kappa_1 \quad . \tag{14}$$

The measured $\bar{\varepsilon}$ from (13) was corrected by the relation (2). This is shown in Figure 50 as a function of η/ℓ. In this case the $\bar{\varepsilon}$ calculated by (14) is 30% larger than that calculated from (13). This indicates that the time constant that was used for the differentiator was too large, by roughly 15%. The general trend for $\bar{\varepsilon}$ from both (13) and (14) is that it increases with η/ℓ, rapidly at first, and then in an apparently asymptotic approach to a constant value. The corrected values are, to within experimental error, constant ($\bar{\bar{\varepsilon}}_{ave} \simeq 26\ \sigma = 8\%$). This makes (2) an appealing correction to use. In Figure 51 the measured skewness of u is shown. Due to the large error involved in this measurement it can be considered to be independent of η/ℓ. This is also true of the flatness of u, Figure 52.

The moments of the derivative $\partial u/\partial t$ are given in Figures 53 and 54, skewness and flatness respectively. These moments also shows no significant dependence on η/ℓ. There are two methods of determining $S(\partial u/\partial t)$. The first is to directly measure the triple correlation, and the other is to use the spectra as follows

$$S_s(\partial u/\partial t) = \frac{116\ \nu^{5/2}}{\bar{\varepsilon}^{3/2}} \int_0^{\infty} \kappa_1^4\ \phi_1\ d\kappa_1 \qquad (15)$$

where it is best to use $\bar{\varepsilon}$ calculated from the spectra.

From Figure 53 it is apparent that (15) gives skewness values roughly 50% larger than the directly measured skewness.

Table 7 is a list of the data used to make Figure 50-54.

One point that should be made is that the only wires to have a significant deviation from the norm are the longest wires. They do differ from the other wires in the one other way. They do not have any plating, the sensor length is from one prong to the next. This does not rule out an additional aerodynamic affect.

VI CONCLUSIONS

The results of this work can be summarized as:

1) The ratio η/ℓ is a factor that affects measurements of the spectra if it is small enough.

2) The effect of changing the wire diameter (in this range) was nil in all measurements.

3) Wyngaard's correction falls within the experimental error.

4) The spectra have a universal shape when normalized with the dissipation measured with the wire used to measure the spectra.

5) The moments of both u and $\partial u/\partial t$ are unaffected by wire length.

6) The correction for the dissipation scale λ and hence dissipation works very well.

On a final reflection one must state that even though the Wyngaard's correction is apparently valid, it is unnecessary. The measurement of spectra at high frequency is at best an order of magnitude analysis. It would be best to merely use the correction for dissipation.

Since η is a 1/4 power function of $\bar{\varepsilon}$, to reduce η by 25%, $\bar{\varepsilon}$ has to be increased by a factor of 3. This corresponds to a dissipation of roughly 80 m^2/s^3, which is quite large for most experimental flows. Thus, if a 1.1 mm wire were used it should not have a η/ℓ less

than 0.08. This coupled with the lack of effect of wire diameter indicates that the 5 μm,1.1 mm wire is the optimum wire to use as it is the largest (easiest to make and handle) with a reasonably good response characteristic.

VII RECOMMENDATIONS

No future work on the length correction should be made until the spectrum of turbulence can be measured more accurately.

For those who wish to measure the spectra a 5 μm, 1.1 mm wire works quite well and is available as a standard probe. The dissipation should be corrected for length using (2).

VIII REFERENCES

Azad, R.S. Arora, S.C. & Reichert, J.K., 1978: "Spectra of Reynolds Stresses in a Developing Pipe Flow", J. Heat Transfer and Fluid Mechanics, Stanford University Press.

Batchelor, G.K., 1967: "The Theory of Homogeneous Turbulence", Cambridge University Press.

Blackman, R.B. & Tukey, J.W., 1958: "The Measurement of Power Spectra From the Point of View of Communications Engineering", Dover.

Bradshaw, P., 1971: "An Introduction to Turbulence and its Measurement", Pergamon Press.

Bradshaw, P., 1978: "Turbulence", 2nd ed., Topics in Applied Physics, Springer-Verlag.

Burhanudin, S., 1980: "Measurement of Wall Sheat Stress with Hot-Wire Anemometer", M.Sc. Thesis, Univ. of Manitoba.

Corrsin, S., 1963: "Turbulence: Experimental Methods", in "Encyclopedia of Physics", Vol. VIII/2, p. 568, Springer-Verlag.

Champagne, F.H. 1978: "The Fine-Scale Structure of The Turbulent Velocity Field", J. Fluid Mech., Vol. 86, Part 1, pp. 67-108.

Dryden, H.L., Schubauer, W.C., Mock Jr. W.C. & Skramstad, H.K., 1937: "Measurements of Intensity and Scale of Wind-Tunnel Turbulence and Their Relation to the Critical Reynolds Number of Spheres", NACA Report No. 581.

Fremuth, P., 1977: "Further Investigations of the Nonlinear Theory for Constant Temperature Hot-wire Anemometers", J. of Physics E.: Scientific Instruments, Vol. 10, pp. 710-713.

Fremuth, P., & Fingerson, L.M., 1977: "Electronic Testing of Frequency Response for Thermal Anemometers", TSI Quarterly, Vol. 3, pp. 7-12.

Frenkiel, F.N., 1949: "The Influence of a hot-wire on the Measurement of Turbulence", Phy. Rev. Second Series, Vol. 75, pp. 1263-1264.

Frenkiel, F.N., 1954: "Effects of Wire Length in Turbulence Investigations with a Hot-wire Anemometer", Aero. Quart., Vol. 5, pp. 1-24.

Frenkiel, F.N. & Klebanoff, P.S., 1975: "On the Lognormality of the Small-Scale Structure of Turbulence", Boundary-Layer Meteorology, Vol. 8, pp. 173-200.

Goldstein, S., 1965: "Modern Developments in Fluid Mechanics", Dover.

Hinze, J.O., 1975: "Turbulence", 2nd ed., McGraw Hill.

Hussain, A.K. M.F., & Reynolds, W.C., 1975: "Measurements in Fully Developed Turbulent Channel Flow", J. Fluids Eng. Trans. ASME, Vol. 97, pp. 568-580.

Kader, B.A. & Yaglom, A.M., 1978: "Similarity Treatment of Moving-Equilibrium Turbulent Boundary Layers in Adverse Pressure Gradients", J. Fluid Mech., Vol. 89, pp. 305-342.

Klebanoff, P.S., 1954: "Characteristics of Turbulence in a Boundary Layer with Zero Pressure Gradient", NACA TN 3178.

Klebanoff, P.S., 1955: "Characteristics of Turbulence in a Boundary Layer with Zero Pressure Gradient", NACA Report No. 1247.

Kline, S.J., Reynolds, W.C., Schraub, F.A. & Runstadler, P.W., 1967: "The Structure of Turbulent Boundary Layers", J. Fluid Mech., Vol. 30, Part 4, pp. 741-773.

Landau, L.D. & Lifshitz, E.M., 1959: "Fluid Mechanics", Course in Theoretical Physics, Vol. 6, Pergamon Press.

Laufer, J. 1954: "The Structure of Turbulence in Fully-Developed Pipe Flow", NACA Report No. 1174.

Lumley, J.L. & Panofsky, H.A., 1964: "The Structure of Atmospheric Turbulence", John-Wiley and Sons.

Monin, A.S., & Yaglom, A.M., 1971: "Statistical Fluid Mechanics: Mechanics of Turbulence", Vol. 1, The MIT Press.

Monin, A.S. & Yaglom, A.M., 1975: "Statistical Fluid Mechanics: Mechanics of Turbulence", Vol. 2, The MIT Press.

Pao, Y.H., 1965: "Structure of Turbulent Velocity and Scalar Fields at Large Wave numbers", Phys. Fluids, Vol. 8, No. 6, pp. 1063-1075.

Paquin, J.E. & Pond, S., 1971: "The Determination of the Kolmogoroff Constants for Velocity, Temperature and Humidity Fluctuations from Second- and Third-order Structure Functions", J. Fluid Mech., Vol. 50, Part 2, pp. 257-269.

Purtell, L.P., Klebanoff, P-S. & Buckly, F.T., 1981: "Turbulent Boundary Layer at Low Reynolds Number", Phys. Fluids, Vol. 24, No. 5, pp. 802-811.

Roberts, J.B., 1973: "On the Correction of Hot-Wire Turbulence Measurements for Spatial Resolution Errors", Aero. J., Vol. 77, No. 752, pp. 406-412.

Schlighting, H., 1979: "Boundary Layer Theory", 7th Ed., McGraw-Hill.

Serag, M.A.-A.E.-S, 1978: "The Influence of the Length and Diameter on the Response Characteristics of a Hot-Wire Probe to the Fine Scale Structure of Turbulence", M.Sc. Thesis, Univ. of Manitoba.

Tennekes, H. & Lumley, J.L., 1972: "A First Course in Turbulence", The MIT Press.

Townsend, A.A., 1976: "The Structure of Turbulent Shear Flow", 2nd Ed., Cambridge University Press.

Uberoi, M.S. & Kovasznay, L.S.G., 1953: "On the Mapping and Measurement of Random Fields", Quart. Appl. Math., Vol. 10, No. 4, pp. 375-393.

Ueda, H. & Hinze, J.O., 1975: "Fine-Structure Turbulence in the Wall Region of a Turbulent Boundary Layer", J. Fluid Mech., Vol. 67, Part 1, pp. 125-143.

Van Driest, E.R., 1956: "On Turbulent Flow near a Wall", J. Aeronaut. Sci., Vol. 23, No. 11, pp. 1007-1011.

Wyngaard, J.C., 1968: "Measurement of Small-Scale Turbulence Structure with Hot Wires", J. Sci. Inst. (J. of Phys. E.) Series 2, Vol. 1, pp. 1105-1108.

Wyngaard, J.C. & Lumley, J.L., 1967: "A Sharp Cutoff Spectral Differentiator", J. Appl. Meteorol., Vol. 6, pp. 952-955.

Wyngaard, J.C. & Pao, Y.H., 1971: "Some Measurements of the Fine Structure of Large Reynolds Number Turbulence", in "Lecture Notes in Physics: Statistical Models and Turbulence", No. 12, pp. 384-401, Springer-Verlag.

TABLE 1

HOT-WIRE GEOMETRY AND RESISTANCES

Probe Number	ℓ (mm)	d (μm)	R_a Ω	R_{op} Ω	Overheat	ℓ/d
1	2.65	5.43	7.77	13.59	0.8	488
2	2.59	5.24	8.22	14.40	0.8	494
3	0.703	5.45	2.88	4.78	0.8	129
4	0.724	5.77	2.76	4.57	0.8	125
5	1.10	5.07	4.07	6.77	0.8	217
6	1.08	4.82	4.17	6.95	0.8	224
7	2.84	2.84	27.69	48.88	0.8	1001
8	2.81	3.41	26.86	47.39	0.8	824
9	1.08	3.60	10.75	18.79	0.8	300
10	1.20	3.72	10.52	18.54	0.8	322
11	1.50	3.49	12.65	22.53	0.8	430
12	1.44	3.49	13.10	23.18	0.8	411
13	0.330	3.85	4.58	7.04	0.8	86
14	0.711	3.60	6.67	10.00	0.8	198

TABLE 2

BOUNDARY LAYER PARAMETERS

U_∞ (m/s)	u_* Cross-Plot (m/s)	u_* Derivative (m/s)	δ_{99} (cm)	δ_1 (mm)	δ_2 (mm)	$Re\delta_{99}$	$Re\delta_1$	$Re\delta_2$	$C_f \times 10^{-3}$
4.0	0.18	0.15	4.0	7.38	5.52	9,940	1,830	1,370	4.3
8.0	0.33	0.31	4.9	7.38	5.52	24,350	3,660	2,740	3.4
12.0	0.48	0.46	4.9	7.38	5.52	36,520	5,490	4,110	3.2

TABLE 3

VISCOUS SUBLAYER BUFFER LAYER LAWS

Y_+	u_+ Van Driest	u_+ Kader & Yaglom	Y_+	u_+ Van Driest	u_+ Kader & Yaglom
1.0	1.00	1.00	31.0	13.44	13.38
2.0	2.00	1.99	32.0	13.54	13.46
3.0	2.99	2.96	33.0	13.65	13.53
4.0	3.96	3.90	34.0	13.74	13.60
5.0	4.89	4.81	35.0	13.84	13.68
6.0	5.76	5.68	36.0	13.93	13.74
7.0	6.55	6.50	37.0	14.02	13.81
8.0	7.26	7.28	38.0	14.10	13.88
9.0	7.90	8.00	39.0	14.18	13.94
10.0	8.46	8.67	40.0	14.26	14.00
11.0	8.97	9.28	41.0	14.33	14.06
12.0	9.42	9.85	42.0	14.41	14.12
13.0	9.82	10.36	43.0	14.47	14.18
14.0	10.19	10.83	44.0	14.54	14.23
15.0	10.52	11.25	45.0	14.61	14.29
16.0	10.82	11.63	46.0	14.68	14.34
17.0	11.09	11.96	47.0	14.74	14.39
18.0	11.35	12.26	48.0	14.80	14.45
19.0	11.56	12.53	49.0	14.86	14.50
20.0	11.79	12.77	50.0	14.92	14.55
21.0	11.99	12.98	51.0	14.97	14.59
22.0	12.18	13.17	52.0	15.03	14.64
23.0	12.36	13.33	53.0	15.08	14.69
24.0	12.52	13.48	54.0	15.13	14.73
25.0	12.67	13.61	55.0	15.18	14.78
26.0	12.82	13.72	56.0	15.23	14.82
27.0	12.96	13.82	57.0	15.28	14.87
28.0	13.08	13.13	58.0	15.23	14.91
29.0	13.21	13.22	59.0	15.38	14.95
30.0	13.33	13.33	60.0	15.42	14.99

TABLE 4

MEASURED SPECTRA ϕ_1

(a) Probe #1 U = 7.84 m/s u' = 0.438 VRMS = 0.876 m/s

f (Hz)	u' (VRMS)	κ_1 (1/m)	$\phi(\kappa_1)$ (m^3/s^2)	$\kappa_1^2\phi(\kappa_1)$ (m/s^2)	$\kappa_1^4\phi(\kappa)$ ($1/ms^2$)
2.1	0.0269	1.68×10^{0}	1.47×10^{-2}	4.15×10^{-2}	1.17×10^{-1}
2.8	0.0311	2.24×10^{0}	1.47×10^{-2}	7.38×10^{-2}	3.70×10^{-1}
3.8	0.0381	3.05×10^{0}	1.63×10^{-2}	1.52×10^{-1}	1.41×10^{0}
5.1	0.0425	4.09×10^{0}	1.51×10^{-2}	2.53×10^{-1}	4.23×10^{0}
6.8	0.0476	5.45×10^{0}	1.42×10^{-2}	4.22×10^{-1}	1.25×10^{1}
9.0	0.0548	7.21×10^{0}	1.43×10^{-2}	7.43×10^{0}	3.86×10^{1}
12	0.0580	9.62×10^{0}	1.20×10^{-2}	1.11×10^{0}	1.03×10^{2}
16	0.0629	1.28×10^{1}	1.05×10^{-2}	1.72×10^{0}	2.82×10^{2}
21	0.0707	1.68×10^{1}	1.01×10^{-2}	2.85×10^{0}	8.05×10^{2}
28	0.0710	2.24×10^{1}	6.67×10^{-3}	3.85×10^{0}	1.93×10^{3}
38	0.0705	3.05×10^{1}	5.57×10^{-3}	5.18×10^{0}	4.82×10^{3}
51	0.0710	4.09×10^{1}	4.22×10^{-3}	7.06×10^{0}	1.18×10^{4}
68	0.0702	5.45×10^{1}	3.09×10^{-3}	9.18×10^{1}	2.73×10^{4}
90	0.0687	7.21×10^{1}	2.24×10^{-3}	1.16×10^{1}	6.05×10^{5}
120	0.0645	9.62×10^{2}	1.48×10^{-3}	1.37×10^{1}	1.27×10^{5}
160	0.0660	1.28×10^{2}	1.16×10^{-3}	1.90×10^{1}	3.11×10^{5}
210	0.0651	1.68×10^{2}	8.60×10^{-4}	2.43×10^{1}	6.85×10^{6}
280	0.0611	2.24×10^{2}	5.68×10^{-4}	2.85×10^{1}	1.43×10^{6}
380	0.0581	3.05×10^{2}	3.78×10^{-4}	3.52×10^{1}	3.27×10^{6}
510	0.0519	4.09×10^{2}	2.25×10^{-4}	3.76×10^{1}	6.30×10^{7}
680	0.0467	5.45×10^{2}	1.36×10^{-5}	4.04×10^{1}	1.20×10^{7}
900	0.0391	7.21×10^{2}	7.24×10^{-5}	3.76×10^{1}	1.96×10^{7}
1200	0.0315	9.62×10^{2}	3.52×10^{-5}	3.26×10^{1}	3.01×10^{7}
1600	0.0243	1.28×10^{3}	1.58×10^{-5}	2.59×10^{1}	4.24×10^{7}
2100	0.0175	1.68×10^{3}	6.21×10^{-6}	1.75×10^{1}	4.95×10^{7}
2800	0.0129	2.24×10^{3}	2.53×10^{-6}	1.25×10^{0}	6.35×10^{7}
3800	0.00855	2.05×10^{3}	8.20×10^{-7}	7.63×10^{0}	7.10×10^{7}
5100	0.00503	4.09×10^{3}	2.11×10^{-8}	3.53×10^{0}	5.90×10^{7}
6800	0.00312	5.45×10^{3}	6.10×10^{-9}	1.81×10^{-1}	5.38×10^{7}
9000	0.00138	7.21×10^{3}	8.98×10^{-9}	4.67×10^{-1}	2.43×10^{7}
12000	0.000678	9.28×10^{3}	1.63×10^{-9}	1.40×10^{-1}	1.21×10^{7}

*These are the measured mean velocity, fluctuating voltage and fluctuating velocity measurements while the spectrum was measured.

(b) Probe #2 U = 7.96 m/s u' = 0.451 VRMS = 0.902 m/s

f (Hz)	u' (VRMS)	κ_1 (1/m)	$\phi(\kappa_1)$ (m^3/s^2)	$\kappa_1^2\phi(\kappa_1)$ (m/s^2)	$\kappa_1^4\phi(\kappa_1)$ ($1/ms^2$)
2.1	0.0278	1.66×10^{0}	1.61×10^{-2}	4.44×10^{-2}	1.22×10^{-1}
2.8	0.0355	2.21×10^{0}	1.96×10^{-2}	9.57×10^{-1}	4.68×10^{0}
3.8	0.0386	3.00×10^{0}	1.71×10^{-2}	1.54×10^{-1}	1.39×10^{0}
5.1	0.0448	4.03×10^{0}	1.72×10^{-2}	2.79×10^{-1}	4.54×10^{0}
6.8	0.0495	5.37×10^{0}	1.58×10^{-2}	4.56×10^{-1}	1.31×10^{-1}
9.0	0.0575	7.10×10^{0}	1.60×10^{-2}	8.07×10^{0}	4.07×10^{1}
12	0.0586	9.47×10^{0}	1.25×10^{-2}	1.12×10^{0}	1.01×10^{2}
16	0.0662	1.26×10^{1}	1.20×10^{-2}	1.91×10^{0}	3.02×10^{2}
21	0.0734	1.66×10^{1}	1.12×10^{-3}	3.09×10^{0}	8.50×10^{3}
28	0.0723	2.21×10^{1}	8.14×10^{-3}	3.98×10^{0}	1.94×10^{3}
38	0.0729	3.00×10^{1}	6.10×10^{-3}	5.49×10^{0}	4.04×10^{4}
51	0.0694	4.03×10^{1}	4.12×10^{-3}	6.69×10^{0}	1.09×10^{4}
68	0.0731	5.37×10^{1}	3.43×10^{-3}	9.89×10^{1}	2.85×10^{4}
90	0.0709	7.10×10^{1}	2.44×10^{-3}	1.23×10^{1}	6.20×10^{5}
120	0.0663	9.47×10^{2}	1.60×10^{-3}	1.43×10^{1}	1.29×10^{5}
160	0.0673	1.26×10^{2}	1.23×10^{-4}	1.95×10^{1}	3.10×10^{5}
210	0.0657	1.66×10^{2}	8.98×10^{-4}	2.47×10^{1}	6.82×10^{6}
280	0.0620	2.21×10^{2}	5.98×10^{-4}	2.92×10^{1}	1.43×10^{6}
380	0.0592	3.00×10^{2}	4.02×10^{-4}	3.62×10^{1}	3.26×10^{6}
510	0.0528	4.03×10^{2}	2.38×10^{-4}	2.87×10^{1}	6.28×10^{7}
680	0.0471	5.37×10^{2}	1.43×10^{-4}	4.12×10^{1}	1.19×10^{7}
900	0.0391	7.10×10^{2}	7.41×10^{-5}	3.74×10^{1}	1.88×10^{7}
1200	0.0318	9.47×10^{2}	3.68×10^{-5}	3.30×10^{1}	2.96×10^{7}
1600	0.0249	1.26×10^{3}	1.69×10^{-6}	2.68×10^{1}	4.26×10^{7}
2100	0.0177	1.66×10^{3}	6.50×10^{-6}	1.79×10^{1}	4.94×10^{7}
2800	0.0126	2.21×10^{3}	2.47×10^{-6}	1.21×10^{0}	5.89×10^{7}
3800	0.00876	3.00×10^{3}	8.80×10^{-7}	7.92×10^{0}	7.13×10^{7}
5100	0.00534	4.03×10^{3}	2.44×10^{-8}	3.96×10^{0}	6.44×10^{7}
6800	0.00293	5.37×10^{3}	5.51×10^{-9}	1.59×10^{-1}	4.58×10^{7}
9000	0.00140	7.10×10^{3}	9.50×10^{-9}	4.79×10^{-1}	2.41×10^{7}
12000	0.000669	9.47×10^{3}	1.63×10^{-9}	1.46×10^{-1}	1.31×10^{7}

(c) Probe #3 U = 7.90 m/s u' = 0.457 VRMS = 0.914 m/s

f (Hz)	u' (V)	κ_1 (1/m)	$\phi(\kappa_1)$ (m^3/s^2)	$\kappa_1^2\phi(\kappa_1)$ (m/s^2)	$\kappa_1^4\phi(\kappa_1)$ ($1/ms^2$)
2.1	0.0307	1.67×10^{0}	1.93×10^{-2}	5.38×10^{-2}	1.50×10^{-1}
2.8	0.0346	2.23×10^{0}	1.84×10^{-2}	9.15×10^{-2}	4.55×10^{-1}
3.8	0.0401	3.02×10^{0}	1.82×10^{-2}	1.66×10^{-1}	1.51×10^{0}
5.1	0.0417	4.06×10^{0}	1.47×10^{-2}	2.42×10^{-1}	3.99×10^{0}
6.8	0.0517	5.41×10^{0}	1.69×10^{-2}	4.95×10^{-1}	1.45×10^{1}
9.0	0.0558	7.16×10^{0}	1.49×10^{-2}	7.64×10^{-1}	3.92×10^{1}
12	0.0579	9.54×10^{0}	1.20×10^{-2}	1.09×10^{0}	9.94×10^{1}
16	0.0650	1.27×10^{1}	1.14×10^{-2}	1.84×10^{0}	2.97×10^{2}
21	0.0704	1.67×10^{1}	1.02×10^{-2}	2.84×10^{0}	7.93×10^{2}
28	0.0731	2.23×10^{1}	8.23×10^{-3}	4.09×10^{0}	2.64×10^{3}
38	0.0721	3.02×10^{1}	5.90×10^{-3}	5.38×10^{0}	4.91×10^{3}
51	0.0696	4.06×10^{1}	4.09×10^{-3}	6.74×10^{0}	1.11×10^{4}
68	0.0728	5.41×10^{1}	3.36×10^{-3}	9.83×10^{0}	2.88×10^{4}
90	0.0711	7.16×10^{1}	2.42×10^{-3}	1.24×10^{1}	6.36×10^{4}
120	0.0661	9.54×10^{1}	1.57×10^{-3}	1.43×10^{1}	1.39×10^{5}
160	0.0672	1.27×10^{2}	1.22×10^{-3}	1.97×10^{1}	3.17×10^{5}
210	0.0666	1.67×10^{2}	9.11×10^{-4}	2.54×10^{1}	7.09×10^{5}
280	0.0634	2.23×10^{2}	6.19×10^{-4}	3.08×10^{1}	1.53×10^{6}
380	0.0605	3.03×10^{2}	4.15×10^{-4}	3.81×10^{1}	3.50×10^{6}
510	0.0567	4.06×10^{2}	2.72×10^{-4}	4.48×10^{1}	7.39×10^{6}
680	0.0506	5.41×10^{2}	1.62×10^{-4}	4.74×10^{1}	1.39×10^{7}
900	0.0442	7.16×10^{2}	9.36×10^{-5}	4.80×10^{1}	2.46×10^{7}
1200	0.0349	9.54×10^{2}	4.38×10^{-5}	3.99×10^{1}	3.63×10^{7}
1600	0.0314	1.27×10^{3}	2.66×10^{-5}	4.29×10^{1}	6.92×10^{7}
2100	0.0222	1.67×10^{3}	1.01×10^{-5}	2.89×10^{1}	7.86×10^{8}
2800	0.0174	2.23×10^{3}	4.66×10^{-6}	2.32×10^{1}	1.15×10^{8}
3800	0.0119	3.03×10^{3}	1.61×10^{-6}	1.48×10^{0}	1.36×10^{8}
5100	0.00747	4.06×10^{3}	4.72×10^{-7}	7.78×10^{0}	1.28×10^{7}
6800	0.00425	5.41×10^{3}	1.15×10^{-7}	3.37×10^{0}	9.85×10^{7}
9000	0.00215	7.16×10^{3}	2.21×10^{-8}	1.13×10^{-1}	5.81×10^{7}
1200	0.00101	9.54×10^{3}	3.66×10^{-9}	3.33×10^{-1}	3.03×10^{7}

(d) Probe #4 U = 8.06 m/s u' = 0.455 VRMS = 0.910 m/s

f (Hz)	u' (VRMS)	κ_1 (1/m)	ϕ (m^3/s^2)	$\kappa_1^2\phi(\kappa_1)$ (m/s^2)	$\kappa_1^4\phi(\kappa_1)$ ($1/ms^2$)
2.1	0.0302	1.64×10^{0}	1.89×10^{-2}	5.08×10^{-2}	1.37×10^{-1}
2.8	0.0333	2.18×10^{0}	1.73×10^{-2}	8.22×10^{-2}	3.91×10^{-1}
3.8	0.0377	2.96×10^{0}	1.63×10^{-2}	1.43×10^{-1}	1.25×10^{0}
51.1	0.0418	3.98×10^{0}	1.49×10^{-2}	2.36×10^{-1}	3.74×10^{1}
6.8	0.0513	5.30×10^{0}	1.69×10^{-2}	4.75×10^{-1}	1.33×10^{1}
9.0	0.0553	7.02×10^{0}	1.48×10^{-2}	7.29×10^{0}	3.59×10^{1}
12	0.0565	9.35×10^{1}	1.16×10^{-2}	1.01×10^{0}	8.87×10^{2}
16	0.0665	1.25×10^{1}	1.20×10^{-2}	1.88×10^{0}	2.93×10^{2}
21	0.0695	1.64×10^{1}	1.00×10^{-2}	2.69×10^{0}	7.23×10^{2}
28	0.0727	2.18×10^{1}	8.23×10^{-3}	3.91×10^{0}	1.86×10^{3}
38	0.0728	2.96×10^{1}	6.08×10^{-3}	5.33×10^{0}	4.67×10^{4}
51	0.0699	3.98×10^{1}	4.18×10^{-3}	6.62×10^{0}	1.05×10^{4}
68	0.0715	5.30×10^{1}	3.28×10^{-3}	9.21×10^{1}	2.59×10^{4}
90	0.0700	7.02×10^{1}	2.37×10^{-3}	1.17×10^{1}	5.79×10^{5}
120	0.0656	9.35×10^{1}	1.56×10^{-3}	1.36×10^{1}	1.19×10^{5}
160	0.0685	1.25×10^{2}	1.28×10^{-3}	2.00×10^{1}	3.13×10^{5}
210	0.0657	1.64×10^{2}	8.96×10^{-4}	2.41×10^{1}	6.48×10^{6}
280	0.0641	2.18×10^{2}	6.40×10^{-4}	3.04×10^{1}	1.45×10^{6}
380	0.0623	2.96×10^{2}	4.45×10^{-4}	3.90×10^{1}	3.42×10^{6}
510	0.0573	3.98×10^{2}	2.81×10^{-4}	4.45×10^{1}	7.05×10^{7}
680	0.0523	5.30×10^{2}	1.75×10^{-4}	4.92×10^{1}	1.38×10^{7}
900	0.0434	7.02×10^{2}	9.12×10^{-5}	4.49×10^{1}	2.21×10^{7}
1200	0.0363	9.25×10^{2}	4.79×10^{-5}	4.19×10^{1}	3.66×10^{7}
1600	0.0316	1.25×10^{3}	2.72×10^{-5}	4.25×10^{1}	6.64×10^{7}
2100	0.0244	1.64×10^{3}	1.24×10^{-6}	3.34×10^{1}	8.97×10^{8}
2800	0.0181	2.18×10^{3}	5.10×10^{-6}	2.42×10^{1}	1.15×10^{8}
3800	0.0125	2.96×10^{3}	1.79×10^{-6}	1.57×10^{0}	1.37×10^{8}
5100	0.00767	3.98×10^{3}	5.03×10^{-7}	7.97×10^{0}	1.26×10^{7}
6800	0.00440	5.30×10^{3}	1.24×10^{-8}	3.48×10^{0}	9.78×10^{7}
9000	0.00229	7.02×10^{3}	2.54×10^{-9}	1.25×10^{-1}	6.17×10^{7}
12000	0.000975	9.38×10^{3}	3.45×10^{-9}	3.02×10^{-1}	2.64×10^{7}

(e) Probe #5 U = 7.92 m/s u' = 0.416 VRMS = 0.922 m/s

f (Hz)	u' (VRMS)	κ_1 (1/m)	$\phi(\kappa_1)$ (m^3/s^2)	$\kappa_1^2\phi(\kappa_1)$ (m/s^2)	$\kappa_1^4\phi(\kappa_1)$ ($1/ms^2$)
2.1	0.0286	1.67×10^{0}	1.73×10^{-2}	4.82×10^{-2}	1.35×10^{-1}
2.8	0.0345	2.22×10^{0}	1.88×10^{-2}	9.27×10^{-2}	4.57×10^{-1}
3.8	0.0375	3.01×10^{0}	1.64×10^{-2}	8.08×10^{-2}	5.38×10^{-1}
5.1	0.0437	4.05×10^{0}	1.66×10^{-2}	2.72×10^{-1}	4.47×10^{0}
6.8	0.0503	5.39×10^{0}	1.65×10^{-2}	4.79×10^{-1}	1.39×10^{1}
9.0	0.0542	7.14×10^{0}	1.45×10^{-2}	7.39×10^{0}	3.77×10^{1}
12	0.0568	9.52×10^{0}	1.19×10^{-2}	1.08×10^{0}	9.77×10^{1}
16	0.0656	1.27×10^{1}	1.19×10^{-2}	1.92×10^{0}	3.10×10^{2}
21	0.0731	1.67×10^{1}	1.13×10^{-2}	3.15×10^{0}	8.79×10^{2}
28	0.0721	2.22×10^{1}	8.23×10^{-3}	4.06×10^{0}	2.00×10^{3}
38	0.0705	3.01×10^{1}	5.80×10^{-3}	5.25×10^{0}	4.76×10^{4}
51	0.0712	4.05×10^{1}	4.41×10^{-3}	7.23×10^{0}	1.19×10^{4}
68	0.0716	5.39×10^{1}	3.34×10^{-3}	9.70×10^{1}	2.82×10^{4}
90	0.0719	7.14×10^{1}	2.55×10^{-3}	1.30×10^{1}	6.63×10^{5}
120	0.0662	9.52×10^{1}	1.62×10^{-3}	1.47×10^{1}	1.33×10^{5}
160	0.0691	1.27×10^{2}	1.32×10^{-3}	2.13×10^{1}	3.43×10^{5}
210	0.0664	1.67×10^{2}	9.30×10^{-4}	2.59×10^{1}	7.23×10^{6}
280	0.0627	2.22×10^{2}	6.22×10^{-4}	3.07×10^{1}	1.51×10^{6}
380	0.0611	3.01×10^{2}	4.35×10^{-4}	3.94×10^{1}	3.57×10^{6}
510	0.0555	4.05×10^{2}	2.68×10^{-4}	4.40×10^{1}	7.21×10^{7}
680	0.0497	5.39×10^{2}	1.61×10^{-4}	4.68×10^{1}	1.36×10^{7}
900	0.0433	7.14×10^{2}	9.23×10^{-5}	4.71×10^{1}	2.40×10^{7}
1200	0.0356	9.52×10^{2}	4.68×10^{-5}	2.24×10^{1}	3.84×10^{7}
1600	0.0311	1.27×10^{3}	2.68×10^{-5}	4.32×10^{1}	6.97×10^{7}
2100	0.0228	1.67×10^{3}	1.10×10^{-6}	3.07×10^{1}	8.56×10^{8}
2800	0.0169	2.22×10^{3}	4.52×10^{-6}	2.23×10^{1}	1.10×10^{8}
3800	0.0115	3.01×10^{3}	1.54×10^{-6}	1.40×10^{1}	1.26×10^{8}
5100	0.00694	4.05×10^{3}	4.19×10^{-7}	6.87×10^{0}	1.13×10^{7}
6800	0.00391	5.39×10^{3}	9.96×10^{-8}	2.89×10^{0}	8.41×10^{7}
9000	0.00196	7.14×10^{3}	1.86×10^{-8}	9.48×10^{-1}	4.83×10^{7}
12000	0.000870	9.52×10^{3}	2.80×10^{-9}	2.54×10^{-1}	2.30×10^{7}

(f) Probe #6 U = 8.04 m/s u' = 0.455 VRMS = 0.910 m/s

f (Hz)	u' (VRMS)	(κ_1) (1/m)	$\phi(\kappa)$ (m^3/s^2)	$\kappa_1^2\phi(\kappa_1)$ (m/s^2)	$\kappa_1^4\phi(\kappa_1)$ ($1/ms^2$)
2.1	0.0277	1.64×10^{0}	1.60×10^{-2}	4.30×10^{-2}	1.16×10^{-1}
2.8	0.0344	2.10×10^{0}	1.85×10^{-2}	8.87×10^{-2}	4.36×10^{-1}
3.8	0.0379	2.97×10^{0}	1.65×10^{-2}	1.46×10^{-1}	1.28×10^{0}
5.1	0.0435	3.99×10^{0}	1.62×10^{-2}	2.58×10^{-1}	4.11×10^{0}
6.8	0.0497	5.31×10^{0}	1.59×10^{-2}	4.48×10^{-1}	1.26×10^{1}
9.0	0.0549	7.03×10^{0}	1.46×10^{-2}	7.22×10^{-1}	3.57×10^{1}
12	0.0577	9.38×10^{0}	1.21×10^{-2}	1.06×10^{0}	9.37×10^{1}
16	0.0647	1.25×10^{1}	1.14×10^{-2}	1.78×10^{0}	2.78×10^{2}
21	0.0715	1.64×10^{1}	1.06×10^{-2}	2.85×10^{0}	7.67×10^{2}
28	0.0725	2.19×10^{1}	8.21×10^{-3}	3.94×10^{0}	1.89×10^{3}
38	0.0719	2.97×10^{1}	5.95×10^{-3}	5.25×10^{0}	4.63×10^{3}
51	0.0716	3.99×10^{1}	4.40×10^{-3}	7.00×10^{0}	1.12×10^{4}
68	0.0712	5.31×10^{1}	3.26×10^{-3}	9.19×10^{0}	2.59×10^{4}
90	0.0712	7.03×10^{1}	2.46×10^{-3}	1.22×10^{1}	6.01×10^{4}
120	0.0664	9.38×10^{1}	1.61×10^{-3}	1.42×10^{1}	1.25×10^{5}
160	0.0673	1.25×10^{2}	1.24×10^{-4}	1.94×10^{1}	3.03×10^{5}
210	0.0656	1.64×10^{2}	8.96×10^{-4}	2.41×10^{1}	6.48×10^{6}
280	0.0648	2.19×10^{2}	6.56×10^{-4}	3.15×10^{1}	1.51×10^{6}
380	0.0613	2.97×10^{2}	4.32×10^{-4}	3.81×10^{1}	3.36×10^{6}
510	0.0567	3.99×10^{2}	2.76×10^{-4}	4.39×10^{1}	7.00×10^{7}
680	0.0506	5.31×10^{2}	1.65×10^{-4}	4.65×10^{1}	1.31×10^{7}
900	0.0440	7.03×10^{2}	9.41×10^{-5}	4.65×10^{1}	2.30×10^{7}
1200	0.0357	9.38×10^{2}	4.64×10^{-5}	4.08×10^{1}	3.59×10^{7}
1600	0.0314	1.25×10^{3}	2.69×10^{-5}	4.20×10^{1}	6.57×10^{7}
2100	0.0228	1.64×10^{3}	1.08×10^{-6}	2.90×10^{1}	7.81×10^{8}
2800	0.0176	2.19×10^{3}	4.84×10^{-6}	2.32×10^{1}	1.11×10^{8}
3800	0.0119	2.97×10^{3}	1.63×10^{-6}	1.44×10^{1}	1.27×10^{8}
5100	0.00704	3.99×10^{3}	4.25×10^{-7}	6.77×10^{0}	1.08×10^{8}
6800	0.00403	5.31×10^{3}	1.04×10^{-7}	2.93×10^{-1}	8.27×10^{7}
9000	0.00199	7.03×10^{3}	1.98×10^{-8}	9.79×10^{-1}	4.84×10^{7}
1200	0.000855	9.38×10^{3}	2.66×10^{-9}	2.34×10^{-1}	2.06×10^{7}

(g) Probe #7 U = 7.70 m/s u' = 0.434 VRMS = 0.868 m/s

f (Hz)	u' (VRMS)	κ_1 (1/m)	$\phi(\kappa_1)$ (m^3/s^2)	$\kappa_1^2\phi(\kappa_1)$ (m/s^2)	$\kappa_1^4\phi(\kappa_1)$ ($1/ms^2$)
2.1	0.0285	1.71×10^{0}	1.65×10^{-2}	4.82×10^{-2}	1.41×10^{-1}
2.8	0.0342	2.28×10^{0}	1.78×10^{-2}	9.25×10^{-2}	4.81×10^{-1}
3.8	0.0362	3.10×10^{0}	1.47×10^{-2}	1.41×10^{-1}	1.36×10^{0}
5.1	0.0411	4.16×10^{0}	1.41×10^{-2}	2.44×10^{-1}	4.22×10^{1}
6.8	0.0485	5.55×10^{0}	1.47×10^{-2}	4.53×10^{-1}	1.39×10^{1}
9.0	0.0510	7.34×10^{0}	1.23×10^{-2}	6.63×10^{0}	3.57×10^{2}
12	0.0560	9.79×10^{0}	1.11×10^{-2}	1.06×10^{0}	1.02×10^{2}
16	0.0639	1.31×10^{1}	1.09×10^{-2}	1.87×10^{0}	3.21×10^{2}
21	0.0669	1.71×10^{1}	9.09×10^{-3}	2.66×10^{0}	7.77×10^{2}
28	0.0686	2.28×10^{1}	7.17×10^{-3}	3.73×10^{0}	1.94×10^{3}
38	0.0678	3.10×10^{1}	5.16×10^{-3}	4.96×10^{0}	4.77×10^{3}
51	0.0675	4.16×10^{1}	3.81×10^{-3}	6.59×10^{0}	1.14×10^{4}
68	0.0685	5.55×10^{1}	2.94×10^{-3}	9.06×10^{1}	2.79×10^{4}
90	0.0666	7.34×10^{1}	2.10×10^{-3}	1.13×10^{1}	6.10×10^{5}
120	0.0606	9.79×10^{2}	1.30×10^{-3}	1.25×10^{1}	1.19×10^{5}
160	0.0640	1.31×10^{2}	1.09×10^{-3}	1.87×10^{1}	3.21×10^{5}
210	0.0618	1.71×10^{2}	7.75×10^{-4}	2.27×10^{1}	6.63×10^{5}
280	0.0579	2.28×10^{2}	5.10×10^{-4}	2.65×10^{1}	1.38×10^{6}
380	0.0559	3.10×10^{2}	3.51×10^{-4}	3.37×10^{1}	3.24×10^{6}
510	0.0501	4.16×10^{2}	2.10×10^{-4}	3.63×10^{1}	6.29×10^{7}
680	0.0443	5.55×10^{2}	1.23×10^{-5}	3.79×10^{1}	1.17×10^{7}
900	0.0377	7.34×10^{2}	6.73×10^{-5}	3.63×10^{1}	1.95×10^{7}
1200	0.0297	9.79×10^{2}	3.13×10^{-5}	3.00×10^{1}	2.88×10^{7}
1600	0.0241	1.31×10^{3}	1.55×10^{-5}	2.66×10^{1}	4.56×10^{7}
2100	0.0171	1.71×10^{3}	5.94×10^{-6}	1.74×10^{1}	5.08×10^{7}
2800	0.0129	2.28×10^{3}	2.53×10^{-7}	1.32×10^{0}	6.84×10^{7}
3800	0.00857	3.10×10^{3}	8.24×10^{-7}	7.92×10^{0}	7.61×10^{7}
5100	0.00506	4.16×10^{3}	2.14×10^{-8}	3.70×10^{0}	6.41×10^{7}
6800	0.00284	5.55×10^{3}	5.06×10^{-9}	1.56×10^{0}	4.80×10^{7}
9000	0.00144	7.34×10^{3}	9.82×10^{-9}	5.29×10^{-1}	2.85×10^{7}
1200	0.000654	9.79×10^{3}	1.52×10^{-9}	1.46×10^{-1}	1.40×10^{7}

(h) Probe #8 U = 8.04 m/s u' = 0.446 VRMS = 0.892 m/s

f (Hz)	u' (VRMS)	κ_1 (1/m)	$\phi(\kappa_1)$ (m^3/s^2)	$\kappa_1^2\phi(\kappa_1)$ (m/s^2)	$\kappa_1^4\phi(\kappa_2)$ ($1/ms^2$)
2.1	0.0295	1.64×10^{0}	1.80×10^{-2}	4.84×10^{-2}	1.30×10^{-1}
2.8	0.0334	2.19×10^{0}	1.73×10^{-2}	8.30×10^{-2}	3.98×10^{-1}
3.8	0.0370	2.97×10^{0}	1.56×10^{-2}	1.38×10^{-1}	1.21×10^{0}
5.1	0.0435	3.99×10^{0}	1.61×10^{-2}	2.56×10^{-1}	4.08×10^{0}
6.8	0.0476	5.31×10^{0}	1.45×10^{-2}	4.09×10^{-1}	1.15×10^{1}
9.0	0.0550	7.03×10^{0}	1.46×10^{-2}	7.22×10^{0}	3.57×10^{1}
12	0.0578	9.28×10^{0}	1.21×10^{-2}	1.04×10^{0}	8.97×10^{1}
16	0.0668	1.25×10^{1}	1.21×10^{-2}	1.89×10^{0}	2.95×10^{2}
21	0.0696	1.64×10^{1}	1.00×10^{-2}	2.69×10^{0}	7.23×10^{2}
28	0.0721	2.19×10^{1}	8.06×10^{-3}	2.87×10^{0}	1.85×10^{3}
38	0.0733	2.97×10^{1}	6.14×10^{-3}	5.42×10^{0}	4.78×10^{3}
51	0.0711	3.99×10^{1}	4.36×10^{-3}	6.85×10^{0}	1.09×10^{4}
68	0.0727	5.31×10^{1}	3.38×10^{-3}	9.53×10^{1}	2.69×10^{4}
90	0.0708	7.03×10^{1}	2.42×10^{-3}	1.20×10^{1}	5.91×10^{4}
120	0.0648	9.28×10^{1}	1.52×10^{-3}	1.31×10^{1}	1.13×10^{5}
160	0.0680	1.25×10^{2}	1.26×10^{-3}	1.91×10^{1}	3.08×10^{5}
210	0.0619	1.64×10^{2}	7.92×10^{-4}	2.14×10^{1}	5.74×10^{5}
280	0.0620	2.19×10^{2}	5.96×10^{-4}	2.73×10^{1}	1.31×10^{6}
380	0.0584	2.97×10^{2}	3.90×10^{-4}	3.44×10^{1}	3.03×10^{6}
510	0.0531	3.99×10^{2}	2.40×10^{-4}	3.82×10^{1}	6.08×10^{6}
680	0.0474	5.31×10^{2}	1.43×10^{-4}	4.03×10^{1}	1.14×10^{7}
900	0.0401	7.03×10^{2}	7.76×10^{-5}	3.84×10^{1}	1.90×10^{7}
1200	0.0318	9.28×10^{2}	3.66×10^{-5}	3.15×10^{1}	2.71×10^{7}
1600	0.0263	1.25×10^{3}	1.88×10^{-6}	2.94×10^{1}	4.59×10^{7}
2100	0.0191	1.64×10^{3}	7.54×10^{-6}	2.03×10^{1}	5.45×10^{7}
2800	0.0135	2.19×10^{3}	2.83×10^{-7}	1.36×10^{0}	6.51×10^{7}
3800	0.00901	2.97×10^{3}	9.28×10^{-7}	8.19×10^{0}	7.22×10^{7}
5100	0.00560	3.99×10^{3}	2.67×10^{-7}	4.25×10^{0}	6.77×10^{7}
6800	0.00321	5.31×10^{3}	6.58×10^{-8}	1.86×10^{0}	5.23×10^{7}
9000	0.00157	7.03×10^{3}	1.19×10^{-8}	5.88×10^{-1}	2.91×10^{7}
12000	0.000717	9.28×10^{3}	1.86×10^{-9}	1.60×10^{-1}	1.38×10^{7}

(i) Proble #9 U = 7.04 m/s u' = 0.421 VRMS = 0.842 m/s

f (Hz)	u' (VRMS)	κ_1 (1/m)	$\phi(\kappa_1)$ (m^3/s^2)	$\kappa_1^2\phi(\kappa_1)$ (m/s^2)	$\kappa_1^4\phi(\kappa_1)$ ($1/ms^2$)
2.1	0.0269	1.87×10^{-2}	1.33×10^{-2}	4.65×10^{-2}	1.63×10^{-1}
2.8	0.0308	2.50×10^{0}	1.31×10^{-2}	8.19×10^{-2}	5.12×10^{0}
3.8	0.0356	3.39×10^{0}	1.28×10^{-2}	1.47×10^{-1}	1.69×10^{0}
5.1	0.0391	4.55×10^{0}	1.15×10^{-2}	2.38×10^{-1}	4.93×10^{1}
6.8	0.0471	6.07×10^{0}	1.26×10^{-2}	4.64×10^{-1}	1.71×10^{1}
9.0	0.0503	8.03×10^{1}	1.08×10^{-3}	6.96×10^{0}	4.49×10^{2}
12	0.0547	1.07×10^{1}	9.60×10^{-3}	1.10×10^{0}	1.26×10^{2}
16	0.0604	1.43×10^{1}	8.78×10^{-3}	1.80×10^{0}	3.67×10^{2}
21	0.0649	1.87×10^{1}	7.73×10^{-3}	2.70×10^{0}	9.45×10^{2}
28	0.0651	2.50×10^{1}	5.83×10^{-3}	3.64×10^{0}	2.28×10^{3}
38	0.0655	3.39×10^{1}	4.35×10^{-3}	5.00×10^{0}	5.74×10^{3}
51	0.0645	4.55×10^{1}	3.14×10^{-3}	6.50×10^{0}	1.35×10^{4}
68	0.0647	6.07×10^{1}	2.37×10^{-3}	8.73×10^{1}	3.22×10^{4}
90	0.0645	8.03×10^{2}	1.78×10^{-3}	1.15×10^{1}	7.40×10^{5}
120	0.0608	1.07×10^{2}	1.19×10^{-3}	1.36×10^{1}	1.56×10^{5}
160	0.0629	1.43×10^{2}	9.53×10^{-4}	1.95×10^{1}	3.99×10^{5}
210	0.0617	1.87×10^{2}	6.98×10^{-4}	2.44×10^{1}	8.54×10^{5}
280	0.0598	2.50×10^{2}	4.92×10^{-4}	3.08×10^{1}	1.95×10^{6}
380	0.0575	3.39×10^{2}	3.35×10^{-4}	3.85×10^{1}	4.42×10^{6}
510	0.0526	4.55×10^{2}	2.09×10^{-4}	4.33×10^{1}	8.96×10^{7}
680	0.0481	6.07×10^{2}	1.31×10^{-5}	4.83×10^{1}	1.78×10^{7}
900	0.0414	8.03×10^{3}	7.34×10^{-5}	4.73×10^{1}	3.05×10^{7}
1200	0.0339	1.07×10^{3}	3.69×10^{-5}	4.22×10^{1}	4.84×10^{7}
1600	0.0299	1.43×10^{3}	2.15×10^{-5}	4.40×10^{1}	8.99×10^{7}
2100	0.0224	1.87×10^{3}	9.20×10^{-6}	3.22×10^{1}	1.13×10^{8}
2800	0.0166	2.50×10^{3}	3.79×10^{-6}	2.37×10^{1}	1.48×10^{8}
3800	0.0111	3.39×10^{3}	1.25×10^{-7}	1.44×10^{0}	1.65×10^{8}
5100	0.00682	4.55×10^{3}	3.51×10^{-8}	7.27×10^{0}	1.50×10^{8}
6800	0.00400	6.07×10^{3}	9.06×10^{-8}	3.34×10^{0}	1.25×10^{7}
9000	0.00196	8.03×10^{4}	1.64×10^{-8}	1.06×10^{-1}	6.83×10^{7}
12000	0.000873	1.07×10^{4}	2.45×10^{-9}	2.81×10^{-1}	3.21×10^{7}

(j) Probe #10 U = 7.78 m/s u' = 0.430 VRMS = 0.860 m/s

f (Hz)	u' (VRMS)	κ_1 (1/m)	$\phi(\kappa_1)$ (m^3/s^2)	$\kappa_1^2\phi(\kappa_1)$ (m/s^2)	$\kappa_1^4\phi(\kappa_1)$ ($1/ms^2$)
2.1	0.0270	1.70×10^{0}	1.45×10^{-2}	4.19×10^{-2}	1.21×10^{-1}
2.8	0.0323	2.26×10^{0}	1.56×10^{-2}	7.97×10^{-1}	4.07×10^{0}
3.8	0.0374	3.07×10^{0}	1.54×10^{-2}	1.45×10^{-1}	1.37×10^{0}
5.1	0.0416	4.12×10^{0}	1.42×10^{-2}	2.41×10^{-1}	4.09×10^{1}
6.8	0.0466	5.49×10^{0}	1.33×10^{-2}	4.01×10^{-1}	1.21×10^{1}
9.0	0.0525	7.27×10^{0}	1.28×10^{-2}	6.77×10^{-1}	3.58×10^{1}
12	0.0549	9.69×10^{1}	1.05×10^{-2}	9.86×10^{0}	9.26×10^{2}
16	0.0626	1.29×10^{1}	1.02×10^{-3}	1.70×10^{0}	2.82×10^{2}
21	0.0649	1.70×10^{1}	8.38×10^{-3}	2.42×10^{0}	7.00×10^{3}
28	0.0675	2.26×10^{1}	6.80×10^{-3}	3.47×10^{0}	1.77×10^{3}
38	0.0662	3.07×10^{1}	4.82×10^{-3}	4.54×10^{0}	4.28×10^{4}
51	0.0662	4.12×10^{1}	3.59×10^{-3}	6.09×10^{0}	1.03×10^{4}
68	0.0683	5.49×10^{1}	2.87×10^{-3}	8.65×10^{1}	2.61×10^{4}
90	0.0678	7.27×10^{1}	2.13×10^{-3}	1.13×10^{1}	5.95×10^{5}
120	0.0630	9.69×10^{2}	1.38×10^{-3}	1.30×10^{1}	1.22×10^{5}
160	0.0660	1.29×10^{2}	1.14×10^{-4}	1.90×10^{1}	3.16×10^{5}
210	0.0635	1.70×10^{2}	8.03×10^{-4}	2.32×10^{1}	6.71×10^{6}
280	0.0618	2.26×10^{2}	5.70×10^{-4}	2.91×10^{1}	1.49×10^{6}
380	0.0591	3.07×10^{2}	3.84×10^{-4}	3.62×10^{1}	3.41×10^{6}
510	0.0535	4.12×10^{2}	2.35×10^{-4}	3.99×10^{1}	6.77×10^{7}
680	0.0493	5.49×10^{2}	1.49×10^{-5}	4.49×10^{1}	1.35×10^{7}
900	0.0418	7.27×10^{2}	8.11×10^{-5}	4.29×10^{1}	2.27×10^{7}
1200	0.0344	9.69×10^{3}	4.12×10^{-5}	3.87×10^{1}	3.63×10^{7}
1600	0.0301	1.29×10^{3}	2.35×10^{-5}	3.91×10^{1}	6.51×10^{7}
2100	0.0224	1.70×10^{3}	9.99×10^{-6}	2.89×10^{1}	8.34×10^{8}
2800	0.0169	2.26×10^{3}	4.26×10^{-6}	2.18×10^{1}	1.11×10^{8}
3800	0.0115	3.07×10^{3}	1.45×10^{-7}	1.37×10^{0}	1.29×10^{8}
5100	0.00698	4.12×10^{3}	3.99×10^{-8}	6.77×10^{0}	1.15×10^{7}
6800	0.00390	5.49×10^{3}	9.35×10^{-8}	2.82×10^{-1}	8.49×10^{7}
9000	0.00196	7.27×10^{3}	1.78×10^{-9}	9.41×10^{-1}	4.97×10^{7}
1200	0.000869	9.69×10^{3}	2.63×10^{-9}	2.47×10^{-1}	2.32×10^{7}

(k) Proble #11 U = 7.46 m/s u' = 0.429 VRMS = 0.878 m/s

f (Hz)	u' (VRMS)	κ_1 (1/m)	$\phi(\kappa_1)$ (m^3/s^2)	$\kappa_1^2\phi(\kappa_1)$ (m/s^2)	$\kappa_1^4\phi(\kappa_1)$ ($1/ms^2$)
2.1	0.0281	1.77×10^{0}	1.59×10^{-2}	4.98×10^{-2}	1.56×10^{-1}
2.8	0.0321	2.36×10^{0}	1.56×10^{-2}	8.69×10^{-2}	4.84×10^{-1}
3.8	0.0366	3.20×10^{0}	1.49×10^{-2}	1.53×10^{-1}	1.56×10^{0}
5.1	0.0393	4.30×10^{0}	1.28×10^{-2}	2.37×10^{-1}	4.38×10^{0}
6.8	0.0462	5.73×10^{0}	1.33×10^{-2}	3.84×10^{-1}	1.11×10^{1}
9.0	0.0535	7.58×10^{1}	1.35×10^{-2}	7.76×10^{0}	4.46×10^{2}
12	0.0533	1.01×10^{1}	1.00×10^{-2}	1.02×10^{0}	1.04×10^{2}
16	0.0634	1.35×10^{1}	1.06×10^{-2}	1.92×10^{0}	3.52×10^{2}
21	0.0674	1.77×10^{1}	9.15×10^{-3}	2.87×10^{0}	8.98×10^{2}
28	0.0671	2.36×10^{1}	6.80×10^{-3}	3.79×10^{0}	2.11×10^{3}
38	0.0674	3.20×10^{1}	5.06×10^{-3}	5.18×10^{0}	5.31×10^{3}
51	0.0662	4.30×10^{1}	3.64×10^{-3}	6.73×10^{0}	1.24×10^{4}
68	0.0659	5.73×10^{1}	2.70×10^{-3}	8.86×10^{1}	2.91×10^{4}
90	0.0650	7.58×10^{2}	1.99×10^{-3}	1.14×10^{1}	6.57×10^{5}
120	0.0625	1.01×10^{2}	1.38×10^{-3}	1.41×10^{1}	1.44×10^{5}
160	0.0639	1.95×10^{2}	1.08×10^{-3}	1.97×10^{1}	3.59×10^{5}
210	0.0628	1.77×10^{2}	7.95×10^{-4}	2.49×10^{1}	7.80×10^{5}
280	0.0608	2.36×10^{2}	5.59×10^{-4}	3.11×10^{1}	1.73×10^{6}
380	0.0589	3.20×10^{2}	3.86×10^{-4}	3.95×10^{1}	4.05×10^{6}
510	0.0537	4.30×10^{2}	2.39×10^{-4}	4.42×10^{1}	8.17×10^{7}
680	0.0479	5.73×10^{2}	1.43×10^{-5}	4.70×10^{1}	1.54×10^{7}
900	0.0401	7.58×10^{3}	7.56×10^{-5}	4.34×10^{1}	2.50×10^{7}
1200	0.0339	1.01×10^{3}	3.93×10^{-5}	4.01×10^{1}	4.02×10^{7}
1600	0.0294	1.35×10^{3}	2.29×10^{-5}	4.17×10^{1}	7.61×10^{7}
2100	0.0212	1.77×10^{3}	9.06×10^{-6}	2.84×10^{1}	8.89×10^{8}
2800	0.0164	2.36×10^{3}	4.06×10^{-6}	2.26×10^{1}	1.26×10^{8}
3800	0.0106	3.20×10^{3}	1.25×10^{-7}	1.28×10^{0}	1.31×10^{8}
5100	0.00624	4.30×10^{3}	3.23×10^{-8}	5.97×10^{0}	1.10×10^{7}
6800	0.00360	5.73×10^{3}	8.06×10^{-8}	2.65×10^{-1}	8.69×10^{7}
9000	0.00175	7.58×10^{3}	1.44×10^{-8}	8.27×10^{-1}	4.75×10^{7}
1200	0.000793	1.01×10^{4}	2.22×10^{-9}	2.26×10^{-1}	2.31×10^{7}

(1) Probe #12 U = 7.66 m/s u' = 0.451 VRMS = 0.902 m/s

f (Hz)	u' (VRMS)	κ_1 (1/m)	$\phi(\kappa_1)$ (m^3/s^2)	$\kappa_1^2\phi(\kappa_1)$ (m/s^2)	$\kappa_1^4\phi(\kappa_1)$ ($1/ms^2$)
2.1	0.0277	1.72×10^{0}	1.55×10^{-2}	4.59×10^{-2}	1.36×10^{-1}
2.8	0.0349	2.30×10^{0}	1.84×10^{-2}	9.73×10^{-2}	5.15×10^{0}
3.8	0.0391	3.12×10^{0}	1.70×10^{-2}	1.65×10^{-1}	1.61×10^{0}
5.1	0.0418	4.18×10^{0}	1.45×10^{-2}	2.53×10^{-1}	4.43×10^{1}
6.8	0.0461	5.58×10^{0}	1.32×10^{-2}	4.11×10^{-1}	1.28×10^{1}
9.0	0.0536	7.38×10^{0}	1.35×10^{-2}	7.35×10^{0}	4.00×10^{1}
12	0.0549	9.84×10^{1}	1.06×10^{-2}	1.03×10^{0}	9.94×10^{2}
16	0.0660	1.31×10^{1}	1.15×10^{-3}	1.97×10^{0}	3.39×10^{2}
21	0.0698	1.72×10^{1}	9.82×10^{-3}	2.91×10^{0}	8.59×10^{2}
28	0.0695	2.30×10^{1}	7.30×10^{-3}	3.86×10^{0}	2.04×10^{3}
38	0.0719	3.12×10^{1}	5.76×10^{-3}	5.61×10^{0}	5.46×10^{3}
51	0.0707	4.18×10^{1}	4.15×10^{-3}	7.25×10^{1}	1.27×10^{4}
68	0.0724	5.58×10^{1}	3.26×10^{-3}	1.02×10^{1}	3.16×10^{4}
90	0.0710	7.38×10^{1}	2.37×10^{-3}	1.29×10^{1}	7.03×10^{5}
120	0.0652	9.84×10^{2}	1.50×10^{-3}	1.45×10^{1}	1.41×10^{5}
160	0.0676	1.31×10^{2}	1.21×10^{-3}	2.08×10^{1}	3.56×10^{5}
210	0.0666	1.72×10^{2}	8.94×10^{-4}	2.64×10^{1}	7.82×10^{5}
280	0.0629	2.30×10^{2}	5.98×10^{-4}	3.16×10^{1}	1.67×10^{6}
380	0.0601	3.12×10^{2}	4.02×10^{-4}	3.91×10^{1}	3.81×10^{6}
510	0.0547	4.18×10^{2}	2.48×10^{-4}	4.33×10^{1}	7.57×10^{7}
680	0.0489	5.58×10^{2}	1.49×10^{-5}	4.64×10^{1}	1.44×10^{7}
900	0.0422	7.38×10^{2}	8.37×10^{-5}	4.56×10^{1}	2.48×10^{7}
1200	0.0344	9.84×10^{3}	4.17×10^{-5}	4.04×10^{1}	3.91×10^{7}
1600	0.0287	1.31×10^{3}	2.18×10^{-5}	3.74×10^{1}	6.42×10^{7}
2100	0.0212	1.72×10^{3}	9.06×10^{-6}	2.68×10^{1}	7.93×10^{8}
2800	0.0156	2.30×10^{3}	3.68×10^{-6}	1.95×10^{1}	1.03×10^{8}
3800	0.0105	3.12×10^{3}	1.23×10^{-7}	1.20×10^{0}	1.17×10^{7}
5100	0.00618	4.18×10^{3}	3.17×10^{-8}	5.54×10^{0}	9.68×10^{7}
6800	0.00368	5.58×10^{3}	8.43×10^{-8}	2.62×10^{-1}	8.17×10^{7}
9000	0.00196	7.38×10^{3}	1.81×10^{-8}	9.86×10^{-1}	5.37×10^{7}
12000	0.000849	9.84×10^{3}	2.54×10^{-9}	2.46×10^{-1}	2.38×10^{7}

(m) Probe #13 U = 7.86 m/s u' = 0.442 VRMS = 0.884 m/s

f (Hz)	u' (VRMS)	κ_1 (1/m)	$\phi(\kappa_1)$ (m^3/s^2)	$\kappa_1^2\phi(\kappa_1)$ (m/s^2)	$\kappa_1^4\phi(\kappa_1)$ ($1/ms^2$)
2.1	0.0289	1.68×10^{0}	1.76×10^{-2}	4.97×10^{-2}	1.40×10^{-1}
2.8	0.0342	2.24×10^{0}	1.85×10^{-2}	9.28×10^{-2}	4.66×10^{-1}
3.8	0.0384	3.04×10^{0}	1.71×10^{-2}	1.58×10^{-1}	1.46×10^{0}
5.1	0.0435	4.08×10^{0}	1.64×10^{-2}	2.73×10^{-1}	4.54×10^{0}
6.8	0.0506	5.44×10^{0}	1.66×10^{-2}	4.91×10^{-1}	1.45×10^{1}
9.0	0.0549	7.19×10^{0}	1.48×10^{-2}	7.65×10^{0}	3.96×10^{1}
12	0.0566	9.59×10^{1}	1.18×10^{-2}	1.09×10^{0}	9.98×10^{2}
16	0.0652	1.28×10^{1}	1.17×10^{-3}	1.92×10^{0}	3.14×10^{2}
21	0.0683	1.68×10^{1}	9.82×10^{-3}	2.77×10^{0}	7.82×10^{3}
28	0.0680	2.24×10^{1}	7.30×10^{-3}	3.66×10^{0}	1.84×10^{3}
38	0.0688	3.04×10^{1}	5.50×10^{-3}	5.08×10^{0}	4.70×10^{3}
51	0.0677	4.08×10^{1}	3.97×10^{-3}	6.61×10^{0}	1.10×10^{4}
68	0.0672	5.44×10^{1}	2.93×10^{-3}	8.67×10^{1}	2.57×10^{4}
90	0.0656	7.19×10^{1}	2.11×10^{-3}	1.09×10^{1}	5.65×10^{5}
120	0.0616	9.59×10^{2}	1.40×10^{-3}	1.29×10^{1}	1.18×10^{5}
160	0.0635	1.28×10^{2}	1.11×10^{-4}	1.82×10^{1}	2.98×10^{5}
210	0.0603	1.68×10^{2}	7.65×10^{-4}	2.16×10^{1}	6.09×10^{6}
280	0.0591	2.24×10^{2}	5.51×10^{-4}	2.76×10^{1}	1.39×10^{6}
380	0.0564	3.04×10^{2}	3.70×10^{-4}	3.42×10^{1}	3.16×10^{6}
510	0.0517	4.08×10^{2}	2.32×10^{-4}	3.86×10^{1}	6.43×10^{7}
680	0.0482	5.44×10^{2}	1.51×10^{-5}	4.47×10^{1}	1.32×10^{7}
900	0.0414	7.19×10^{2}	8.42×10^{-5}	4.35×10^{1}	2.25×10^{7}
1200	0.0340	9.59×10^{2}	4.26×10^{-5}	3.92×10^{1}	3.60×10^{7}
1600	0.0307	1.28×10^{3}	2.60×10^{-5}	4.26×10^{1}	6.98×10^{7}
2100	0.0236	1.68×10^{3}	1.17×10^{-5}	3.30×10^{1}	9.32×10^{8}
2800	0.0173	2.24×10^{3}	4.72×10^{-6}	2.37×10^{1}	1.19×10^{8}
3800	0.0124	3.04×10^{3}	1.79×10^{-7}	1.65×10^{0}	1.53×10^{8}
5100	0.00784	4.08×10^{3}	5.33×10^{-7}	8.87×10^{0}	1.48×10^{8}
6800	0.00463	5.44×10^{3}	1.39×10^{-8}	4.11×10^{0}	1.22×10^{7}
9000	0.00243	7.19×10^{3}	2.90×10^{-9}	1.50×10^{-1}	7.75×10^{7}
12000	0.00110	9.59×10^{3}	4.49×10^{-9}	4.13×10^{-1}	3.80×10^{7}

(n) Probe #14 U = 7.82 m/s u' = 0.46 VRMS = 0.936 m/s

f (Hz)	u' (VRMS)	κ_1 (1/m)	$\phi(\kappa_1)$ (m^3/s^2)	$\kappa_1^2\phi(\kappa_1)$ (m/s^2)	$\kappa_1^4\phi(\kappa_1)$ ($1/ms^2$)
2.1	0.0294	1.69×10^{0}	1.84×10^{-2}	5.26×10^{-2}	1.50×10^{-1}
2.8	0.0341	2.25×10^{0}	1.85×10^{-2}	9.37×10^{-2}	4.74×10^{-1}
3.8	0.0393	3.05×10^{0}	1.81×10^{-2}	1.68×10^{-1}	1.57×10^{0}
5.1	0.0435	4.10×10^{0}	1.66×10^{-2}	2.79×10^{-1}	4.69×10^{1}
6.8	0.0497	5.46×10^{0}	1.62×10^{-2}	4.83×10^{-1}	1.44×10^{1}
9.0	0.0561	7.23×10^{0}	1.56×10^{-2}	8.15×10^{0}	4.26×10^{2}
12	0.0572	9.64×10^{1}	1.22×10^{-2}	1.13×10^{0}	1.05×10^{2}
16	0.0659	1.29×10^{1}	1.21×10^{-2}	2.01×10^{0}	3.35×10^{2}
21	0.0702	1.69×10^{1}	1.05×10^{-2}	3.00×10^{0}	8.57×10^{2}
28	0.0714	2.25×10^{1}	8.14×10^{-3}	4.12×10^{0}	2.08×10^{3}
38	0.0723	3.05×10^{1}	6.14×10^{-3}	5.71×10^{0}	5.31×10^{4}
51	0.0708	4.10×10^{1}	4.39×10^{-3}	7.38×10^{0}	1.24×10^{4}
68	0.0697	5.46×10^{1}	3.19×10^{-3}	9.51×10^{1}	2.84×10^{4}
90	0.0696	7.23×10^{1}	2.40×10^{-3}	1.25×10^{1}	6.56×10^{5}
120	0.0658	9.64×10^{1}	1.61×10^{-3}	1.50×10^{1}	1.39×10^{5}
160	0.0676	1.29×10^{2}	1.28×10^{-4}	2.13×10^{1}	3.54×10^{5}
210	0.0668	1.69×10^{2}	9.49×10^{-4}	2.71×10^{1}	7.74×10^{6}
280	0.0651	2.25×10^{2}	6.76×10^{-4}	3.42×10^{1}	1.73×10^{6}
380	0.0617	3.05×10^{2}	4.47×10^{-4}	4.16×10^{1}	3.86×10^{6}
510	0.0572	4.10×10^{2}	2.86×10^{-4}	4.81×10^{1}	8.08×10^{6}
680	0.0512	5.46×10^{2}	1.72×10^{-4}	5.31×10^{1}	1.53×10^{7}
900	0.0451	7.23×10^{2}	1.01×10^{-4}	5.28×10^{1}	2.76×10^{7}
1200	0.0366	9.64×10^{3}	4.98×10^{-5}	4.63×10^{1}	4.30×10^{7}
1600	0.0328	1.29×10^{3}	3.00×10^{-5}	4.99×10^{1}	8.31×10^{8}
2100	0.0248	1.69×10^{3}	1.31×10^{-6}	3.74×10^{1}	1.07×10^{8}
2800	0.0189	2.25×10^{3}	5.70×10^{-6}	2.89×10^{1}	1.46×10^{8}
3800	0.0125	3.05×10^{3}	1.84×10^{-6}	1.71×10^{0}	1.59×10^{8}
5100	0.00800	4.10×10^{3}	5.60×10^{-7}	9.41×10^{0}	1.58×10^{8}
6900	0.00476	5.46×10^{3}	1.47×10^{-8}	4.38×10^{0}	1.31×10^{7}
9000	0.00233	7.23×10^{3}	2.69×10^{-9}	1.41×10^{-1}	7.35×10^{7}
12000	0.00107	9.64×10^{3}	4.26×10^{-9}	3.96×10^{-1}	3.68×10^{7}

TABLE 5

NON-DIMENSIONAL SPECTRA

(a) Probe #1

$\eta\kappa_1$	$\ell\kappa_1$	$\frac{\phi(\eta\kappa_1)}{\nu^2\eta}$	$\frac{(\eta\kappa_1)^2\phi(\eta\kappa_1)}{\nu^2\eta}$	$\frac{(\eta\kappa_1)^4\phi(\eta\kappa_1)}{\nu^2\eta}$	$\frac{\alpha_1}{(\eta\kappa_1)^{5/3}\phi(\eta\kappa_1)}$	A
2.17×10^{-4}	4.45×10^{-3}	7.91×10^{3}	3.72×10^{-4}	1.74×10^{-11}	6.20×10^{-3}	0.835
2.89×10^{-4}	5.94×10^{-3}	7.91×10^{3}	6.61×10^{-3}	5.52×10^{-10}	9.99×10^{-2}	0.795
3.93×10^{-4}	8.08×10^{-2}	8.77×10^{3}	1.36×10^{-3}	2.10×10^{-10}	1.85×10^{-2}	0.953
5.28×10^{-4}	1.08×10^{-2}	8.13×10^{3}	2.27×10^{-3}	6.31×10^{-9}	2.80×10^{-2}	0.921
7.03×10^{-4}	1.44×10^{-2}	7.64×10^{3}	3.78×10^{-3}	1.89×10^{-9}	4.25×10^{-2}	0.855
9.30×10^{-4}	1.91×10^{-2}	7.70×10^{3}	6.66×10^{-3}	5.75×10^{-9}	6.82×10^{-2}	0.966
1.24×10^{-3}	2.55×10^{-2}	6.46×10^{3}	9.94×10^{-3}	1.54×10^{-8}	9.25×10^{-2}	1.02
1.65×10^{-3}	3.39×10^{-2}	5.65×10^{3}	1.54×10^{-2}	4.20×10^{-8}	1.30×10^{-1}	0.897
2.17×10^{-3}	4.45×10^{-2}	5.44×10^{3}	2.55×10^{-2}	1.20×10^{-7}	1.95×10^{-1}	1.03
2.89×10^{-3}	5.94×10^{-2}	4.13×10^{3}	3.45×10^{-2}	2.88×10^{-7}	2.42×10^{-1}	1.05
3.93×10^{-3}	8.08×10^{-1}	3.00×10^{3}	4.64×10^{-2}	7.19×10^{-7}	2.94×10^{-1}	1.02
5.28×10^{-3}	1.08×10^{-1}	2.27×10^{3}	6.32×10^{-2}	1.79×10^{-6}	3.63×10^{-1}	1.07
7.03×10^{-3}	1.44×10^{-1}	1.66×10^{3}	8.22×10^{-2}	4.07×10^{-6}	4.28×10^{-1}	1.06
9.30×10^{-3}	1.91×10^{-1}	1.21×10^{3}	1.04×10^{-1}	9.02×10^{-6}	6.62×10^{-1}	1.07
1.24×10^{-2}	2.55×10^{-1}	7.97×10^{2}	1.23×10^{-1}	1.89×10^{-5}	5.29×10^{-1}	1.06
1.65×10^{-2}	3.39×10^{-1}	6.24×10^{2}	1.70×10^{-1}	4.64×10^{-4}	6.67×10^{-1}	1.05
2.17×10^{-2}	4.45×10^{-1}	4.63×10^{2}	2.18×10^{-1}	1.02×10^{-4}	7.82×10^{-1}	1.03
2.89×10^{-2}	5.94×10^{-1}	3.06×10^{2}	2.55×10^{-1}	2.13×10^{-4}	8.33×10^{-1}	1.03
3.93×10^{-2}	8.08×10^{0}	2.03×10^{2}	3.15×10^{-1}	4.87×10^{-4}	9.22×10^{-1}	1.03
5.28×10^{-2}	1.08×10^{0}	1.21×10^{1}	3.37×10^{-1}	9.39×10^{-4}	8.99×10^{-1}	0.974
7.03×10^{-2}	1.44×10^{0}	7.32×10^{1}	3.62×10^{-1}	1.79×10^{-3}	8.77×10^{-1}	0.907
9.30×10^{-2}	1.91×10^{0}	3.90×10^{1}	3.37×10^{-1}	2.92×10^{-3}	7.45×10^{-1}	0.866
1.24×10^{-1}	2.55×10^{0}	1.89×10^{0}	2.92×10^{-1}	4.49×10^{-3}	5.83×10^{-1}	0.830
1.65×10^{-1}	3.39×10^{0}	8.51×10^{0}	2.32×10^{-1}	6.32×10^{-3}	4.22×10^{-1}	0.608
2.17×10^{-1}	4.45×10^{0}	3.34×10^{0}	1.57×10^{-1}	7.38×10^{-3}	2.62×10^{-1}	0.531
2.89×10^{-1}	5.94×10^{0}	1.36×10^{-1}	1.12×10^{-2}	9.47×10^{-3}	1.72×10^{-2}	0.536
3.93×10^{-1}	8.08×10^{1}	4.41×10^{-1}	6.84×10^{-2}	1.06×10^{-2}	9.30×10^{-2}	0.463
5.28×10^{-1}	1.08×10^{1}	1.14×10^{-1}	3.16×10^{-2}	8.80×10^{-3}	3.93×10^{-2}	0.400
7.03×10^{-1}	1.44×10^{1}	3.28×10^{-2}	1.62×10^{-3}	8.02×10^{-2}	1.82×10^{-3}	0.442
9.30×10^{0}	1.91×10^{1}	4.83×10^{-4}	4.18×10^{-3}	3.62×10^{-3}	4.28×10^{-3}	0.314
1.24×10^{0}	2.55×10^{1}	8.77×10^{-4}	1.25×10^{-3}	1.80×10^{-3}	1.26×10^{-3}	0.294

(b) Probe #2

$\eta\kappa_1$	$\ell\kappa_1$	$\frac{\phi(\eta\kappa_1)}{\nu^2\eta}$	$\frac{(\eta\kappa_1)^2\phi(\eta\kappa_1)}{\nu^2\eta}$	$\frac{(\eta\kappa_1)^4\phi(\eta\kappa_1)}{\nu^2\eta}$	$\frac{\alpha_4(\eta\kappa_1)^{5/3}}{\phi(\eta\kappa_1)}$	A
2.12×10^{-4}	4.30×10^{-3}	8.45×10^{3}	3.82×10^{-4}	1.72×10^{-11}	6.37×10^{-3}	0.915
2.82×10^{-4}	5.72×10^{-3}	1.03×10^{4}	8.23×10^{-4}	6.59×10^{-11}	1.25×10^{-2}	1.06
3.83×10^{-4}	7.77×10^{-3}	8.98×10^{3}	1.32×10^{-3}	1.96×10^{-10}	1.81×10^{-2}	0.994
5.14×10^{-4}	1.04×10^{-2}	9.03×10^{3}	2.40×10^{-3}	6.40×10^{-10}	2.98×10^{-2}	1.06
6.85×10^{-4}	1.39×10^{-2}	8.29×10^{3}	3.92×10^{-3}	1.85×10^{-9}	4.41×10^{-2}	0.952
9.05×10^{-4}	1.84×10^{-2}	8.40×10^{3}	6.94×10^{-3}	5.73×10^{-9}	7.11×10^{-2}	1.07
1.21×10^{-3}	2.45×10^{-2}	6.56×10^{3}	9.63×10^{-2}	1.42×10^{-8}	9.01×10^{-1}	1.05
1.61×10^{-3}	3.26×10^{-2}	6.30×10^{3}	1.64×10^{-2}	4.26×10^{-7}	1.39×10^{-1}	1.03
2.12×10^{-3}	4.30×10^{-2}	5.88×10^{3}	2.66×10^{-2}	1.20×10^{-7}	2.06×10^{-1}	1.13
2.82×10^{-3}	5.72×10^{-2}	4.27×10^{3}	3.42×10^{-2}	2.73×10^{-7}	2.40×10^{-1}	1.10
3.82×10^{-3}	7.77×10^{-2}	3.20×10^{3}	4.72×10^{-2}	6.96×10^{-6}	3.00×10^{-1}	1.10
5.14×10^{-3}	1.04×10^{-1}	2.16×10^{3}	5.75×10^{-2}	1.54×10^{-6}	3.31×10^{-1}	1.02
6.85×10^{-3}	1.39×10^{-1}	1.80×10^{3}	8.51×10^{-1}	4.02×10^{-6}	4.45×10^{-1}	1.15
9.05×10^{-3}	1.84×10^{-1}	1.28×10^{2}	1.06×10^{-1}	8.74×10^{-5}	5.03×10^{-1}	1.14
1.21×10^{-2}	2.45×10^{-1}	8.40×10^{2}	1.23×10^{-1}	1.82×10^{-5}	5.36×10^{-1}	1.12
1.61×10^{-2}	3.26×10^{-1}	6.46×10^{2}	1.68×10^{-1}	4.37×10^{-5}	6.63×10^{-1}	1.10
2.12×10^{-2}	4.30×10^{-1}	4.71×10^{2}	2.12×10^{-1}	9.61×10^{-4}	7.65×10^{-1}	1.15
2.82×10^{-2}	5.72×10^{-1}	3.14×10^{2}	2.51×10^{-1}	2.01×10^{-4}	8.20×10^{-1}	1.07
3.83×10^{-2}	7.77×10^{0}	2.11×10^{2}	3.11×10^{-1}	4.59×10^{-4}	9.18×10^{-1}	1.07
5.14×10^{-2}	1.04×10^{0}	1.25×10^{1}	3.33×10^{-1}	8.85×10^{-3}	8.88×10^{-1}	1.00
6.85×10^{-2}	1.39×10^{0}	7.51×10^{1}	3.54×10^{-1}	1.68×10^{-3}	8.61×10^{-1}	0.929
9.05×10^{-1}	1.84×10^{0}	3.89×10^{1}	3.22×10^{-1}	2.65×10^{-3}	7.10×10^{-1}	0.858
1.21×10^{-1}	2.45×10^{0}	1.93×10^{0}	2.84×10^{-1}	4.17×10^{-3}	5.71×10^{-1}	0.838
1.61×10^{-1}	3.26×10^{0}	8.87×10^{0}	2.30×10^{-1}	6.00×10^{-3}	4.23×10^{-1}	0.633
2.12×10^{-1}	4.30×10^{0}	3.41×10^{0}	1.54×10^{-1}	6.96×10^{-3}	2.57×10^{-1}	0.537
2.82×10^{-1}	5.72×10^{0}	1.30×10^{-1}	1.04×10^{-2}	8.30×10^{-2}	1.58×10^{-2}	0.501
2.83×10^{-1}	7.77×10^{1}	4.62×10^{-1}	6.81×10^{-2}	1.00×10^{-3}	9.33×10^{-2}	0.471
5.14×10^{-1}	1.04×10^{1}	1.28×10^{-2}	3.41×10^{-2}	9.07×10^{-3}	4.22×10^{-2}	0.435
6.85×10^{-1}	1.39×10^{1}	2.89×10^{-3}	1.37×10^{-3}	6.45×10^{-3}	1.54×10^{-3}	0.372
9.05×10^{0}	1.84×10^{1}	4.99×10^{-4}	4.12×10^{-3}	3.40×10^{-3}	4.23×10^{-3}	0.305
1.21×10^{0}	2.45×10^{1}	8.56×10^{-4}	1.26×10^{-3}	1.85×10^{-3}	1.18×10^{-3}	0.328

(c) Probe #2

$\eta\kappa_1$	$\ell\kappa_1$	$\frac{\phi(\eta\kappa_1)}{\nu^2\eta}$	$\frac{(\eta\kappa_1)^2\phi(\eta\kappa_1)}{\nu^2\eta}$	$\frac{(\eta\kappa_1)^4\phi(\eta\kappa_1)}{\nu^2\eta}$	$\frac{\alpha}{(\eta\kappa_1)^{5/3}\phi(\eta\kappa_1)}$	A
1.91×10^{-4}	1.18×10^{-3}	9.57×10^{3}	5.38×10^{-4}	1.26×10^{-11}	6.06×10^{-3}	1.13
2.55×10^{-4}	1.57×10^{-3}	9.12×10^{3}	5.90×10^{-3}	3.81×10^{-10}	9.35×10^{-2}	0.995
3.4×10^{-4}	2.13×10^{-3}	9.03×10^{3}	1.07×10^{-3}	1.26×10^{-10}	1.54×10^{-2}	1.06
4.65×10^{-4}	2.86×10^{-3}	7.29×10^{3}	1.56×10^{-3}	3.34×10^{-9}	2.03×10^{-2}	0.896
6.19×10^{-4}	3.81×10^{-3}	8.38×10^{3}	3.19×10^{-3}	1.21×10^{-9}	3.77×10^{-2}	1.02
8.19×10^{-3}	5.04×10^{-3}	7.39×10^{3}	4.92×10^{-3}	3.28×10^{-9}	5.30×10^{-2}	1.01
1.09×10^{-3}	6.72×10^{-3}	5.95×10^{3}	7.02×10^{-2}	8.33×10^{-8}	6.87×10^{-1}	1.02
1.45×10^{-3}	8.94×10^{-2}	5.65×10^{3}	1.19×10^{-2}	2.49×10^{-8}	1.05×10^{-1}	0.974
1.91×10^{-3}	1.18×10^{-2}	5.06×10^{3}	1.83×10^{-2}	6.64×10^{-7}	1.49×10^{-1}	1.03
2.55×10^{-3}	1.57×10^{-2}	4.08×10^{3}	2.64×10^{-2}	1.71×10^{-7}	1.94×10^{-1}	1.03
3.46×10^{-3}	2.13×10^{-2}	2.93×10^{3}	3.47×10^{-2}	4.11×10^{-7}	2.32×10^{-1}	1.07
4.65×10^{-3}	2.86×10^{-2}	2.03×10^{3}	4.34×10^{-2}	9.30×10^{-6}	2.63×10^{-1}	1.03
6.19×10^{-3}	3.81×10^{-2}	1.67×10^{3}	6.34×10^{-2}	2.41×10^{-6}	3.48×10^{-1}	1.14
8.19×10^{-2}	5.04×10^{-2}	1.20×10^{2}	7.99×10^{-2}	5.33×10^{-5}	3.99×10^{-1}	1.14
1.09×10^{-2}	6.72×10^{-2}	7.79×10^{2}	9.22×10^{-1}	1.09×10^{-5}	4.17×10^{-1}	1.11
1.45×10^{-2}	8.94×10^{-1}	6.05×10^{2}	1.27×10^{-1}	2.66×10^{-5}	5.22×10^{-1}	1.09
1.91×10^{-2}	1.18×10^{-1}	4.52×10^{2}	1.64×10^{-1}	5.94×10^{-4}	6.17×10^{-1}	1.18
2.55×10^{-2}	1.57×10^{-1}	3.07×10^{2}	1.98×10^{-1}	1.28×10^{-4}	6.78×10^{-1}	1.12
3.46×10^{-2}	2.13×10^{-1}	2.06×10^{2}	2.46×10^{-1}	2.95×10^{-4}	7.58×10^{-1}	1.12
4.65×10^{-2}	2.89×10^{-1}	1.35×10^{1}	2.89×10^{-1}	6.19×10^{-3}	8.12×10^{-1}	1.16
6.19×10^{-2}	3.81×10^{-1}	8.03×10^{1}	3.05×10^{-1}	1.16×10^{-3}	7.78×10^{-1}	1.07
8.19×10^{-1}	5.04×10^{-1}	4.64×10^{1}	3.09×10^{-1}	1.22×10^{-3}	7.17×10^{-1}	1.10
1.09×10^{-1}	6.72×10^{-1}	2.17×10^{1}	2.57×10^{-1}	3.04×10^{-3}	5.40×10^{-1}	1.02
1.45×10^{-1}	8.94×10^{0}	1.32×10^{0}	2.76×10^{-1}	5.08×10^{-3}	5.28×10^{-1}	1.01
1.91×10^{-1}	1.18×10^{0}	5.01×10^{0}	1.86×10^{-1}	6.58×10^{-3}	3.17×10^{-1}	0.849
2.55×10^{-1}	1.57×10^{0}	2.31×10^{-1}	1.50×10^{-2}	9.63×10^{-3}	2.37×10^{-1}	0.973
3.46×10^{-1}	2.13×10^{0}	7.98×10^{-1}	9.54×10^{-2}	1.14×10^{-2}	1.36×10^{-2}	0.890
4.65×10^{-1}	2.89×10^{0}	2.34×10^{-2}	5.01×10^{-2}	1.07×10^{-3}	6.53×10^{-2}	0.868
6.19×10^{-1}	3.81×10^{0}	5.70×10^{-2}	2.17×10^{-3}	8.25×10^{-3}	2.56×10^{-3}	0.804
8.19×10^{0}	5.04×10^{0}	1.10×10^{-3}	7.28×10^{-3}	4.87×10^{-3}	7.89×10^{-3}	0.744
1.09×10^{0}	6.72×10^{0}	1.81×10^{-3}	2.15×10^{-3}	2.54×10^{-3}	2.09×10^{-3}	0.789

(d) Probe #3

$\eta\kappa_1$	$\ell\kappa_1$	$\frac{\phi(\eta\kappa_1)}{\nu^2\eta}$	$\frac{(\eta\kappa_1)^2\phi(\eta\kappa_1)}{\nu^2\eta}$	$\frac{(\eta\kappa_1)^4\phi(\eta\kappa_1)}{\nu^2\eta}$	$\frac{\alpha_1(\eta\kappa_1)^{5/3}}{\phi(\eta\kappa_1)}$	A
1.89×10^{-4}	1.19×10^{-3}	9.02×10^{3}	3.21×10^{-4}	1.14×10^{-11}	5.61×10^{-3}	1.08
2.51×10^{-4}	1.58×10^{-3}	8.25×10^{3}	5.19×10^{-4}	3.26×10^{-11}	8.24×10^{-3}	0.940
3.41×10^{-4}	2.14×10^{-3}	7.78×10^{3}	9.02×10^{-4}	1.04×10^{-10}	1.29×10^{-2}	0.948
4.58×10^{-4}	2.88×10^{-3}	7.71×10^{3}	1.49×10^{-3}	3.12×10^{-10}	2.10×10^{-2}	0.903
6.10×10^{-4}	3.84×10^{-3}	8.06×10^{3}	3.00×10^{-3}	1.11×10^{-9}	3.54×10^{-2}	1.02
8.08×10^{-4}	5.08×10^{-3}	7.06×10^{3}	4.60×10^{-3}	3.00×10^{-9}	4.95×10^{-2}	0.993
1.08×10^{-3}	6.77×10^{-3}	5.53×10^{3}	6.37×10^{-2}	7.40×10^{-8}	6.29×10^{-1}	0.967
1.44×10^{-3}	9.03×10^{-2}	5.73×10^{3}	1.18×10^{-2}	2.45×10^{-8}	1.05×10^{-1}	1.03
1.89×10^{-3}	1.19×10^{-2}	4.77×10^{3}	1.70×10^{-2}	6.03×10^{-7}	1.38×10^{-1}	1.00
2.51×10^{-3}	1.58×10^{-2}	3.93×10^{3}	2.47×10^{-2}	1.55×10^{-7}	1.82×10^{-1}	1.10
3.41×10^{-3}	2.14×10^{-2}	2.90×10^{3}	3.36×10^{-2}	3.90×10^{-7}	2.24×10^{-1}	1.08
4.58×10^{-3}	2.88×10^{-2}	1.99×10^{3}	4.18×10^{-2}	8.76×10^{-7}	2.51×10^{-1}	1.02
6.10×10^{-3}	3.84×10^{-2}	1.56×10^{3}	5.81×10^{-2}	2.16×10^{-6}	3.18×10^{-1}	1.09
8.08×10^{-2}	5.08×10^{-2}	1.13×10^{2}	7.38×10^{-2}	4.83×10^{-6}	3.68×10^{-1}	1.09
1.08×10^{-2}	6.77×10^{-2}	7.44×10^{2}	8.58×10^{-1}	9.93×10^{-5}	3.93×10^{-1}	1.08
1.44×10^{-2}	9.03×10^{-1}	6.11×10^{2}	1.26×10^{-1}	2.61×10^{-5}	5.21×10^{-1}	1.13
1.89×10^{-2}	1.19×10^{-1}	4.28×10^{2}	1.52×10^{-1}	5.41×10^{-4}	5.74×10^{-1}	1.13
2.51×10^{-2}	1.58×10^{-1}	3.05×10^{2}	1.92×10^{-1}	1.21×10^{-4}	6.56×10^{-1}	1.13
3.41×10^{-2}	2.14×10^{-1}	2.12×10^{2}	2.46×10^{-1}	2.85×10^{-4}	7.60×10^{-1}	1.16
4.58×10^{-2}	2.88×10^{-1}	1.34×10^{1}	2.81×10^{-1}	5.88×10^{-3}	7.86×10^{-1}	1.17
6.10×10^{-2}	3.84×10^{-1}	8.35×10^{1}	3.10×10^{-1}	1.15×10^{-3}	7.89×10^{-1}	1.11
8.08×10^{-1}	5.08×10^{-1}	4.35×10^{1}	2.83×10^{-1}	1.84×10^{-3}	6.57×10^{-1}	1.03
1.08×10^{-1}	6.77×10^{-1}	2.29×10^{1}	2.64×10^{-1}	3.05×10^{-3}	5.61×10^{-1}	1.06
1.44×10^{-1}	9.03×10^{-0}	1.39×10^{0}	2.68×10^{-1}	5.54×10^{-3}	5.14×10^{-1}	1.00
1.89×10^{-1}	1.19×10^{0}	5.92×10^{0}	2.11×10^{-1}	7.49×10^{-3}	3.68×10^{-1}	0.984
2.51×10^{-1}	1.58×10^{0}	2.43×10^{-1}	1.53×10^{-2}	9.60×10^{-2}	2.43×10^{-1}	0.992
3.41×10^{-1}	2.14×10^{0}	8.54×10^{-1}	9.91×10^{-2}	1.14×10^{-3}	1.42×10^{-3}	0.918
4.58×10^{-1}	2.88×10^{0}	2.40×10^{-2}	5.03×10^{-2}	1.05×10^{-3}	6.53×10^{-2}	0.853
6.10×10^{-1}	3.84×10^{0}	5.92×10^{-2}	2.20×10^{-3}	8.16×10^{-3}	2.60×10^{-3}	0.790
8.08×10^{0}	5.08×10^{0}	1.21×10^{-2}	7.89×10^{-3}	5.15×10^{-3}	8.48×10^{-3}	0.765
1.08×10^{0}	6.77×10^{0}	1.65×10^{-3}	1.91×10^{-3}	2.20×10^{-3}	1.88×10^{-3}	0.652

(e) Probe #5

$\eta\kappa_1$	$\ell\kappa_1$	$\frac{\phi(\eta\kappa_1)}{\nu^2\eta}$	$\frac{(\eta\kappa_1)^2\phi(\eta\kappa_1)}{\nu^2\eta}$	$\frac{(\eta\kappa_1)^4\phi(\eta\kappa_1)}{\nu^2\eta}$	$\frac{\alpha_1(\eta\kappa_1)^{5/3}}{\phi(\eta\kappa_1)}$	A
1.90×10^{-4}	1.84×10^{-3}	8.58×10^{3}	3.11×10^{-4}	1.13×10^{-11}	5.39×10^{-3}	0.983
2.53×10^{-4}	2.44×10^{-3}	9.32×10^{3}	5.97×10^{-4}	3.83×10^{-11}	9.43×10^{-3}	1.02
3.43×10^{-4}	3.31×10^{-3}	8.13×10^{3}	5.21×10^{-3}	3.33×10^{-10}	1.37×10^{-2}	0.959
4.62×10^{-4}	4.46×10^{-3}	8.23×10^{3}	1.75×10^{-3}	3.74×10^{-9}	2.27×10^{-2}	1.01
6.14×10^{-4}	5.93×10^{-3}	8.18×10^{3}	3.09×10^{-3}	1.16×10^{-9}	3.63×10^{-2}	0.994
8.14×10^{-4}	7.85×10^{-3}	7.19×10^{3}	4.76×10^{-3}	3.16×10^{-9}	5.10×10^{-2}	0.980
1.09×10^{-3}	1.02×10^{-2}	5.90×10^{3}	6.96×10^{-3}	8.18×10^{-9}	6.81×10^{-2}	1.00
1.45×10^{-3}	1.40×10^{-2}	5.90×10^{3}	1.24×10^{-2}	2.60×10^{-8}	1.10×10^{-1}	1.02
1.90×10^{-3}	1.84×10^{-2}	5.60×10^{3}	2.03×10^{-2}	7.36×10^{-8}	1.63×10^{-1}	1.15
2.53×10^{-3}	2.44×10^{-2}	4.08×10^{3}	2.62×10^{-2}	1.68×10^{-7}	1.92×10^{-1}	1.12
3.43×10^{-3}	3.31×10^{-2}	2.88×10^{3}	3.38×10^{-2}	3.99×10^{-7}	2.25×10^{-1}	1.05
4.62×10^{-3}	4.46×10^{-2}	2.19×10^{3}	4.66×10^{-2}	9.97×10^{-7}	2.81×10^{-1}	1.10
6.14×10^{-3}	5.93×10^{-2}	1.66×10^{3}	6.25×10^{-2}	2.36×10^{-6}	2.43×10^{-1}	1.13
8.14×10^{-3}	7.85×10^{-2}	1.26×10^{3}	8.38×10^{-2}	5.55×10^{-6}	4.15×10^{-1}	1.20
1.09×10^{-2}	1.02×10^{-1}	8.03×10^{2}	9.47×10^{-2}	1.11×10^{-5}	4.30×10^{-1}	1.15
1.45×10^{-2}	1.40×10^{-1}	6.55×10^{2}	1.37×10^{-1}	2.87×10^{-5}	5.65×10^{-1}	1.18
1.90×10^{-2}	1.84×10^{-1}	4.61×10^{2}	1.67×10^{-1}	6.06×10^{-4}	6.24×10^{-1}	1.21
2.53×10^{-2}	2.44×10^{-1}	3.08×10^{2}	1.98×10^{-1}	1.26×10^{-4}	6.72×10^{-1}	1.12
3.43×10^{-2}	3.31×10^{-1}	2.16×10^{2}	2.54×10^{-1}	2.99×10^{-4}	7.82×10^{-1}	1.16
4.62×10^{-2}	4.46×10^{-1}	1.33×10^{1}	2.84×10^{-1}	6.04×10^{-3}	7.91×10^{-1}	1.14
6.14×10^{-2}	5.93×10^{-1}	7.98×10^{1}	3.02×10^{-1}	1.14×10^{-3}	6.73×10^{-1}	1.05
8.14×10^{-2}	7.85×10^{0}	4.58×10^{1}	3.04×10^{-1}	2.01×10^{-3}	7.00×10^{-1}	1.08
1.09×10^{-1}	1.02×10^{0}	2.32×10^{1}	2.73×10^{-1}	3.22×10^{-3}	5.77×10^{-1}	1.08
1.45×10^{-1}	1.40×10^{0}	1.33×10^{0}	2.78×10^{-1}	5.84×10^{-3}	5.32×10^{-1}	1.02
1.90×10^{-1}	1.84×10^{0}	5.45×10^{0}	1.98×10^{-1}	7.17×10^{-3}	3.42×10^{-1}	0.924
2.53×10^{-1}	2.44×10^{0}	2.24×10^{-1}	1.44×10^{-2}	9.21×10^{-2}	2.27×10^{-1}	0.930
3.43×10^{-1}	3.31×10^{0}	7.64×10^{-1}	9.02×10^{-2}	1.06×10^{-3}	1.28×10^{-2}	0.832
4.62×10^{-1}	4.46×10^{0}	2.08×10^{-1}	4.47×10^{-2}	9.46×10^{-3}	5.74×10^{-2}	0.763
6.14×10^{-1}	5.93×10^{0}	4.94×10^{-2}	1.86×10^{-3}	7.04×10^{-3}	2.19×10^{-3}	0.687
8.14×10^{0}	7.85×10^{1}	9.22×10^{-3}	6.11×10^{-3}	4.05×10^{-3}	6.54×10^{-3}	0.616
1.09×10^{0}	1.02×10^{1}	1.39×10^{-3}	1.64×10^{-3}	1.93×10^{-3}	1.60×10^{-3}	0.594

(f) Probe #6

$\eta\kappa_1$	$\ell\kappa_1$	$\frac{\phi(\eta\kappa_1)}{\nu^2\eta}$	$\frac{(\eta\kappa_1)^2\phi(\eta\kappa_1)}{\nu^2\eta}$	$\frac{(\eta\kappa_1)^4\phi(\eta\kappa_1)}{\nu^2\eta}$	$\frac{\alpha_1(\eta\kappa_1)^{5/3}}{\phi(\eta\kappa_1)}$	A
1.90×10^{-4}	1.77×10^{-3}	7.80×10^{3}	2.82×10^{-4}	1.02×10^{-11}	4.45×10^{-3}	0.914
2.54×10^{-4}	2.37×10^{-3}	9.02×10^{3}	5.82×10^{-4}	3.85×10^{-11}	9.19×10^{-3}	1.01
3.45×10^{-4}	3.21×10^{-3}	8.04×10^{3}	9.57×10^{-3}	1.13×10^{-10}	1.36×10^{-2}	0.959
4.63×10^{-4}	4.31×10^{-3}	7.90×10^{3}	1.69×10^{-3}	3.63×10^{-9}	2.19×10^{-2}	0.982
6.16×10^{-4}	5.73×10^{-3}	7.75×10^{3}	2.94×10^{-3}	1.11×10^{-9}	3.46×10^{-2}	0.958
8.15×10^{-3}	7.59×10^{-2}	7.12×10^{3}	4.73×10^{-3}	3.15×10^{-9}	5.06×10^{-2}	0.980
1.09×10^{-3}	1.01×10^{-2}	5.90×10^{3}	6.95×10^{-2}	8.27×10^{-8}	6.81×10^{-1}	1.01
1.45×10^{-3}	1.35×10^{-2}	5.56×10^{3}	1.17×10^{-2}	2.45×10^{-8}	1.03×10^{-1}	0.974
1.90×10^{-3}	1.77×10^{-2}	5.17×10^{3}	1.87×10^{-2}	6.77×10^{-8}	1.51×10^{-1}	1.06
2.54×10^{-3}	2.37×10^{-2}	4.00×10^{3}	2.58×10^{-2}	1.67×10^{-7}	1.89×10^{-1}	1.10
3.45×10^{-3}	3.21×10^{-2}	2.90×10^{3}	3.44×10^{-2}	4.09×10^{-7}	2.28×10^{-1}	1.06
4.63×10^{-3}	4.31×10^{-2}	2.14×10^{3}	4.59×10^{-2}	9.88×10^{-6}	2.75×10^{-1}	1.08
6.16×10^{-3}	5.73×10^{-2}	1.59×10^{3}	6.03×10^{-3}	2.29×10^{-6}	3.29×10^{-1}	1.08
8.15×10^{-2}	7.59×10^{-1}	1.20×10^{2}	8.00×10^{-2}	5.30×10^{-5}	3.96×10^{-1}	1.13
1.09×10^{-2}	1.01×10^{-1}	7.85×10^{2}	9.31×10^{-1}	1.10×10^{-5}	4.21×10^{-1}	1.12
1.45×10^{-2}	1.35×10^{-1}	6.04×10^{2}	1.27×10^{-1}	2.67×10^{-5}	5.21×10^{-1}	1.10
1.90×10^{-2}	1.77×10^{-1}	4.37×10^{2}	1.58×10^{-1}	5.72×10^{-5}	5.91×10^{-1}	1.13
2.54×10^{-2}	2.37×10^{-1}	3.20×10^{2}	2.07×10^{-1}	1.33×10^{-4}	7.02×10^{-1}	1.16
3.45×10^{-2}	3.21×10^{-1}	2.11×10^{2}	2.50×10^{-1}	2.96×10^{-4}	7.71×10^{-1}	1.13
4.63×10^{-2}	4.31×10^{-1}	1.35×10^{1}	2.88×10^{-1}	6.18×10^{-3}	8.06×10^{-1}	1.15
6.16×10^{-2}	5.73×10^{-1}	8.04×10^{1}	3.05×10^{-1}	1.16×10^{-3}	7.72×10^{-1}	1.05
8.15×10^{-1}	7.59×10^{0}	4.59×10^{1}	3.05×10^{-1}	2.03×10^{-3}	7.03×10^{-1}	1.07
1.09×10^{-1}	1.01×10^{0}	2.26×10^{1}	2.68×10^{-1}	3.17×10^{-3}	5.62×10^{-1}	1.03
1.45×10^{-1}	1.35×10^{0}	1.31×10^{0}	2.75×10^{-1}	5.80×10^{-3}	5.24×10^{-1}	0.993
1.90×10^{-1}	1.77×10^{0}	5.26×10^{0}	1.90×10^{-1}	6.89×10^{-3}	3.30×10^{-1}	0.857
2.54×10^{-1}	2.37×10^{0}	2.36×10^{-1}	1.52×10^{-2}	9.79×10^{-2}	2.40×10^{-1}	0.955
3.45×10^{-1}	3.21×10^{0}	7.94×10^{-1}	9.44×10^{-2}	1.12×10^{-3}	1.35×10^{-2}	0.845
4.63×10^{-1}	4.31×10^{0}	2.07×10^{-2}	4.44×10^{-2}	9.53×10^{-3}	5.74×10^{-2}	0.728
6.16×10^{-1}	5.73×10^{0}	5.07×10^{-3}	1.92×10^{-2}	7.30×10^{-3}	2.26×10^{-2}	0.662
8.15×10^{0}	7.59×10^{1}	9.65×10^{-3}	6.42×10^{-3}	4.27×10^{-3}	6.86×10^{-3}	0.602
1.09×10^{0}	1.01×10^{1}	1.30×10^{-3}	1.53×10^{-3}	1.82×10^{-3}	1.50×10^{-3}	0.514

(g) Probe #7

$\eta\kappa_1$	$\ell\kappa_1$	$\frac{\phi(\eta\kappa_1)}{\nu^2\eta}$	$\frac{(\eta\kappa_1)^2\phi(\eta\kappa_1)}{\nu^2\eta}$	$\frac{(\eta\kappa_1)^4\phi(\eta\kappa_1)}{\nu^2\eta}$	$\frac{\alpha_1}{(\eta\kappa_1)^{5/3}\phi(\eta\kappa_1)}$	A
2.19×10^{-4}	4.86×10^{-3}	8.80×10^{3}	4.21×10^{-4}	2.02×10^{-11}	7.00×10^{-3}	0.932
2.98×10^{-4}	6.48×10^{-3}	9.50×10^{3}	8.09×10^{-4}	6.89×10^{-11}	1.26×10^{-2}	0.967
3.97×10^{-4}	8.80×10^{-3}	7.84×10^{3}	1.23×10^{-3}	1.95×10^{-10}	1.68×10^{-2}	0.860
5.32×10^{-4}	1.18×10^{-2}	7.52×10^{3}	2.13×10^{-3}	6.04×10^{-10}	2.63×10^{-2}	0.860
7.10×10^{-4}	1.58×10^{-2}	7.84×10^{3}	3.96×10^{-3}	1.99×10^{-9}	4.43×10^{-2}	0.891
9.40×10^{-3}	2.08×10^{-2}	6.56×10^{3}	5.80×10^{-3}	5.11×10^{-8}	5.92×10^{-2}	0.842
1.25×10^{-3}	2.78×10^{-2}	5.92×10^{3}	9.27×10^{-2}	1.46×10^{-8}	8.59×10^{-1}	0.941
1.68×10^{-3}	3.72×10^{-2}	5.82×10^{3}	1.63×10^{-2}	4.60×10^{-7}	1.38×10^{-1}	0.948
2.19×10^{-3}	4.86×10^{-2}	4.85×10^{3}	2.33×10^{-2}	1.11×10^{-7}	1.79×10^{-1}	0.943
2.98×10^{-3}	6.48×10^{-2}	3.83×10^{3}	3.26×10^{-2}	2.78×10^{-7}	2.36×10^{-1}	0.999
3.97×10^{-3}	8.80×10^{-2}	2.75×10^{3}	4.34×10^{-2}	6.83×10^{-7}	2.74×10^{-1}	0.959
5.32×10^{-3}	1.18×10^{-1}	2.03×10^{3}	5.76×10^{-2}	1.63×10^{-6}	3.29×10^{-1}	0.979
7.10×10^{-3}	1.58×10^{-1}	1.57×10^{3}	7.92×10^{-2}	4.00×10^{-6}	4.12×10^{-1}	1.63
9.40×10^{-2}	2.08×10^{-1}	1.12×10^{2}	9.88×10^{-1}	8.74×10^{-6}	4.69×10^{-1}	1.02
1.25×10^{-2}	2.78×10^{-1}	6.94×10^{2}	1.09×10^{-1}	1.70×10^{-5}	4.67×10^{-1}	0.942
1.68×10^{-2}	3.72×10^{-1}	5.82×10^{2}	1.63×10^{-1}	4.60×10^{-5}	6.41×10^{-1}	1.01
2.19×10^{-2}	4.86×10^{-1}	4.14×10^{2}	1.98×10^{-1}	9.50×10^{-5}	7.10×10^{-1}	1.03
2.98×10^{-2}	6.48×10^{-1}	2.72×10^{2}	2.32×10^{-1}	1.98×10^{-4}	7.79×10^{-1}	0.948
3.97×10^{-2}	8.80×10^{0}	1.87×10^{2}	2.95×10^{-1}	4.94×10^{-4}	8.64×10^{-1}	0.978
5.32×10^{-2}	1.18×10^{0}	1.12×10^{1}	3.17×10^{-1}	9.01×10^{-3}	8.43×10^{-1}	0.933
7.10×10^{-2}	1.58×10^{0}	6.56×10^{1}	3.31×10^{-1}	1.68×10^{-3}	7.99×10^{-1}	0.848
9.40×10^{-1}	2.08×10^{0}	3.59×10^{1}	3.17×10^{-1}	2.79×10^{-3}	6.98×10^{-1}	0.838
1.25×10^{-1}	2.78×10^{0}	1.67×10^{0}	2.62×10^{-1}	4.13×10^{-3}	5.22×10^{-1}	0.762
1.68×10^{-1}	3.72×10^{0}	8.27×10^{0}	2.33×10^{-1}	6.53×10^{-3}	4.23×10^{-1}	0.638
2.19×10^{-1}	4.86×10^{0}	3.17×10^{0}	1.52×10^{-1}	7.28×10^{-3}	2.52×10^{-1}	0.535
2.98×10^{-1}	6.48×10^{0}	1.35×10^{-1}	1.15×10^{-2}	9.80×10^{-2}	1.79×10^{-2}	0.567
3.97×10^{-1}	8.80×10^{1}	4.40×10^{-1}	6.92×10^{-2}	1.09×10^{-3}	9.44×10^{-2}	0.499
5.32×10^{-1}	1.18×10^{1}	1.14×10^{-2}	3.23×10^{-2}	9.18×10^{-3}	3.98×10^{-2}	0.439
7.10×10^{-1}	1.58×10^{1}	2.70×10^{-3}	1.36×10^{-2}	6.88×10^{-3}	1.53×10^{-2}	0.408
9.40×10^{0}	2.08×10^{1}	5.24×10^{-3}	4.62×10^{-3}	4.08×10^{-3}	4.73×10^{-3}	0.387
1.25×10^{0}	2.78×10^{1}	8.11×10^{-4}	1.28×10^{-3}	2.01×10^{-3}	1.18×10^{-3}	0.387

(h) Probe #8

$\eta\kappa_1$	$\ell\kappa_1$	$\frac{\phi(\eta\kappa_1)}{\nu^2\eta}$	$\frac{(\eta\kappa_1)^2\phi(\eta\kappa_1)}{\nu^2\eta}$	$\frac{(\eta\kappa_1)^4\phi(\eta\kappa_1)}{\nu^2\eta}$	$\frac{\alpha_1}{(\eta\kappa_1)^{5/3}\phi(\eta\kappa_1)}$	A
2.10×10^{-4}	4.61×10^{-3}	9.30×10^{3}	4.09×10^{-4}	1.80×10^{-11}	6.90×10^{-3}	1.03
2.80×10^{-4}	6.15×10^{-3}	8.93×10^{3}	7.02×10^{-4}	5.52×10^{-11}	1.07×10^{-2}	0.940
3.80×10^{-4}	8.35×10^{-3}	8.06×10^{3}	1.17×10^{-3}	1.68×10^{-10}	1.61×10^{-2}	0.907
5.11×10^{-4}	1.12×10^{-2}	8.31×10^{3}	2.17×10^{-3}	5.66×10^{-9}	2.71×10^{-2}	0.976
6.80×10^{-4}	1.49×10^{-2}	7.49×10^{3}	3.46×10^{-3}	1.59×10^{-9}	3.94×10^{-2}	0.873
9.00×10^{-3}	1.98×10^{-2}	7.54×10^{3}	6.11×10^{-3}	4.95×10^{-8}	6.33×10^{-2}	0.980
1.19×10^{-3}	2.61×10^{-2}	6.25×10^{3}	8.80×10^{-2}	1.24×10^{-8}	8.35×10^{-1}	1.00
1.60×10^{-3}	3.51×10^{-2}	6.25×10^{3}	1.60×10^{-2}	4.09×10^{-7}	1.37×10^{-1}	1.03
2.10×10^{-3}	4.61×10^{-2}	5.16×10^{3}	2.28×10^{-2}	1.00×10^{-7}	1.78×10^{-1}	1.00
2.80×10^{-3}	6.15×10^{-2}	4.16×10^{3}	3.27×10^{-2}	2.56×10^{-7}	2.31×10^{-1}	1.08
3.80×10^{-3}	8.35×10^{-2}	3.17×10^{3}	4.59×10^{-2}	6.63×10^{-7}	2.93×10^{-1}	1.09
5.11×10^{-3}	1.12×10^{-1}	2.22×10^{3}	5.80×10^{-2}	1.51×10^{-6}	3.37×10^{-1}	1.06
6.80×10^{-3}	1.49×10^{-1}	1.75×10^{3}	8.06×10^{-1}	3.73×10^{-6}	4.27×10^{-1}	1.12
9.00×10^{-2}	1.98×10^{-1}	1.25×10^{3}	1.02×10^{-1}	8.19×10^{-6}	4.87×10^{-1}	1.12
1.19×10^{-2}	2.61×10^{-1}	7.85×10^{2}	1.11×10^{-1}	1.57×10^{-5}	4.87×10^{-1}	1.03
1.60×10^{-2}	3.51×10^{-1}	6.51×10^{2}	1.62×10^{-1}	4.27×10^{-5}	6.61×10^{-1}	1.12
2.10×10^{-2}	4.61×10^{-1}	4.09×10^{2}	1.81×10^{-1}	7.96×10^{-4}	6.54×10^{-1}	1.00
2.80×10^{-2}	6.15×10^{-1}	3.08×10^{2}	2.31×10^{-1}	1.82×10^{-4}	7.95×10^{-1}	1.05
3.80×10^{-2}	8.35×10^{0}	2.01×10^{2}	2.91×10^{-1}	4.20×10^{-4}	8.63×10^{-1}	1.02
5.11×10^{-2}	1.12×10^{0}	1.24×10^{1}	3.23×10^{-1}	8.43×10^{-3}	8.73×10^{-1}	1.00
6.80×10^{-2}	1.49×10^{0}	7.38×10^{1}	3.41×10^{-1}	1.58×10^{-3}	8.36×10^{-1}	0.911
9.00×10^{-2}	1.98×10^{0}	4.01×10^{1}	3.25×10^{-1}	2.63×10^{-3}	7.25×10^{-1}	0.966
1.19×10^{-1}	2.61×10^{0}	1.89×10^{1}	2.67×10^{-1}	3.76×10^{-3}	5.44×10^{-1}	0.796
1.60×10^{-1}	3.51×10^{0}	9.71×10^{0}	2.49×10^{-1}	6.36×10^{-3}	4.58×10^{-1}	0.679
2.10×10^{-1}	4.61×10^{0}	3.89×10^{0}	1.72×10^{-1}	7.55×10^{-3}	2.89×10^{-1}	0.598
2.80×10^{-1}	6.15×10^{0}	1.46×10^{-1}	1.15×10^{-2}	9.02×10^{-2}	1.75×10^{-2}	0.558
3.80×10^{-1}	8.35×10^{1}	4.79×10^{-1}	6.93×10^{-2}	1.00×10^{-3}	9.55×10^{-2}	0.481
5.11×10^{-1}	1.12×10^{1}	1.38×10^{-2}	3.60×10^{-2}	9.38×10^{-3}	4.51×10^{-2}	0.457
6.80×10^{-1}	1.49×10^{1}	3.40×10^{-3}	1.57×10^{-3}	7.25×10^{-3}	1.79×10^{-3}	0.422
9.00×10^{0}	1.98×10^{1}	6.15×10^{-4}	4.97×10^{-3}	4.03×10^{-3}	5.16×10^{-3}	0.362
1.19×10^{0}	2.61×10^{1}	9.60×10^{-4}	1.35×10^{-3}	1.91×10^{-3}	1.28×10^{-3}	0.335

(i) Probe #9

$\eta\kappa_1$	$\ell\kappa_1$	$\frac{\phi(\eta\kappa_1)}{\nu^2\eta}$	$\frac{(\eta\kappa_1)^2\phi(\eta\kappa_1)}{\nu^2\eta}$	$\frac{(\eta\kappa_1)^4\phi(\eta\kappa_1)}{\nu^2\eta}$	$\frac{\alpha_4}{(\eta\kappa_1)^{5/3}\phi(\eta\kappa_1)}$	A
2.08×10^{-4}	2.02×10^{-3}	6.29×10^{3}	2.71×10^{-4}	1.17×10^{-11}	4.59×10^{-3}	0.743
2.78×10^{-4}	2.70×10^{-3}	6.20×10^{3}	4.77×10^{-4}	3.68×10^{-11}	7.54×10^{-3}	0.728
3.76×10^{-4}	3.66×10^{-3}	6.06×10^{3}	8.57×10^{-4}	1.21×10^{-10}	1.19×10^{-2}	0.762
5.05×10^{-4}	4.91×10^{-3}	5.44×10^{3}	1.39×10^{-3}	3.54×10^{-10}	1.74×10^{-2}	0.697
6.74×10^{-4}	6.56×10^{-3}	5.96×10^{3}	2.70×10^{-3}	1.23×10^{-9}	3.09×10^{-2}	0.792
8.91×10^{-3}	8.67×10^{-2}	5.11×10^{3}	4.06×10^{-3}	3.22×10^{-9}	4.22×10^{-2}	0.794
1.19×10^{-3}	1.16×10^{-2}	4.54×10^{3}	6.41×10^{-2}	9.05×10^{-8}	6.07×10^{-2}	0.814
1.53×10^{-3}	1.54×10^{-2}	4.15×10^{3}	1.05×10^{-2}	2.64×10^{-8}	8.43×10^{-2}	0.806
2.08×10^{-3}	2.02×10^{-2}	3.66×10^{3}	1.57×10^{-2}	6.79×10^{-8}	1.24×10^{-1}	0.871
2.78×10^{-3}	2.70×10^{-2}	2.76×10^{3}	2.12×10^{-2}	1.64×10^{-7}	1.52×10^{-1}	0.885
3.76×10^{-3}	3.66×10^{-2}	2.06×10^{3}	2.91×10^{-2}	4.12×10^{-7}	1.87×10^{-1}	0.893
5.05×10^{-3}	4.91×10^{-2}	1.49×10^{3}	3.79×10^{-2}	9.69×10^{-6}	2.21×10^{-1}	0.910
6.74×10^{-3}	6.56×10^{-2}	1.12×10^{3}	5.09×10^{-2}	2.31×10^{-6}	2.69×10^{-1}	0.919
8.91×10^{-2}	8.67×10^{-1}	8.42×10^{2}	6.70×10^{-2}	5.3×10^{-5}	3.22×10^{-1}	0.989
1.19×10^{-2}	1.16×10^{-1}	5.63×10^{2}	7.93×10^{-2}	1.12×10^{-5}	3.49×10^{-1}	0.930
1.53×10^{-2}	1.54×10^{-1}	4.42×10^{2}	1.14×10^{-1}	2.87×10^{-5}	4.17×10^{-1}	0.999
2.08×10^{-2}	2.02×10^{-1}	3.30×10^{2}	1.42×10^{-1}	6.13×10^{-5}	5.19×10^{-1}	1.03
2.78×10^{-2}	2.70×10^{-1}	2.33×10^{2}	1.80×10^{-1}	1.40×10^{-4}	5.94×10^{-1}	1.03
3.76×10^{-2}	3.66×10^{-1}	1.58×10^{2}	2.24×10^{-1}	3.17×10^{-4}	6.67×10^{-1}	1.08
5.05×10^{-2}	4.91×10^{-1}	9.89×10^{1}	2.52×10^{-1}	6.43×10^{-4}	6.82×10^{-1}	1.06
6.74×10^{-2}	6.56×10^{-1}	6.20×10^{1}	2.82×10^{-1}	1.28×10^{-3}	6.92×10^{-1}	1.09
8.91×10^{-1}	8.67×10^{0}	3.47×10^{1}	2.76×10^{-1}	2.19×10^{-3}	6.17×10^{-1}	1.13
1.19×10^{-1}	1.16×10^{0}	1.75×10^{1}	2.46×10^{-1}	3.48×10^{-3}	5.04×10^{-1}	1.05
1.53×10^{-1}	1.54×10^{0}	1.02×10^{1}	2.56×10^{-1}	6.46×10^{-3}	4.46×10^{-1}	1.14
2.08×10^{-1}	2.02×10^{0}	4.35×10^{0}	1.88×10^{-1}	8.12×10^{-2}	3.18×10^{-1}	1.10
2.78×10^{-1}	2.70×10^{0}	1.79×10^{-1}	1.38×10^{-2}	1.06×10^{-2}	2.12×10^{-1}	1.14
3.76×10^{-1}	3.66×10^{0}	5.91×10^{-1}	8.38×10^{-2}	1.18×10^{-2}	1.16×10^{-2}	1.10
5.05×10^{-1}	4.91×10^{0}	1.66×10^{-2}	4.24×10^{-2}	1.08×10^{-2}	5.36×10^{-2}	1.10
6.74×10^{-1}	6.56×10^{0}	4.29×10^{-3}	1.95×10^{-3}	8.98×10^{-3}	2.22×10^{-2}	1.27
8.91×10^{0}	8.67×10^{0}	7.76×10^{-3}	6.18×10^{-3}	4.90×10^{-3}	6.40×10^{-3}	1.15
1.19×10^{0}	1.16×10^{1}	1.16×10^{-3}	1.64×10^{-3}	2.31×10^{-3}	1.55×10^{-3}	1.11

(j) Probe #10

$\eta\kappa_1$	$\ell\kappa_1$	$\frac{\phi(\eta\kappa_1)}{\nu^2\eta}$	$\frac{(\eta\kappa_1)^2\phi(\eta\kappa_1)}{\nu^2\eta}$	$\frac{(\eta\kappa_1)^4\phi(\eta\kappa_1)}{\nu^2\eta}$	$\frac{\alpha_1(\eta\kappa_1)^{5/3}}{\phi(\eta\kappa_1)}$	A
2.01×10^{-4}	2.04×10^{-3}	7.16×10^{3}	2.88×10^{-4}	1.16×10^{-11}	4.95×10^{-3}	0.824
2.67×10^{-4}	2.71×10^{-3}	7.70×10^{3}	5.48×10^{-4}	3.90×10^{-10}	7.83×10^{-2}	0.843
3.62×10^{-4}	3.68×10^{-3}	7.60×10^{3}	9.97×10^{-3}	1.31×10^{-10}	1.40×10^{-2}	0.901
4.86×10^{-4}	4.94×10^{-3}	7.01×10^{3}	1.66×10^{-3}	3.92×10^{-9}	2.09×10^{-2}	0.866
6.48×10^{-4}	6.59×10^{-3}	6.57×10^{3}	2.76×10^{-3}	1.16×10^{-9}	3.19×10^{-2}	0.806
8.58×10^{-4}	8.72×10^{-3}	6.32×10^{3}	4.66×10^{-3}	3.43×10^{-9}	4.90×10^{-2}	0.871
$1.1r\times10^{-3}$	1.16×10^{-2}	5.19×10^{3}	6.78×10^{-3}	8.87×10^{-9}	6.46×10^{-2}	0.890
1.52×10^{-3}	1.55×10^{-2}	5.04×10^{3}	1.17×10^{-2}	2.70×10^{-8}	1.01×10^{-1}	0.879
2.01×10^{-3}	2.04×10^{-2}	4.14×10^{3}	1.66×10^{-2}	6.70×10^{-7}	1.33×10^{-1}	0.864
2.67×10^{-3}	2.71×10^{-2}	3.36×10^{3}	2.39×10^{-2}	1.69×10^{-7}	1.73×10^{-1}	0.939
3.62×10^{-3}	3.68×10^{-2}	2.38×10^{3}	3.12×10^{-2}	4.10×10^{-7}	2.03×10^{-1}	0.886
4.86×10^{-3}	4.94×10^{-2}	1.77×10^{3}	4.19×10^{-2}	9.86×10^{-7}	2.47×10^{-1}	0.913
6.48×10^{-3}	6.59×10^{-2}	1.42×10^{3}	5.95×10^{-2}	2.50×10^{-6}	3.20×10^{-1}	0.990
8.58×10^{-3}	8.72×10^{-2}	1.05×10^{3}	7.77×10^{-2}	5.70×10^{-6}	3.78×10^{-1}	1.02
$1.1r\times10^{-2}$	1.16×10^{-1}	6.81×10^{2}	8.94×10^{-1}	1.17×10^{-5}	3.93×10^{-1}	0.993
1.52×10^{-2}	1.55×10^{-1}	5.63×10^{2}	1.31×10^{-1}	3.03×10^{-5}	5.25×10^{-1}	1.04
2.01×10^{-2}	2.04×10^{-1}	3.97×10^{2}	1.60×10^{-1}	6.42×10^{-4}	5.90×10^{-1}	1.06
2.67×10^{-2}	2.71×10^{-1}	2.81×10^{2}	2.00×10^{-1}	1.43×10^{-4}	6.70×10^{-1}	1.05
3.62×10^{-2}	3.68×10^{-1}	1.90×10^{2}	2.49×10^{-1}	3.26×10^{-4}	7.56×10^{-1}	1.05
4.86×10^{-2}	4.94×10^{-1}	1.16×10^{1}	2.74×10^{-1}	6.48×10^{-4}	7.51×10^{-1}	1.03
6.48×10^{-2}	6.59×10^{-1}	7.36×10^{1}	3.09×10^{-1}	1.29×10^{-3}	7.69×10^{-1}	1.00
8.58×10^{-1}	8.72×10^{0}	4.00×10^{1}	2.95×10^{-1}	2.17×10^{-3}	6.68×10^{-1}	0.989
1.14×10^{-1}	1.16×10^{0}	2.03×10^{1}	2.66×10^{-1}	3.48×10^{-3}	5.44×10^{-1}	0.983
1.52×10^{-1}	1.55×10^{0}	1.16×10^{0}	2.69×10^{-1}	6.23×10^{-3}	5.02×10^{-1}	0.925
2.01×10^{-1}	2.04×10^{0}	4.93×10^{0}	1.99×10^{-1}	7.98×10^{-2}	3.40×10^{-1}	0.884
2.67×10^{-1}	2.71×10^{0}	2.10×10^{-1}	1.50×10^{-2}	1.06×10^{-2}	2.32×10^{-1}	0.928
3.62×10^{-1}	3.68×10^{0}	7.17×10^{-1}	9.42×10^{-2}	1.24×10^{-2}	1.32×10^{-2}	0.843
4.86×10^{-1}	4.94×10^{0}	1.97×10^{-1}	4.66×10^{-2}	1.10×10^{-3}	5.92×10^{-2}	0.784
6.48×10^{-1}	6.59×10^{0}	4.62×10^{-2}	1.94×10^{-3}	8.13×10^{-3}	2.24×10^{-3}	0.708
8.58×10^{0}	8.72×10^{1}	8.79×10^{-3}	6.47×10^{-3}	4.76×10^{-3}	6.81×10^{-3}	0.659
1.14×10^{0}	1.16×10^{1}	1.30×10^{-3}	1.70×10^{-3}	2.22×10^{-3}	1.62×10^{-3}	0.626

(k) Probe #11

$\eta\kappa_1$	$\ell\kappa_1$	$\frac{\phi(\eta\kappa_1)}{\nu^2\eta}$	$\frac{(\eta\kappa_1)^2\phi(\eta\kappa_1)}{\nu^2\eta}$	$\frac{(\eta\kappa_1)^4\phi(\eta\kappa_1)}{\nu^2\eta}$	$\frac{\alpha_1(\eta\kappa_1)^{5/3}}{\phi(\eta\kappa_1)}$	A
2.09×10^{-4}	2.66×10^{-3}	8.10×10^{3}	3.53×10^{-4}	1.54×10^{-11}	5.96×10^{-3}	0.893
2.78×10^{-4}	3.54×10^{-3}	7.94×10^{3}	6.16×10^{-4}	4.78×10^{-11}	9.40×10^{-3}	0.852
3.78×10^{-4}	4.80×10^{-3}	7.59×10^{3}	1.08×10^{-3}	1.54×10^{-11}	1.50×10^{-2}	0.876
5.07×10^{-4}	6.45×10^{-3}	6.52×10^{3}	1.68×10^{-3}	4.32×10^{-10}	2.10×10^{-2}	0.780
6.76×10^{-4}	8.60×10^{-3}	6.77×10^{3}	2.72×10^{-3}	1.10×10^{-9}	3.53×10^{-2}	0.821
8.94×10^{-4}	1.14×10^{-2}	6.87×10^{3}	5.50×10^{-3}	4.40×10^{-9}	5.70×10^{-2}	0.944
1.19×10^{-3}	1.52×10^{-2}	5.09×10^{3}	7.23×10^{-3}	1.03×10^{-8}	6.80×10^{-2}	0.847
1.59×10^{-3}	2.03×10^{-2}	5.40×10^{3}	1.37×10^{-2}	3.48×10^{-8}	1.17×10^{-1}	0.938
2.09×10^{-3}	2.66×10^{-2}	4.66×10^{3}	2.04×10^{-2}	8.87×10^{-8}	1.59×10^{-1}	0.983
2.78×10^{-3}	3.54×10^{-2}	3.46×10^{3}	2.69×10^{-2}	2.08×10^{-7}	1.90×10^{-1}	0.977
3.78×10^{-3}	4.80×10^{-2}	2.58×10^{3}	3.67×10^{-2}	5.24×10^{-6}	2.37×10^{-1}	0.973
5.07×10^{-3}	6.45×10^{-2}	1.85×10^{3}	4.77×10^{-2}	1.22×10^{-6}	2.77×10^{-1}	0.968
6.76×10^{-3}	8.60×10^{-1}	1.37×10^{3}	6.28×10^{-2}	2.87×10^{-6}	3.31×10^{-1}	0.978
8.94×10^{-3}	1.14×10^{-1}	1.01×10^{3}	8.08×10^{-1}	6.49×10^{-5}	3.89×10^{-1}	1.02
1.19×10^{-2}	1.52×10^{-1}	7.03×10^{2}	1.00×10^{-1}	1.42×10^{-5}	4.36×10^{-1}	1.03
1.59×10^{-2}	2.03×10^{-1}	5.50×10^{2}	1.40×10^{-1}	3.54×10^{-5}	5.53×10^{-1}	1.05
2.09×10^{-2}	2.66×10^{-1}	4.05×10^{2}	1.77×10^{-1}	7.70×10^{-4}	6.42×10^{-1}	1.10
2.78×10^{-2}	3.54×10^{-1}	2.85×10^{2}	2.21×10^{-1}	1.71×10^{-4}	7.27×10^{-1}	1.09
3.78×10^{-2}	4.80×10^{-1}	1.97×10^{2}	2.80×10^{-1}	4.00×10^{-4}	8.39×10^{-1}	1.13
5.07×10^{-2}	6.45×10^{-1}	1.22×10^{1}	3.13×10^{-1}	8.07×10^{-3}	8.47×10^{-1}	1.11
6.76×10^{-2}	8.60×10^{0}	7.28×10^{1}	3.33×10^{-1}	1.52×10^{-3}	8.17×10^{-1}	1.06
8.94×10^{-2}	1.14×10^{0}	3.85×10^{1}	3.08×10^{-1}	2.47×10^{-3}	6.88×10^{-1}	1.03
1.19×10^{-1}	1.52×10^{0}	2.00×10^{1}	2.84×10^{-1}	4.04×10^{-3}	5.76×10^{-1}	1.01
1.59×10^{-1}	2.03×10^{0}	1.17×10^{0}	2.96×10^{-1}	7.51×10^{-3}	5.46×10^{-1}	1.03
2.09×10^{-1}	2.66×10^{0}	4.61×10^{0}	2.01×10^{-1}	8.78×10^{-2}	3.39×10^{-1}	0.913
2.78×19^{-1}	3.54×10^{0}	2.07×10^{-1}	1.60×10^{-2}	1.24×10^{-2}	2.45×10^{-1}	1.02
3.78×10^{-1}	4.80×10^{0}	6.37×10^{-1}	9.08×10^{-2}	1.29×10^{-2}	1.26×10^{-2}	0.862
5.07×10^{-1}	6.45×10^{0}	1.64×10^{-2}	4.23×10^{-2}	1.09×10^{-3}	5.29×10^{-2}	0.775
6.76×10^{-1}	8.60×10^{1}	4.10×10^{-3}	1.88×10^{-3}	8.58×10^{-3}	2.13×10^{-3}	0.775
8.94×10^{-1}	1.14×10^{1}	7.33×10^{-3}	5.86×10^{-3}	4.69×10^{-3}	6.08×10^{-3}	0.699
1.19×10^{-1}	1.52×10^{1}	1.13×10^{-3}	1.60×10^{-3}	2.28×10^{-3}	1.51×10^{-3}	0.692

(1) Probe #12

$\eta\kappa_1$	$\ell\kappa_1$	$\frac{\phi(\eta\kappa_1)}{\nu^2\eta}$	$\frac{(\eta\kappa_1)^2\phi(\eta\kappa_1)}{\nu^2\eta}$	$\frac{(\eta\kappa_1)^4\phi(\eta\kappa_1)}{\nu^2\eta}$	$\frac{\alpha_1(\eta\kappa_1)^{5/3}}{\phi(\eta\kappa_1)}$	A
2.03×10^{-4}	2.48×10^{-3}	7.54×10^{3}	3.11×10^{-4}	1.28×10^{-11}	5.29×10^{-3}	0.876
2.71×10^{-4}	3.31×10^{-3}	8.95×10^{3}	6.59×10^{-4}	4.86×10^{-11}	1.02×10^{-2}	1.00
3.68×10^{-4}	4.49×10^{-3}	8.27×10^{3}	1.12×10^{-3}	1.52×10^{-10}	1.56×10^{-2}	1.00
4.03×10^{-4}	6.02×10^{-3}	7.05×10^{3}	1.71×10^{-3}	4.18×10^{-10}	2.17×10^{-2}	0.884
6.58×10^{-4}	8.04×10^{-3}	6.42×10^{3}	2.78×10^{-3}	1.21×10^{-9}	3.20×10^{-2}	0.805
8.71×10^{-4}	1.06×10^{-2}	6.57×10^{3}	4.98×10^{-3}	3.77×10^{-3}	5.22×10^{-2}	0.931
1.16×10^{-3}	1.42×10^{-2}	5.16×10^{3}	6.98×10^{-3}	9.37×10^{-8}	6.61×10^{-2}	0.898
1.55×10^{-3}	1.89×10^{-2}	5.56×10^{3}	1.33×10^{-2}	3.20×10^{-8}	1.15×10^{-1}	1.00
2.03×10^{-3}	2.48×10^{-2}	4.78×10^{3}	1.97×10^{-2}	8.10×10^{-8}	1.56×10^{-1}	1.03
2.71×10^{-3}	3.31×10^{-2}	3.55×10^{3}	2.61×10^{-2}	1.92×10^{-7}	1.87×10^{-1}	1.03
3.68×10^{-3}	4.49×10^{-2}	2.80×10^{3}	3.80×10^{-2}	5.15×10^{-7}	2.46×10^{-1}	1.08
4.93×10^{-3}	6.02×10^{-2}	2.02×10^{3}	4.91×10^{-2}	1.20×10^{-6}	2.88×10^{-1}	1.07
6.58×10^{-3}	8.04×10^{-2}	1.59×10^{3}	6.91×10^{-2}	2.98×10^{-6}	3.67×10^{-1}	1.15
8.71×10^{-3}	1.06×10^{-1}	1.15×10^{2}	8.74×10^{-2}	6.63×10^{-6}	4.24×10^{-1}	1.17
1.16×10^{-2}	1.42×10^{-1}	7.30×10^{2}	9.82×10^{-2}	1.33×10^{-5}	4.34×10^{-1}	1.09
1.55×10^{-2}	1.89×10^{-1}	5.89×10^{2}	1.41×10^{-1}	3.36×10^{-5}	5.68×10^{-1}	1.11
2.03×10^{-2}	2.48×10^{-1}	4.13×10^{2}	1.79×10^{-1}	7.37×10^{-5}	6.24×10^{-1}	1.20
2.71×10^{-2}	3.31×10^{-1}	2.91×10^{2}	2.14×10^{-1}	1.57×10^{-4}	7.12×10^{-1}	1.12
3.68×10^{-2}	4.49×10^{-1}	1.96×10^{2}	2.65×10^{-1}	3.59×10^{-4}	7.98×10^{-1}	1.13
4.93×10^{-2}	6.02×10^{-1}	1.21×10^{1}	2.93×10^{-1}	7.14×10^{-4}	8.02×10^{-1}	1.11
6.58×10^{-2}	8.04×10^{0}	7.25×10^{1}	3.14×10^{-1}	1.36×10^{-3}	7.78×10^{-1}	1.04
8.71×10^{-1}	1.06×10^{0}	4.07×10^{1}	3.09×10^{-1}	2.34×10^{-3}	6.97×10^{-1}	1.06
1.16×10^{-1}	1.42×10^{0}	2.03×10^{1}	2.74×10^{-1}	3.69×10^{-3}	5.60×10^{-1}	1.02
1.55×10^{-1}	1.89×10^{0}	1.06×10^{0}	2.53×10^{-1}	6.05×10^{-3}	4.74×10^{-1}	0.897
2.03×10^{-1}	2.48×10^{0}	4.41×10^{0}	1.81×10^{-1}	7.48×10^{-3}	3.09×10^{-1}	0.831
2.71×10^{-1}	3.31×10^{0}	1.79×10^{-1}	1.32×10^{-2}	9.71×10^{-3}	2.03×10^{-1}	0.848
3.68×10^{-1}	4.49×10^{0}	5.98×10^{-1}	8.13×10^{-2}	1.10×10^{-2}	1.13×10^{-1}	0.764
4.93×10^{-1}	6.02×10^{0}	1.54×10^{-2}	3.75×10^{-3}	9.13×10^{-3}	4.74×10^{-2}	0.662
6.58×10^{-1}	8.04×10^{1}	4.10×10^{-3}	1.77×10^{-3}	7.70×10^{-3}	2.04×10^{-3}	0.697
8.71×10^{0}	1.06×10^{1}	8.80×10^{-3}	6.70×10^{-3}	5.06×10^{-3}	6.99×10^{-3}	0.739
1.16×10^{0}	1.42×10^{1}	1.24×10^{-3}	1.67×10^{-3}	2.24×10^{-3}	1.56×10^{-3}	0.668

(m) Probe #13

$\eta\kappa_1$	$\ell\kappa_1$	$\frac{\phi(\eta\kappa_1)}{\nu^2\eta}$	$\frac{(\eta\kappa_1)^2\phi(\eta\kappa_1)}{\nu^2\eta}$	$\frac{(\eta\kappa_1)^4\phi(\eta\kappa_1)}{\nu^2\kappa}$	$\frac{\alpha_1(\eta\kappa_1)^{5/3}}{\phi(\eta\kappa_1)}$
1.94×10^{-4}	5.54×10^{-4}	8.27×10^{3}	3.09×10^{-4}	1.15×10^{-11}	5.38×10^{-3}
2.58×10^{-4}	7.39×10^{-4}	8.70×10^{3}	5.77×10^{-4}	3.83×10^{-11}	9.10×10^{-3}
3.50×10^{-4}	1.00×10^{-3}	8.04×10^{3}	9.82×10^{-3}	1.20×10^{-10}	1.40×10^{-2}
4.70×10^{-4}	1.35×10^{-3}	7.71×10^{3}	1.70×10^{-3}	3.73×10^{-9}	2.19×10^{-2}
6.27×10^{-4}	1.80×10^{-3}	7.80×10^{3}	3.05×10^{-3}	1.19×10^{-9}	3.58×10^{-2}
8.29×10^{-4}	2.37×10^{-3}	6.96×10^{3}	4.76×10^{-3}	3.26×10^{-9}	5.09×10^{-2}
1.11×10^{-3}	3.16×10^{-3}	5.55×10^{3}	6.78×10^{-3}	8.21×10^{-9}	6.60×10^{-2}
1.48×10^{-3}	4.22×10^{-3}	5.50×10^{3}	1.19×10^{-2}	2.58×10^{-8}	1.06×10^{-1}
1.94×10^{-3}	5.54×10^{-3}	4.62×10^{3}	1.72×10^{-2}	6.43×10^{-7}	1.39×10^{-1}
2.58×10^{-3}	7.32×10^{-2}	3.43×10^{3}	2.28×10^{-2}	1.51×10^{-7}	1.66×10^{-1}
3.50×10^{-3}	1.00×10^{-2}	2.59×10^{3}	3.16×10^{-2}	3.86×10^{-7}	2.09×10^{-1}
4.70×10^{-3}	1.35×10^{-2}	1.87×10^{3}	4.11×10^{-2}	9.04×10^{-6}	2.47×10^{-1}
6.27×10^{-3}	1.80×10^{-2}	1.38×10^{2}	5.39×10^{-2}	2.11×10^{-6}	2.94×10^{-1}
8.29×10^{-3}	2.37×10^{-2}	9.92×10^{2}	6.78×10^{-2}	4.64×10^{-6}	3.37×10^{-1}
1.11×10^{-2}	3.16×10^{-2}	6.58×10^{2}	8.02×10^{-2}	9.70×10^{-6}	3.63×10^{-1}
1.48×10^{-2}	4.22×10^{-2}	5.22×10^{2}	1.13×10^{-1}	2.45×10^{-5}	4.66×10^{-1}
1.94×10^{-2}	5.54×10^{-2}	3.60×10^{2}	1.34×10^{-1}	5.01×10^{-4}	5.04×10^{-1}
2.58×10^{-2}	7.39×10^{-1}	2.59×10^{2}	1.72×10^{-1}	1.14×10^{-4}	5.83×10^{-1}
3.50×10^{-2}	1.00×10^{-1}	1.74×10^{2}	2.13×10^{-1}	2.60×10^{-4}	6.52×10^{-1}
4.70×10^{-2}	1.35×10^{-1}	1.09×10^{1}	2.40×10^{-1}	5.29×10^{-3}	6.67×10^{-1}
6.27×10^{-2}	1.80×10^{-1}	7.10×10^{1}	2.78×10^{-1}	1.09×10^{-3}	7.03×19^{-1}
8.29×10^{-1}	2.37×10^{-1}	3.96×10^{1}	2.70×10^{-1}	1.85×10^{-3}	6.24×10^{-1}
1.11×10^{-1}	3.16×10^{-1}	2.00×10^{1}	2.44×10^{-1}	2.96×10^{-3}	5.13×10^{-1}
1.48×10^{-1}	4.22×10^{-1}	1.22×10^{0}	2.65×10^{-1}	5.74×10^{-3}	5.05×10^{-1}
1.94×10^{-1}	5.54×10^{-1}	5.50×10^{0}	2.05×10^{-1}	7.66×10^{-3}	3.58×10^{-1}
2.58×10^{-1}	7.39×10^{0}	2.23×10^{-1}	1.47×10^{-1}	9.79×10^{-2}	2.33×10^{-1}
3.50×10^{-1}	1.00×10^{0}	8.42×10^{-1}	1.03×10^{-1}	1.26×10^{-2}	1.46×10^{-1}
4.70×10^{-1}	1.35×10^{0}	2.51×10^{-2}	5.51×10^{-2}	1.22×10^{-2}	7.13×10^{-2}
6.27×10^{-1}	1.80×10^{0}	6.53×10^{-2}	2.56×10^{-2}	1.00×10^{-2}	3.00×10^{-2}
8.29×10^{0}	2.37×10^{0}	1.36×10^{-3}	9.33×10^{-3}	6.37×10^{-3}	9.95×10^{-3}
1.11×10^{0}	3.16×10^{0}	2.11×10^{-3}	2.56×10^{-3}	3.12×10^{-3}	2.51×10^{-3}

(n) Probe #14

$\eta\kappa_1$	$\ell\kappa_1$	$\frac{\phi(\eta\kappa_1)}{\nu^2\eta}$	$\frac{(\eta\kappa_1)^2\phi(\eta\kappa_1)}{\nu^2\eta}$	$\frac{(\eta\kappa_1)^4\phi(\eta\kappa_1)}{\nu^2\eta}$	$\frac{\alpha_1}{(\eta\kappa_1)^{5/3}\phi(\eta\kappa_1)}$	A
1.88×10^{-4}	1.20×10^{-3}	8.58×10^{3}	1.06×10^{-11}	5.29×10^{-3}	5.29×10^{-3}	1.05
2.50×10^{-4}	1.60×10^{-3}	8.63×10^{3}	5.38×10^{-4}	3.36×10^{-11}	8.56×10^{-3}	1.00
3.39×10^{-4}	2.17×10^{-3}	8.44×10^{3}	9.65×10^{-4}	1.11×10^{-10}	1.39×10^{-2}	1.06
4.56×10^{-4}	2.92×10^{-3}	7.74×10^{3}	1.60×10^{-3}	3.32×10^{-10}	2.09×10^{-2}	1.01
6.07×10^{-4}	3.88×10^{-3}	7.55×10^{3}	2.77×10^{-3}	1.02×10^{-9}	3.29×10^{-2}	0.988
8.03×10^{-4}	5.14×10^{-3}	7.27×10^{3}	4.68×10^{-3}	3.02×10^{-9}	5.04×10^{-2}	0.993
1.07×10^{-3}	6.85×10^{-3}	5.69×10^{3}	6.49×10^{-3}	7.43×10^{-9}	6.37×10^{-2}	1.03
1.43×10^{-3}	9.17×10^{-2}	5.64×10^{3}	1.15×10^{-2}	2.37×10^{-8}	1.02×10^{-1}	1.04
1.88×10^{-3}	1.20×10^{-2}	4.90×10^{3}	1.72×10^{-2}	6.07×10^{-8}	1.40×10^{-1}	1.08
2.50×10^{-3}	1.60×10^{-2}	3.79×10^{3}	2.37×10^{-2}	1.47×10^{-7}	1.75×10^{-1}	1.12
3.39×10^{-3}	2.17×10^{-2}	2.96×10^{3}	3.28×10^{-2}	3.76×10^{-7}	2.19×10^{-1}	1.12
4.56×10^{-3}	2.92×10^{-2}	2.05×10^{3}	4.24×10^{-2}	8.78×10^{-7}	2.57×10^{-1}	1.11
6.07×10^{-3}	3.88×10^{-2}	1.49×10^{3}	5.46×10^{-2}	2.01×10^{-6}	3.01×10^{-1}	1.09
8.03×10^{-2}	5.14×10^{-2}	1.12×10^{2}	7.17×10^{-2}	4.64×10^{-6}	3.61×10^{-1}	1.15
1.07×10^{-2}	6.85×10^{-2}	7.51×10^{2}	8.62×10^{-2}	9.84×10^{-6}	3.90×10^{-1}	1.16
1.43×10^{-2}	9.17×10^{-1}	5.91×10^{2}	1.22×10^{-1}	2.51×10^{-5}	4.98×10^{-1}	1.16
1.88×10^{-2}	1.20×10^{-1}	4.43×10^{2}	1.56×10^{-1}	5.48×10^{-5}	5.89×10^{-1}	1.25
2.50×10^{-2}	1.60×10^{-1}	3.15×10^{2}	1.96×10^{-1}	1.22×10^{-4}	6.73×10^{-1}	1.23
3.39×10^{-2}	2.17×10^{-1}	2.08×10^{2}	2.39×10^{-1}	2.73×10^{-4}	7.39×10^{-1}	1.21
4.56×10^{-2}	2.92×10^{-1}	1.33×10^{1}	2.79×10^{-1}	5.72×10^{-4}	7.74×10^{-1}	1.24
6.07×10^{-2}	3.88×10^{-1}	8.02×10^{1}	3.05×10^{-1}	1.08×10^{-3}	7.52×10^{-1}	1.15
8.03×10^{-1}	5.14×10^{-1}	4.71×10^{1}	3.03×10^{-1}	1.95×10^{-3}	7.04×10^{-1}	1.22
1.07×10^{-1}	6.85×10^{-1}	2.32×10^{1}	2.66×10^{-1}	3.04×10^{-3}	5.59×10^{-1}	1.18
1.43×10^{-1}	9.17×10^{0}	1.40×10^{0}	2.87×10^{-1}	5.88×10^{-3}	5.47×10^{-1}	1.18
1.88×10^{-1}	1.20×10^{0}	6.11×10^{0}	2.15×10^{-1}	7.57×10^{-3}	3.77×10^{-1}	1.14
2.50×10^{-1}	1.60×10^{0}	2.66×10^{-1}	1.66×10^{-2}	1.03×10^{-2}	2.64×10^{-1}	1.23
3.39×10^{-1}	2.17×10^{0}	8.58×10^{-1}	9.82×10^{-2}	1.13×10^{-2}	1.41×10^{-2}	1.04
4.56×10^{-1}	2.92×10^{0}	2.61×10^{-2}	5.41×10^{-2}	1.12×10^{-2}	7.05×10^{-2}	1.07
6.07×10^{-1}	3.88×10^{0}	6.85×10^{-2}	2.52×10^{-2}	9.27×10^{-3}	2.98×10^{-2}	1.08
8.03×10^{0}	5.14×10^{0}	1.25×10^{-2}	8.10×10^{-3}	5.20×10^{-3}	8.67×10^{-3}	0.961
1.07×10^{0}	6.85×10^{0}	2.00×10^{-3}	2.28×10^{-3}	2.60×10^{-3}	2.24×10^{-3}	0.982

TABLE 6

RELATIVE ATTENUATION CALCULATED FROM WYNGAARD'S CORRECTION

$(\kappa_1 \ell)$	A $(n/\ell = 0.05)$	A $(n/\ell = 0.08)$	A $(n/\ell = 0.10)$	A $(n/\ell = 0.16)$
0.100	1.000	1.00	1.000	1.000
0.200	0.999	1.000	1.000	1.000
0.316	0.971	0.972	0.972	0.982
0.500	0.955	0.957	0.958	0.973
1.00	0.916	0.920	0.921	0.951
2.00	0.835	0.847	0.849	0.906
3.16	0.704	0.717	0.720	0.825
5.00	0.651	0.658	0.672	0.795
10.0	0.555	0.575	0.577	0.736

TABLE 7

DISSIPATION AND THE MOMENTS FOR DIFFERENT WIRE LENGTHS

Probe Number	$\bar{\varepsilon}$ (m^2/s^3)	$\bar{\varepsilon}_s$ (m^2/s^3)	$\bar{\varepsilon}_c$ (m^2/s^3)	S(u)	F(u)	S(∂u/∂t)	S_s(∂u/∂t)	F(∂u/∂t)	u' (m/s)
1	13.408	17.730	23.337	0.074	2.688	0.338	0.558	4.563	0.876
2	14.216	17.858	24.389	0.048	2.803	0.351	0.543	4.582	0.902
3	20.522	26.887	24.086	0.003	2.712	0.340	0.560	4.812	0.914
4	21.155	27.560	24.989	0.081	2.732	0.355	0.557	4.877	0.910
5	20.472	26.281	26.374	0.021	2.717	0.366	0.521	4.849	0.922
6	20.363	25.624	26.116	0.021	2.758	0.381	0.546	4.807	0.910
7	13.829	17.910	25.705	0.066	2.498	0.363	0.587	4.581	0.868
8	14.453	18.976	26.407	0.049	2.634	0.329	0.542	4.762	0.892
9	23.652	31.276	31.749	0.040	2.794	0.392	0.626	4.815	0.842
10	19.040	25.505	25.349	0.051	2.637	0.415	0.579	4.795	0.860
11	18.387	26.512	26.171	0.036	2.795	0.393	0.558	4.813	0.878
12	19.302	25.461	26.897	0.039	2.684	0.345	0.570	3.824	0.902
13	21.709	28.448	23.448	0.019	2.666	0.316	0.652	4.727	0.884
14	24.282	32.592	28.814	0.027	2.724	0.354	0.556	4.752	0.936

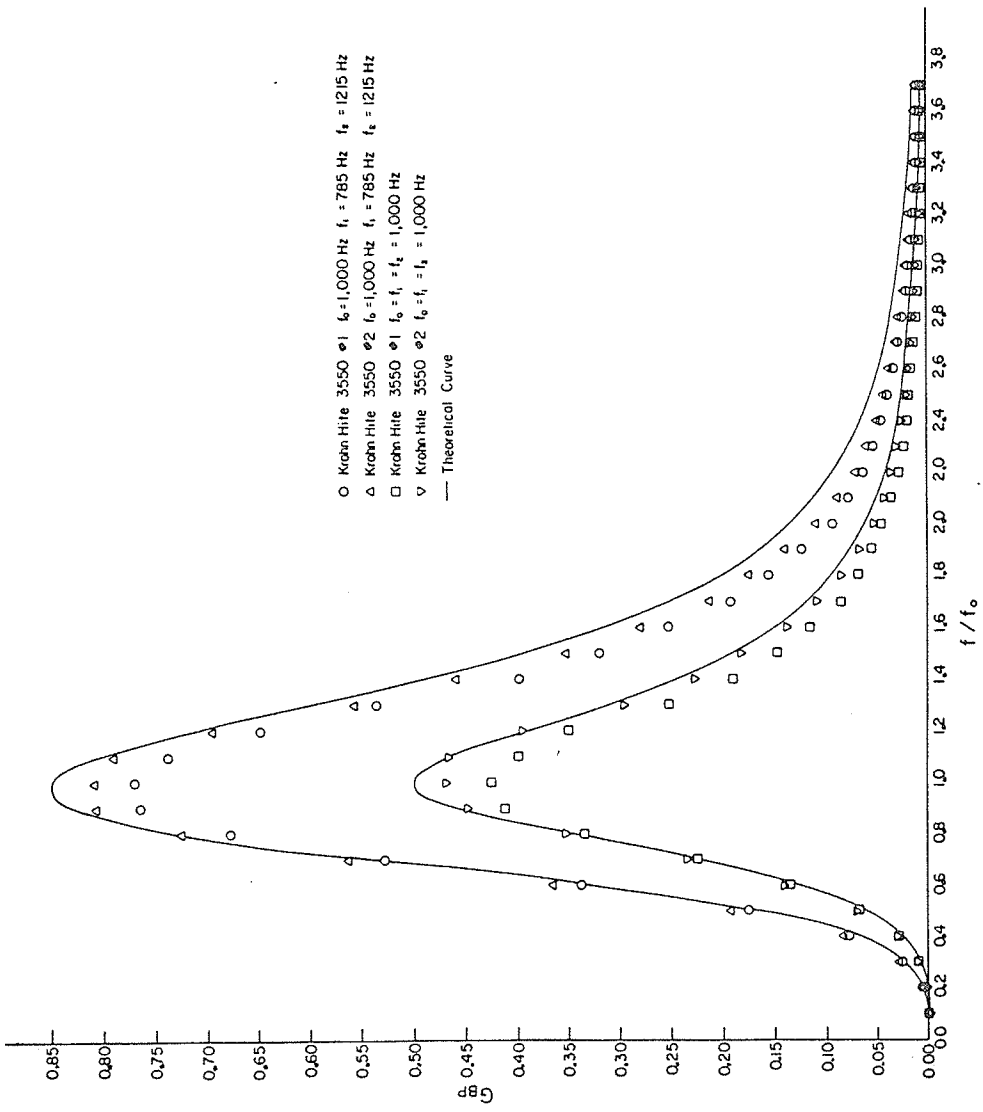

Figure 1: Bandpass Amplitude Attenuation Versus Frequency.

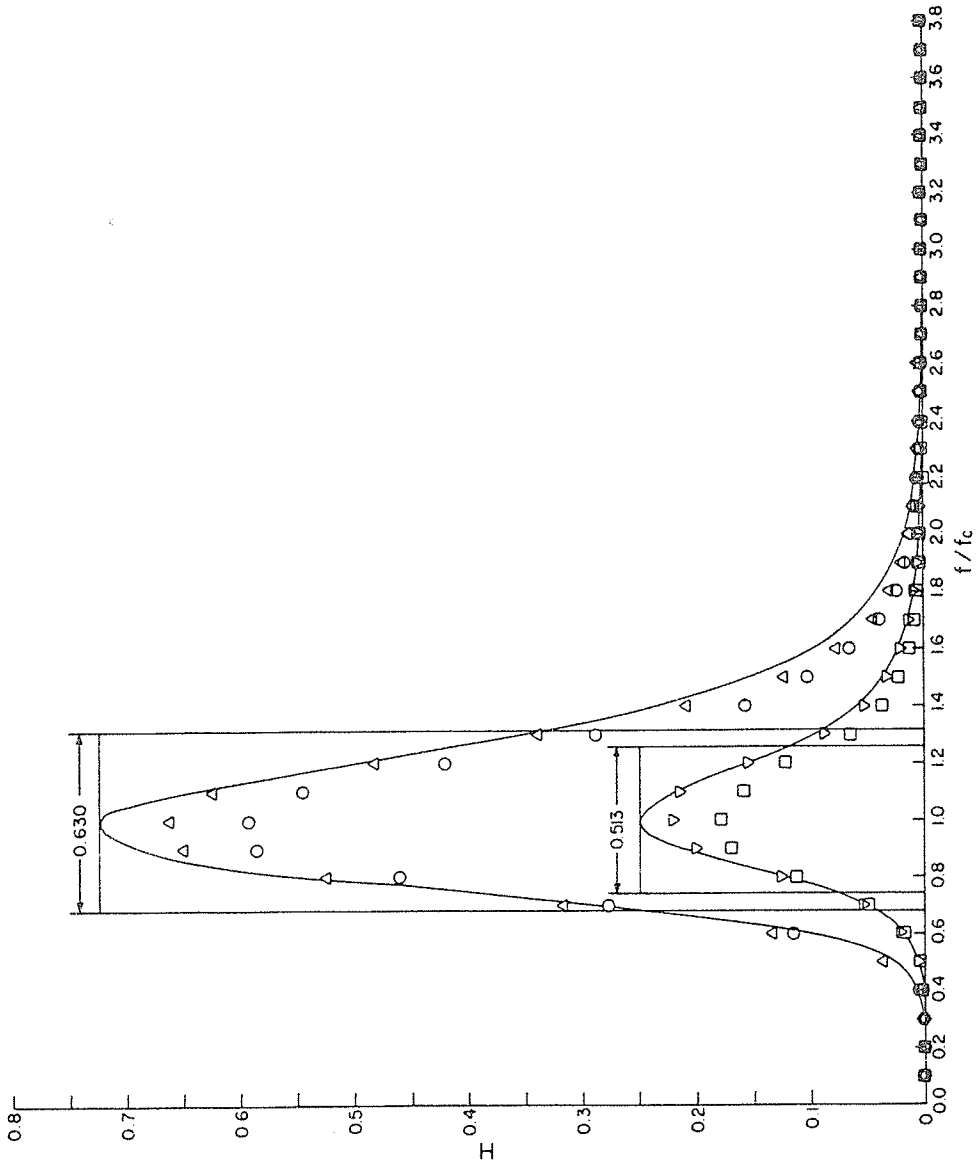

Figure 2: Bandpass Power Attenuation Versus Frequency. Symbols as in Figure 1.

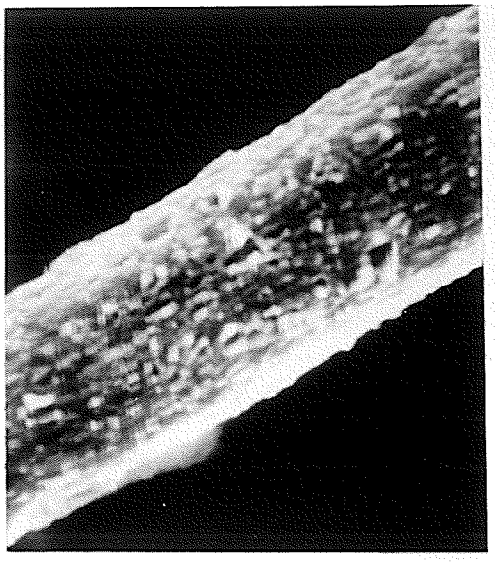

FIG. 3a
PROBE 1
MAG. = 5530X

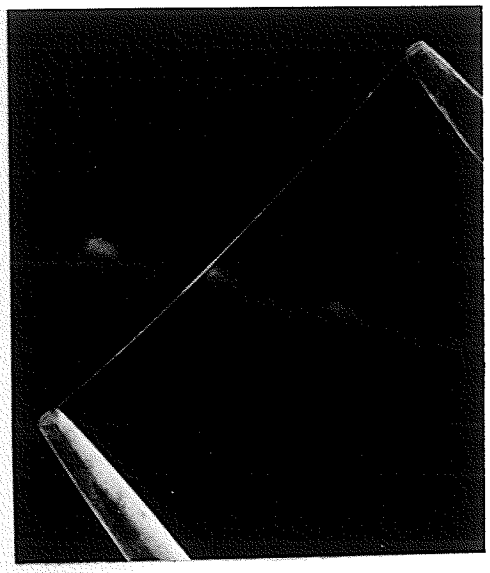

FIG. 3b
PROBE 1
MAG. = 25X

FIG. 3c
PROBE 2
MAG = 4060X

FIG. 3d
PROBE 2
MAG = 1710X

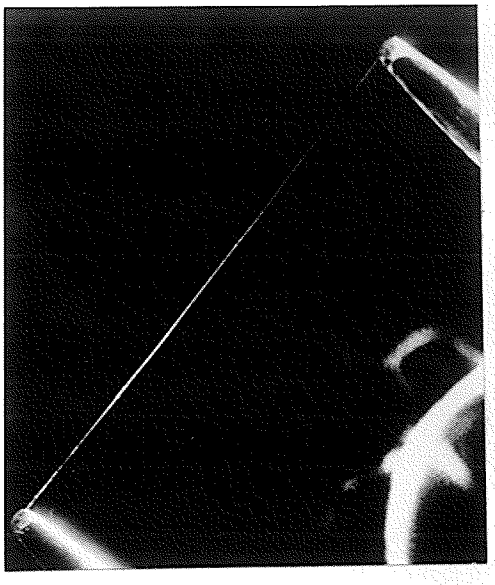

FIG. 3e
PROBE 2
MAG.=29X

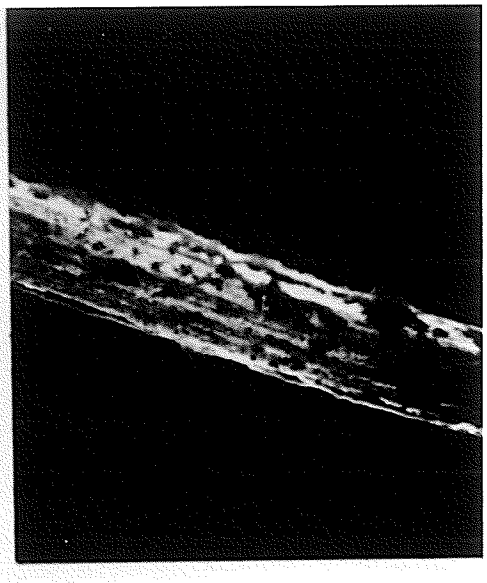

FIG. 3f
PROBE 3
MAG.=2660X

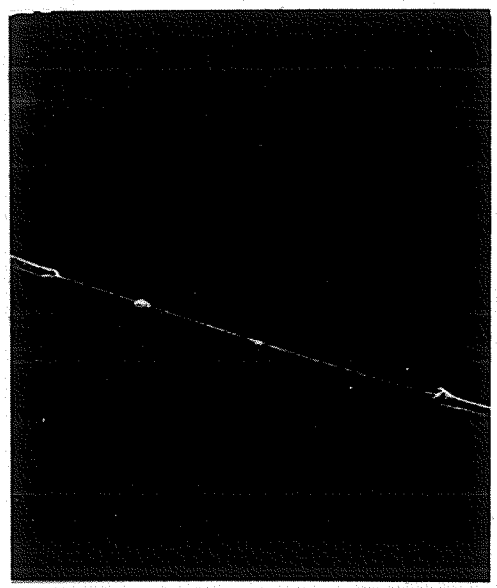

FIG. 3g
PROBE 3
MAG.=74X

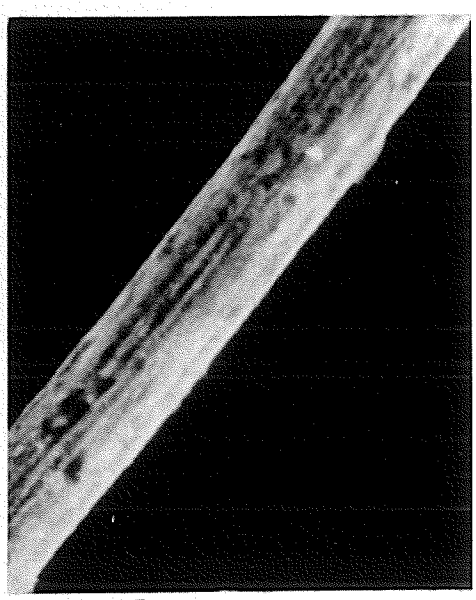

FIG. 3h
PROBE 4
MAG.=2660X

FIG. 3q
PROBE 8
MAG. = 18.5X

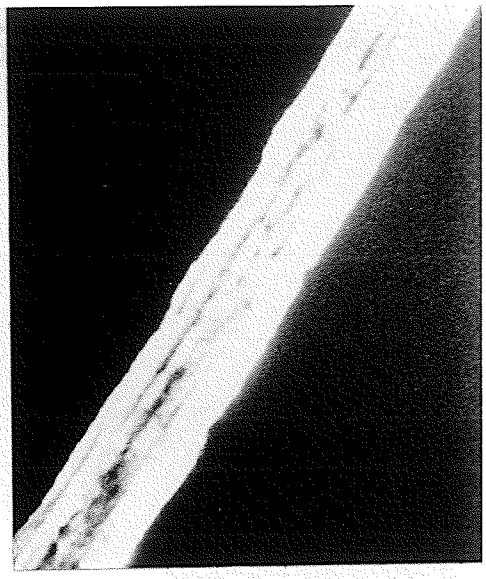

FIG. 3r
PROBE 9
MAG. = 3800X

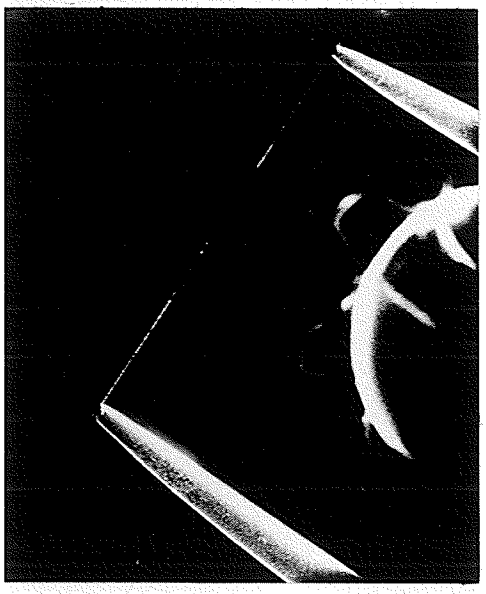

FIG. 3s
PROBE 9
MAG. = 19X

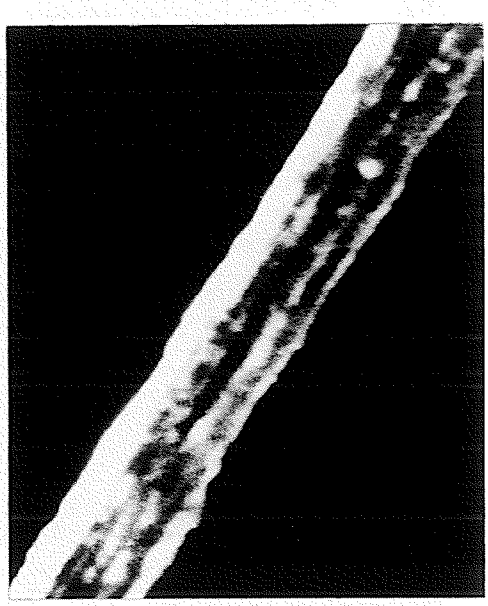

FIG. 3t
PROBE 10
MAG. = 3900X

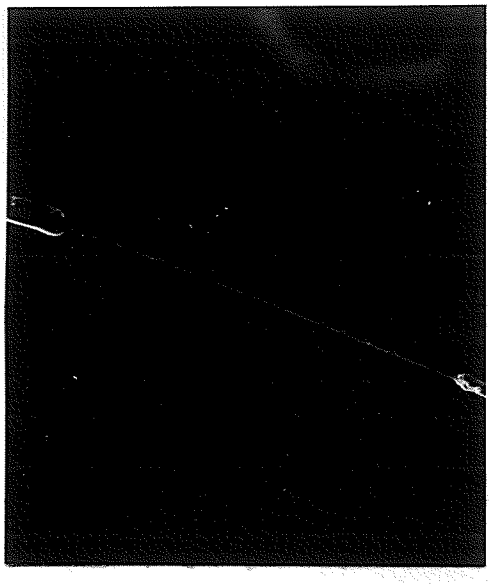

FIG. 3i
PROBE 4
MAG.= 76X

FIG. 3j
PROBE 5
MAG.=2660X

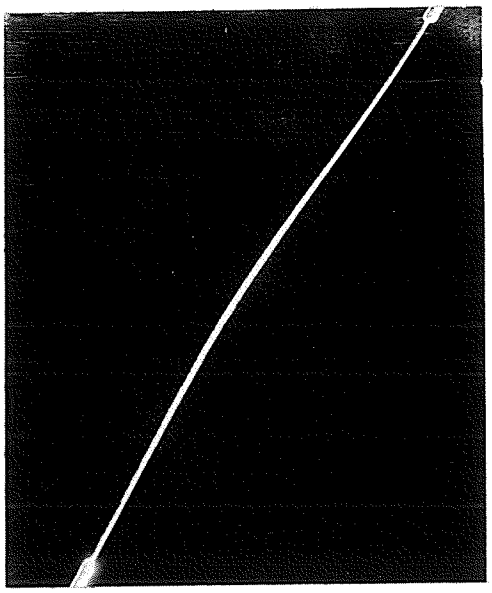

FIG. 3k
PROBE 5
MAG.= 76X

FIG. 3l
PROBE 6
MAG.=2660X

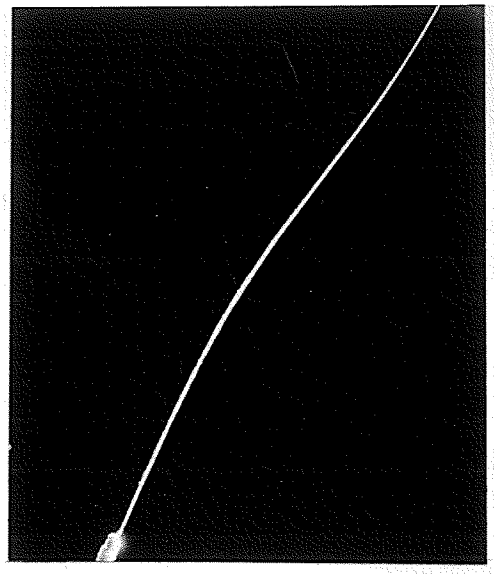

FIG. 3m
PROBE 6
MAG.= 76X

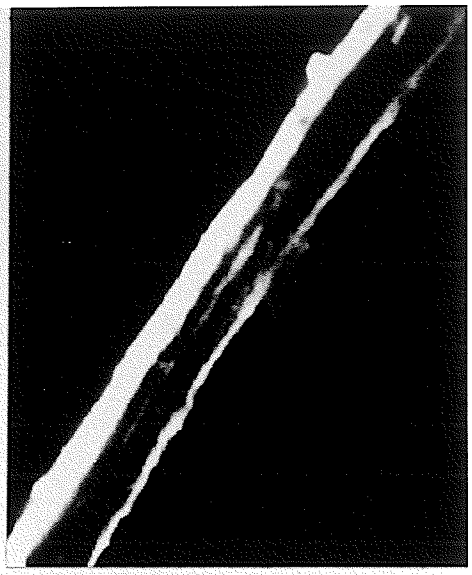

FIG.3n
PROBE 7
MAG.= 3800X

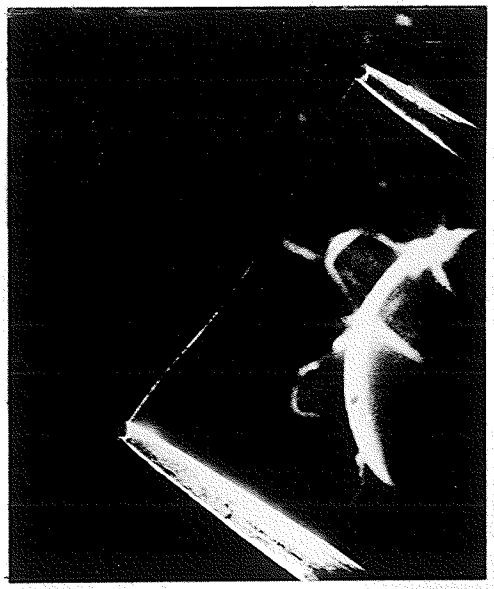

FIG.3o
PROBE 7
MAG.= 19X

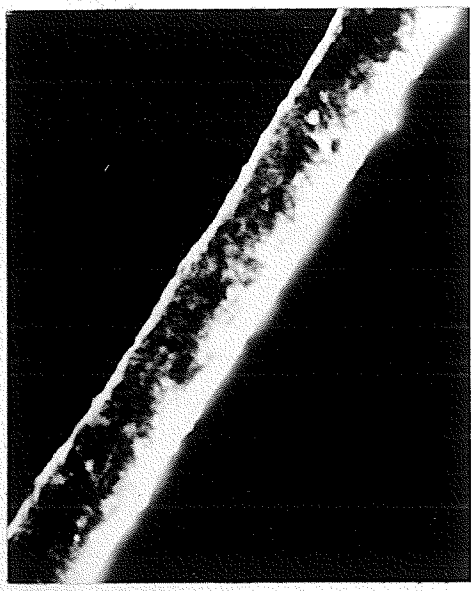

FIG. 3p
PROBE 8
MAG.= 3800X

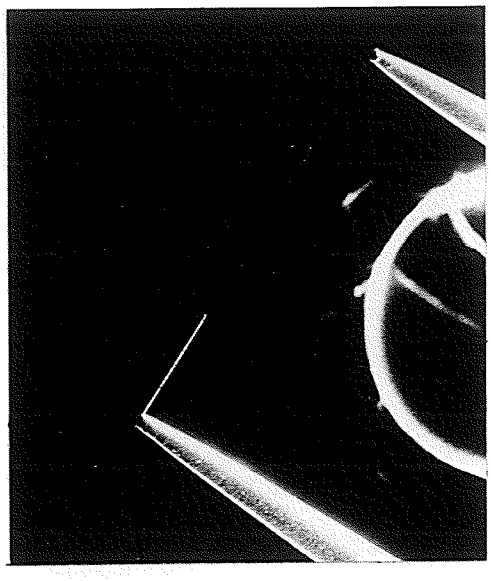

FIG. 3u
PROBE 10
MAG.=19X

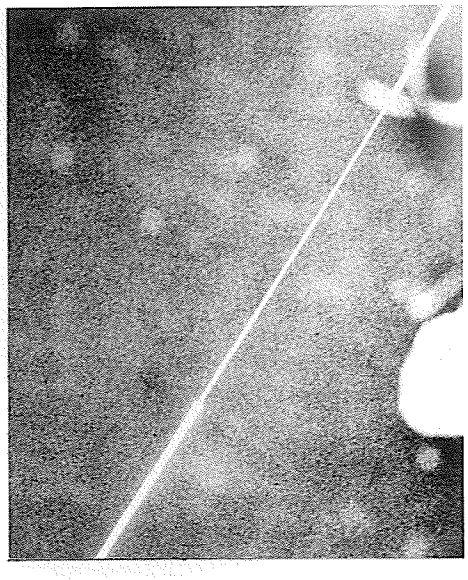

FIG.3v
PROBE 10
MAG.=38X

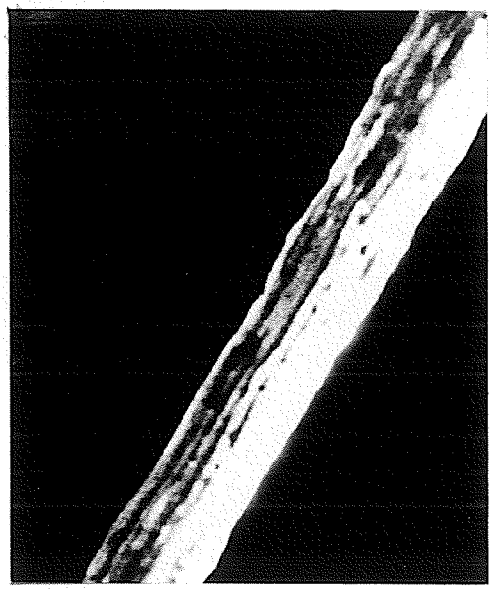

FIG. 3w
PROBE 11
MAG.=3900X

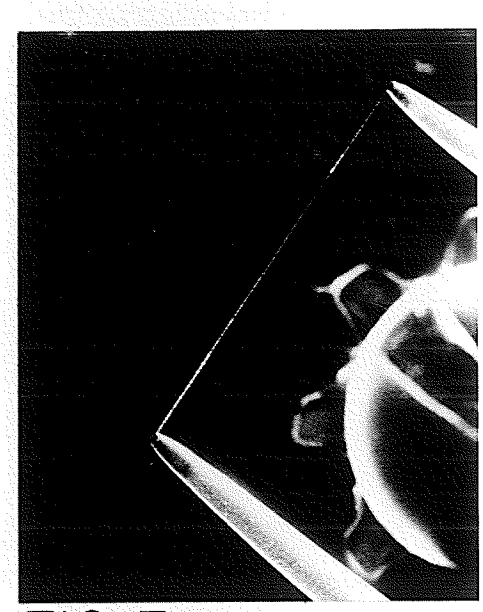

FIG. 3x
PROBE 11
MAG.=19X

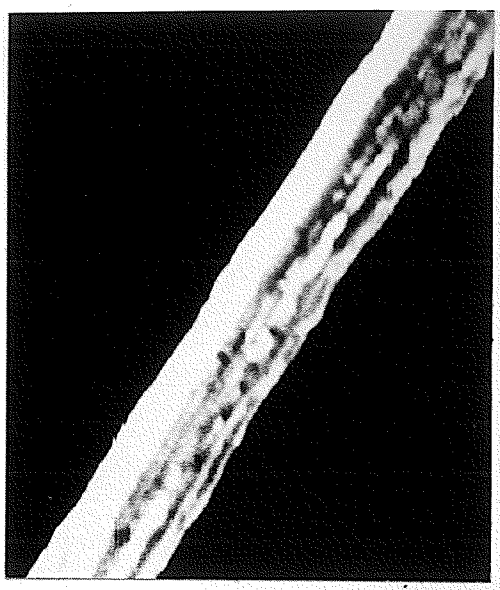

FIG. 3y
PROBE 12
MAG. = 3900X

FIG. 3z
PROBE 12
MAG. = 19.5 X

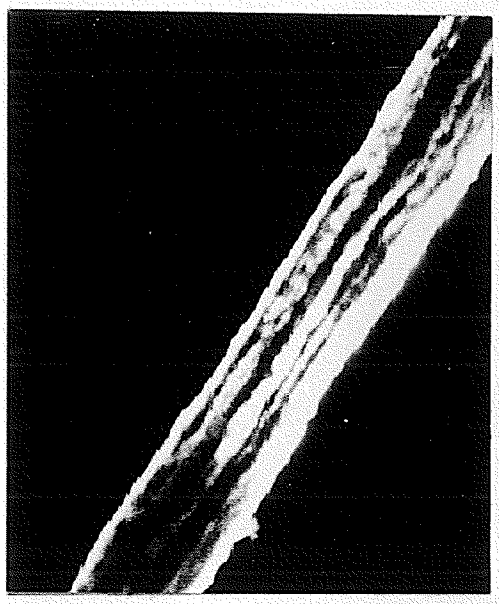

FIG. 3aa
PROBE 13
MAG. = 3800X

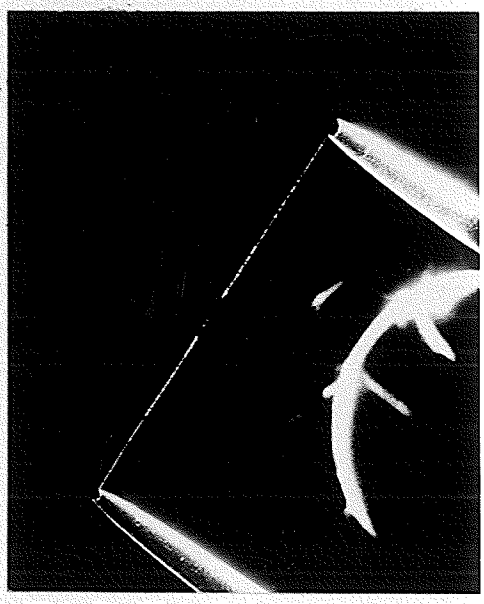

FIG. 3bb
PROBE 13
MAG. = 19.5 X

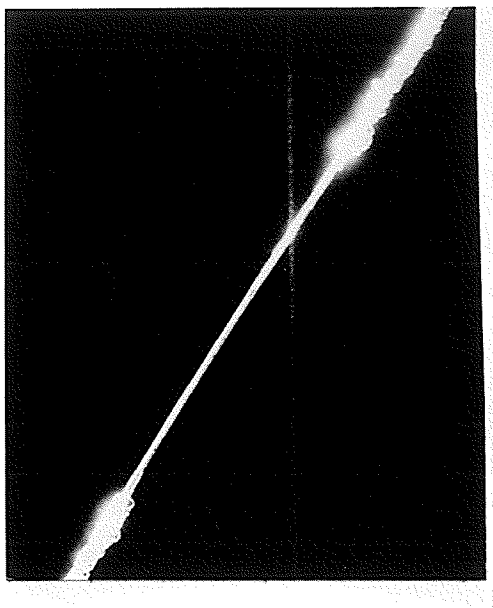

FIG. 3cc
PROBE 13
MAG.=156X

FIG.3dd
PROBE 14
MAG.=3900X

FIG. 3ee
PROBE 14
MAG.=19X

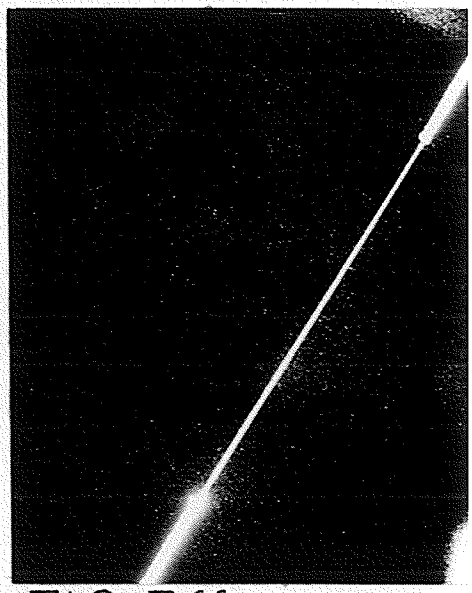

FIG. 3ff
PROBE 14
MAG.=76X

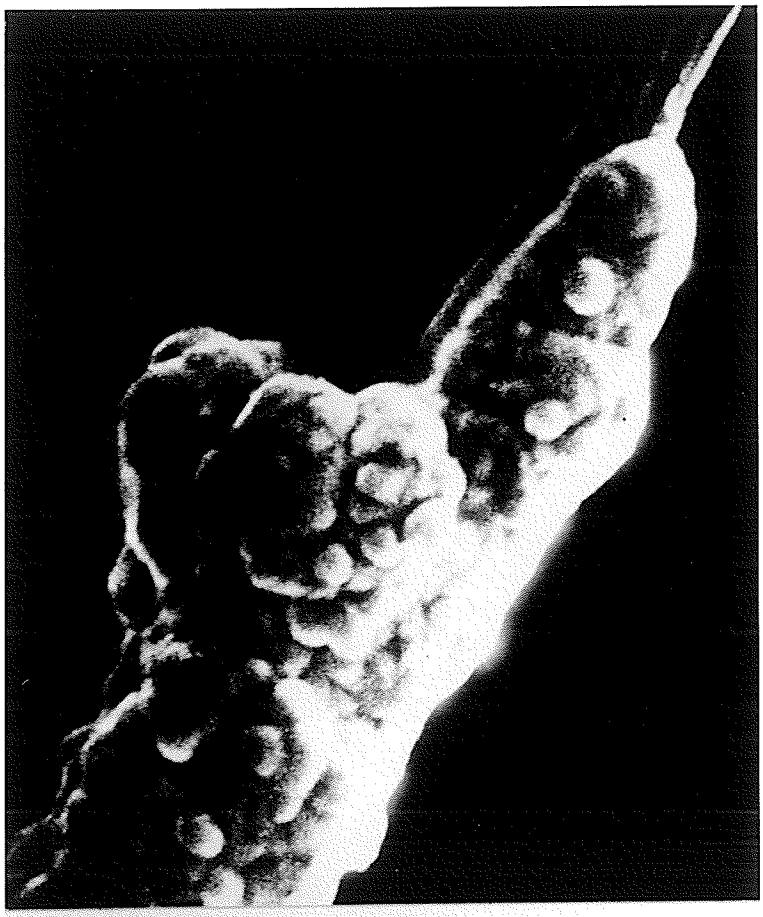

FIG. 3gg
PROBE 14
MAG.=1900X

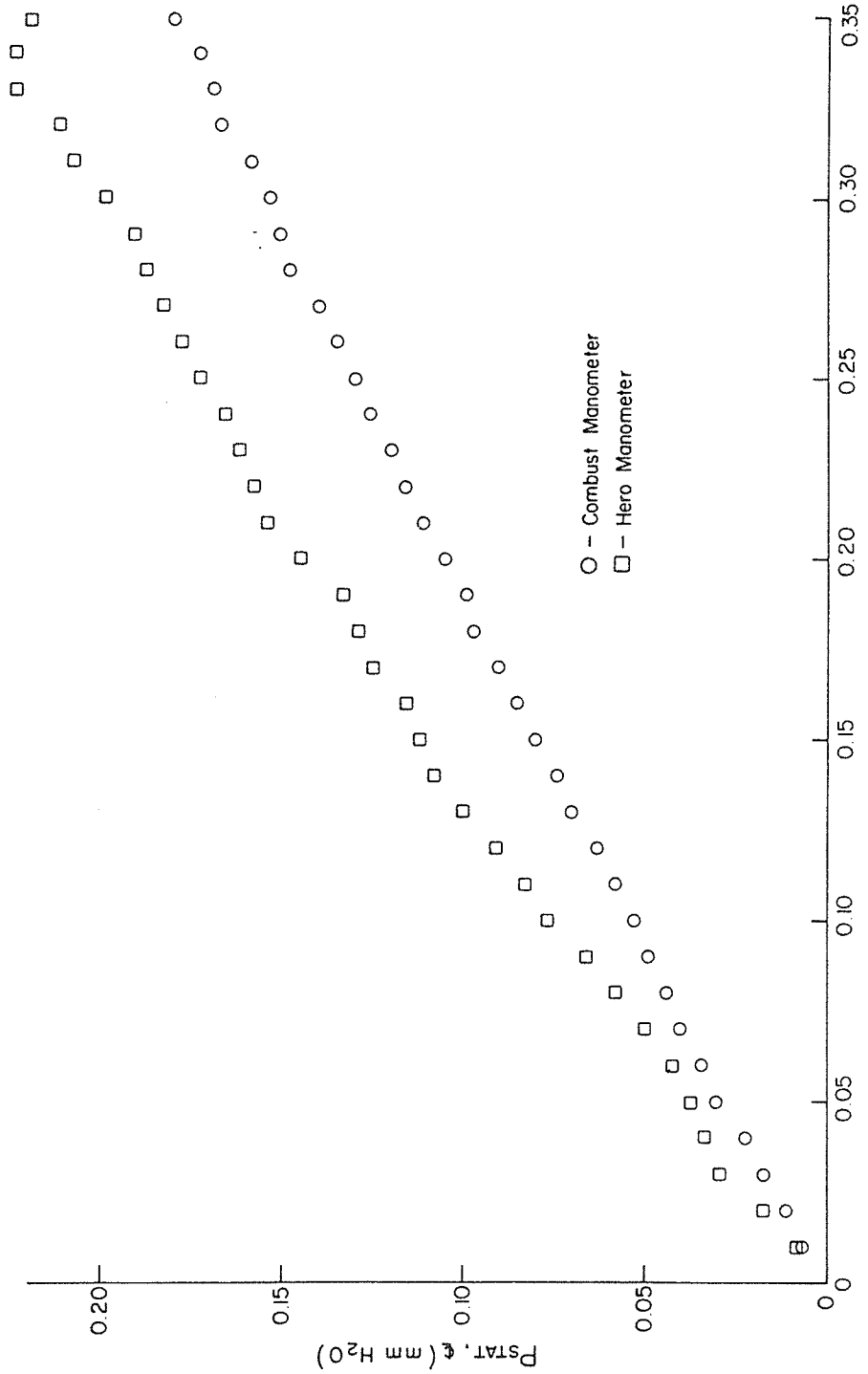

Figure 4: Static Pressure Versus Cone Pressure.

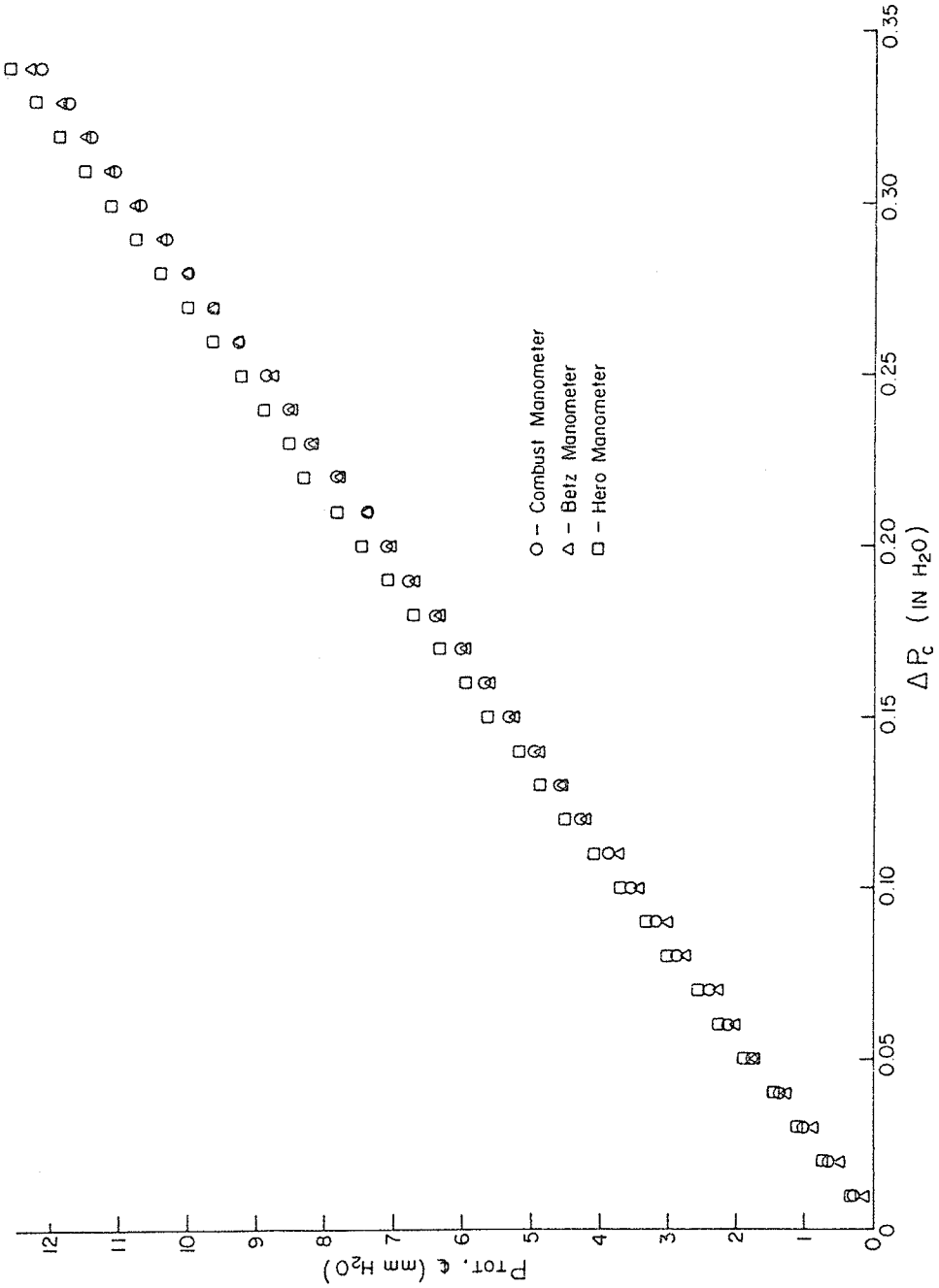

Figure 5: Total Pressure Versus Cone Pressure.

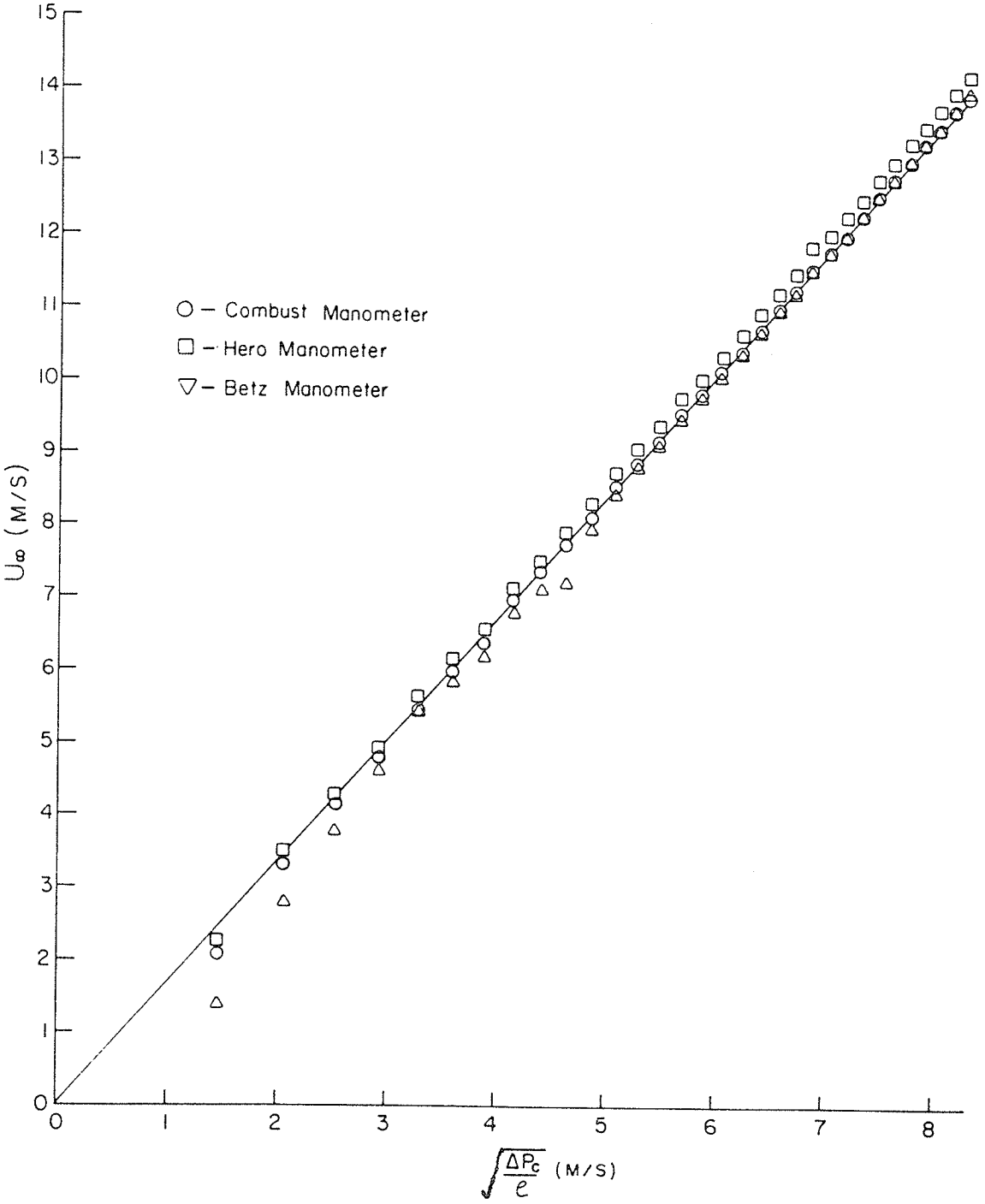

Figure 6: Centerline Velocity Versus Cone Pressure.

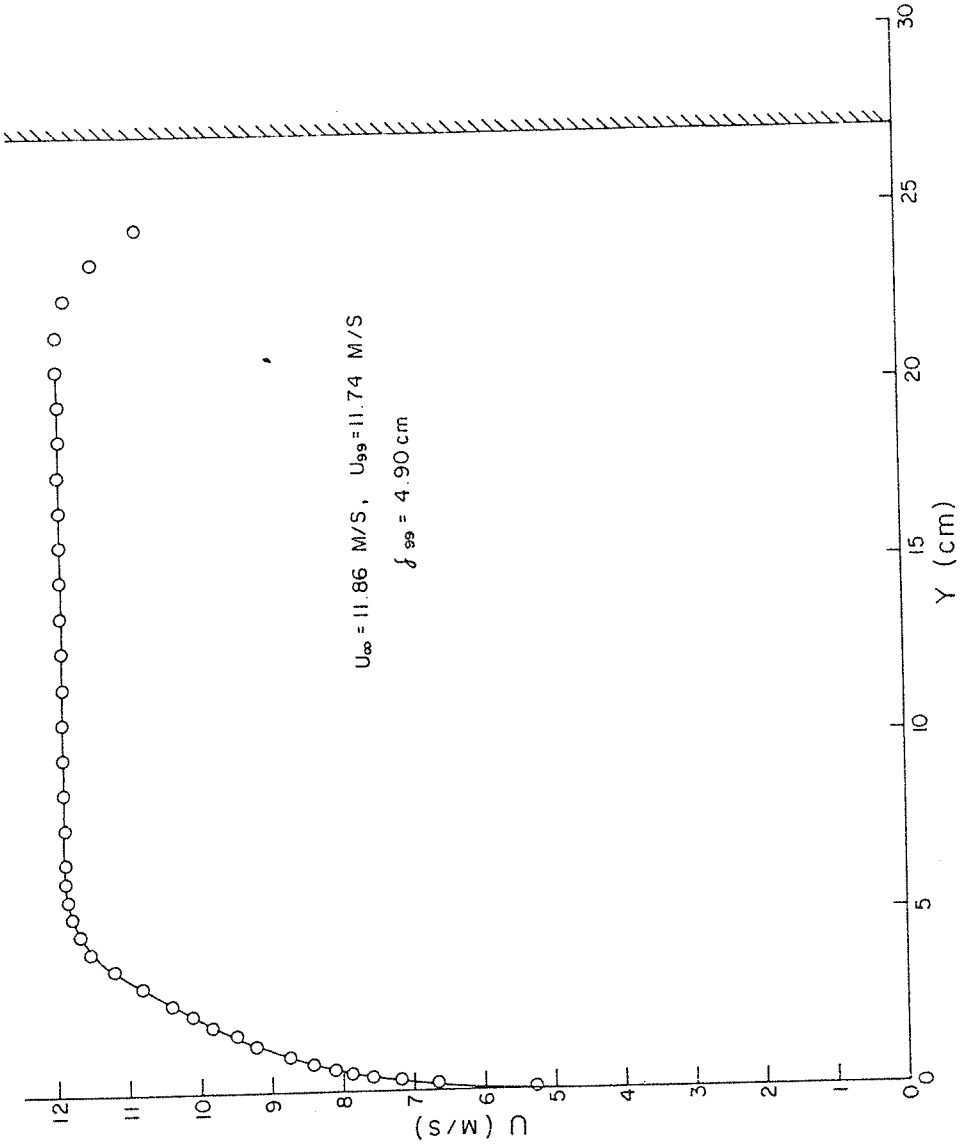

Figure 7: Velocity Distribution at U_∞ = 12 m/s, Pitot Tube.

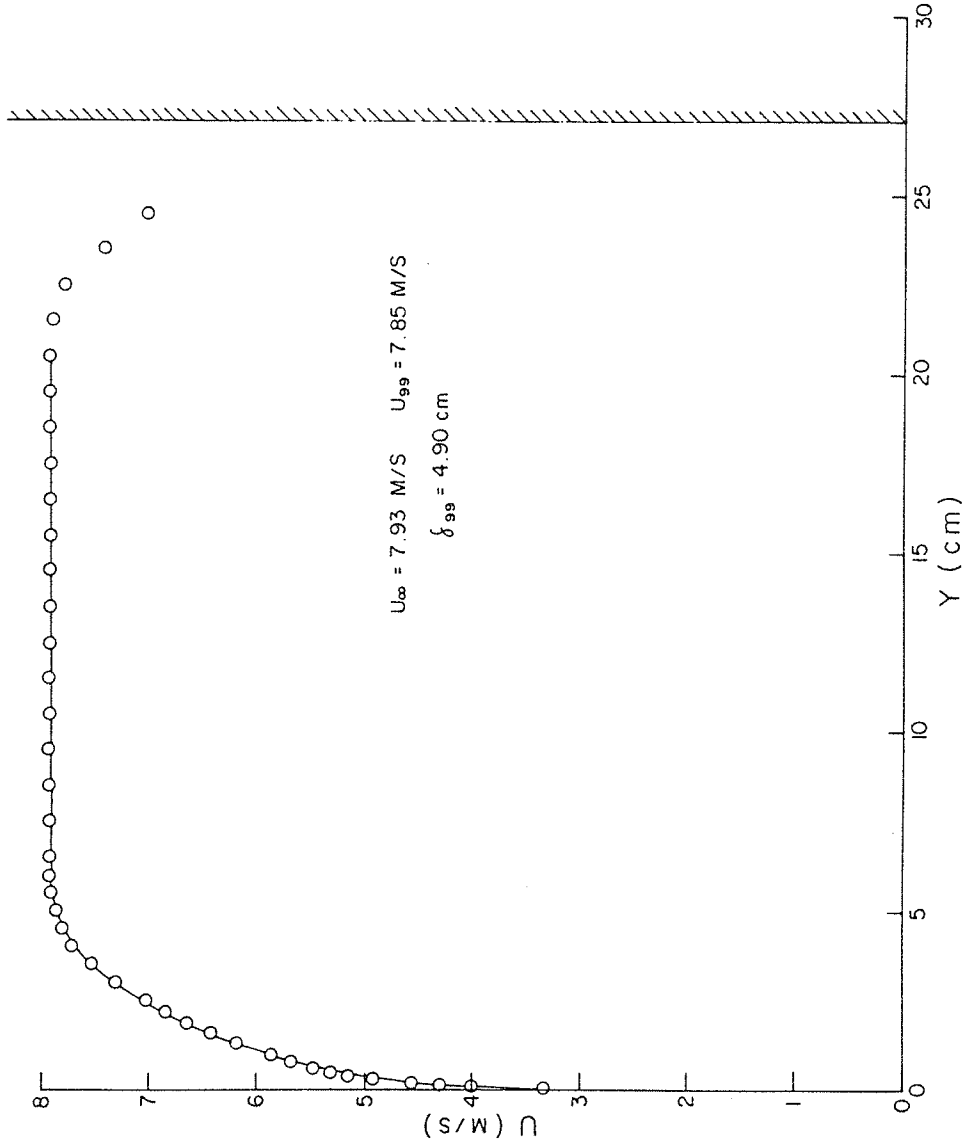

Figure 8: Velocity Distribution at U_∞ = 8 m/s, Pitot Tube.

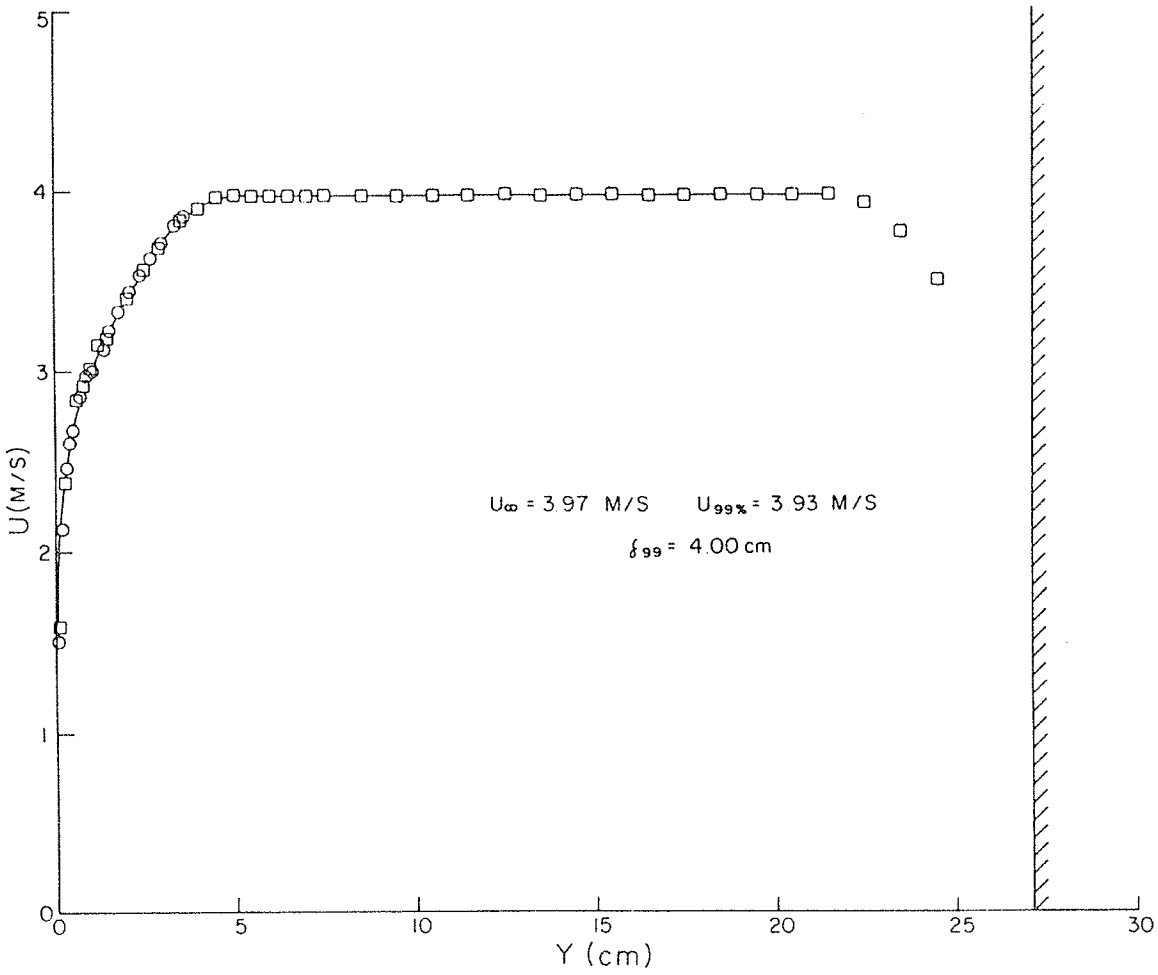

Figure 9: Velocity Distribution at U_∞ = 4 m/s, Pitot Tube.

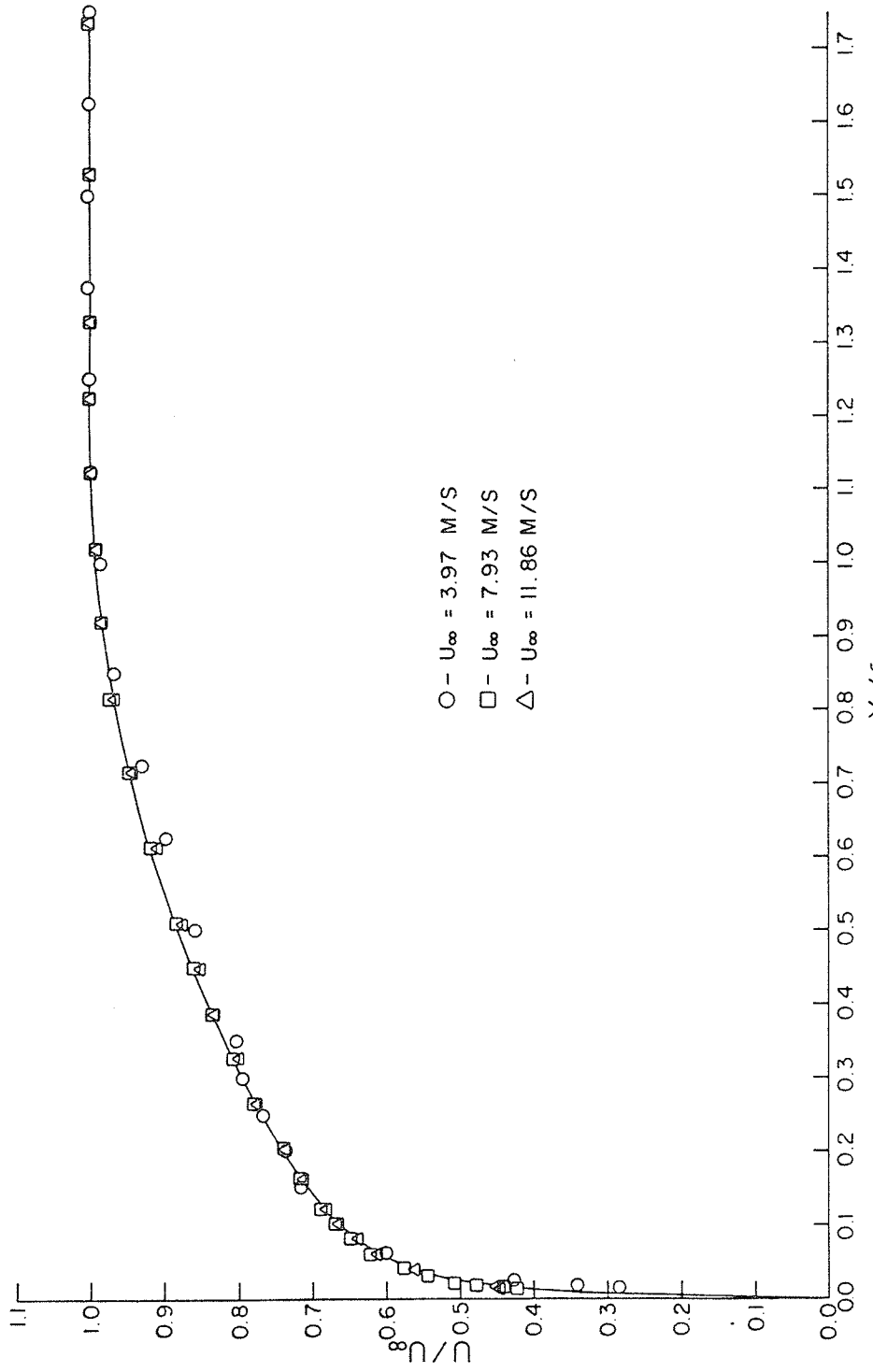

Figure 10: Normalized Velocity (U/U_∞) versus Y/δ, Pitot Tube.

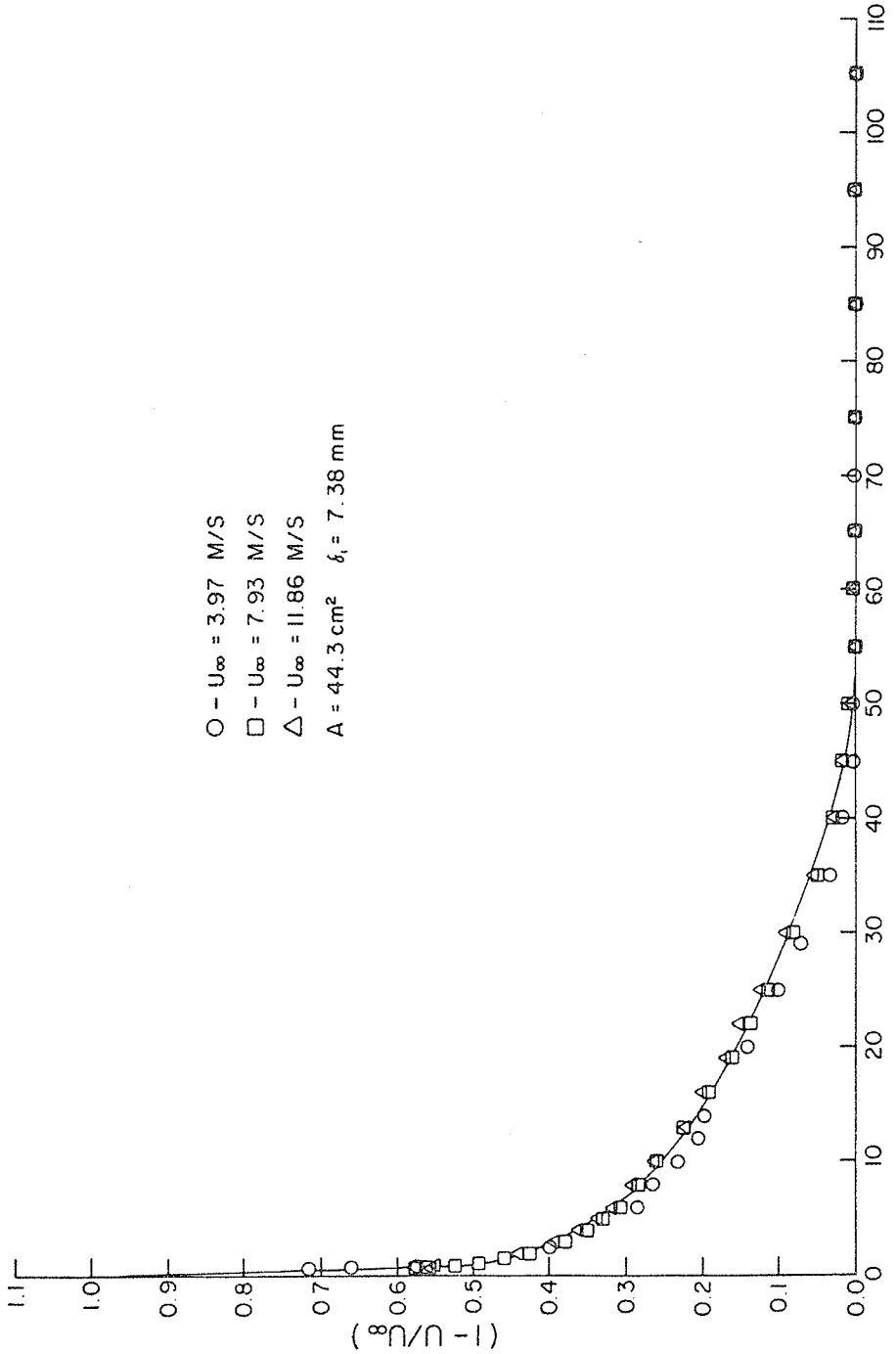

Figure 11: Displacement Thickness ($1-U/U_\infty$) Plot, Pitot Tube.

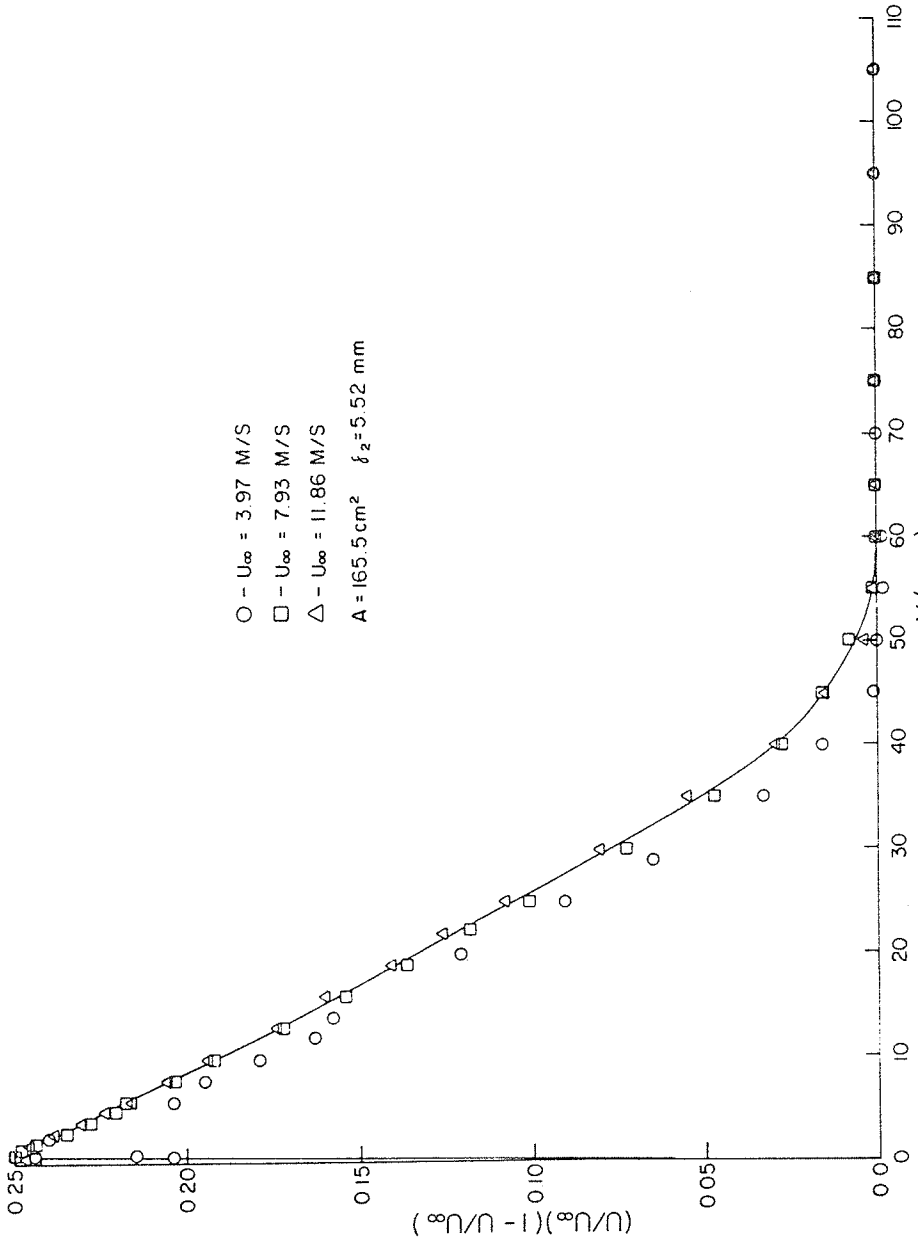

Figure 12: Momentum Thickness $U(1-U/U_\infty)/U_\infty$ Plot, Pitot Tube.

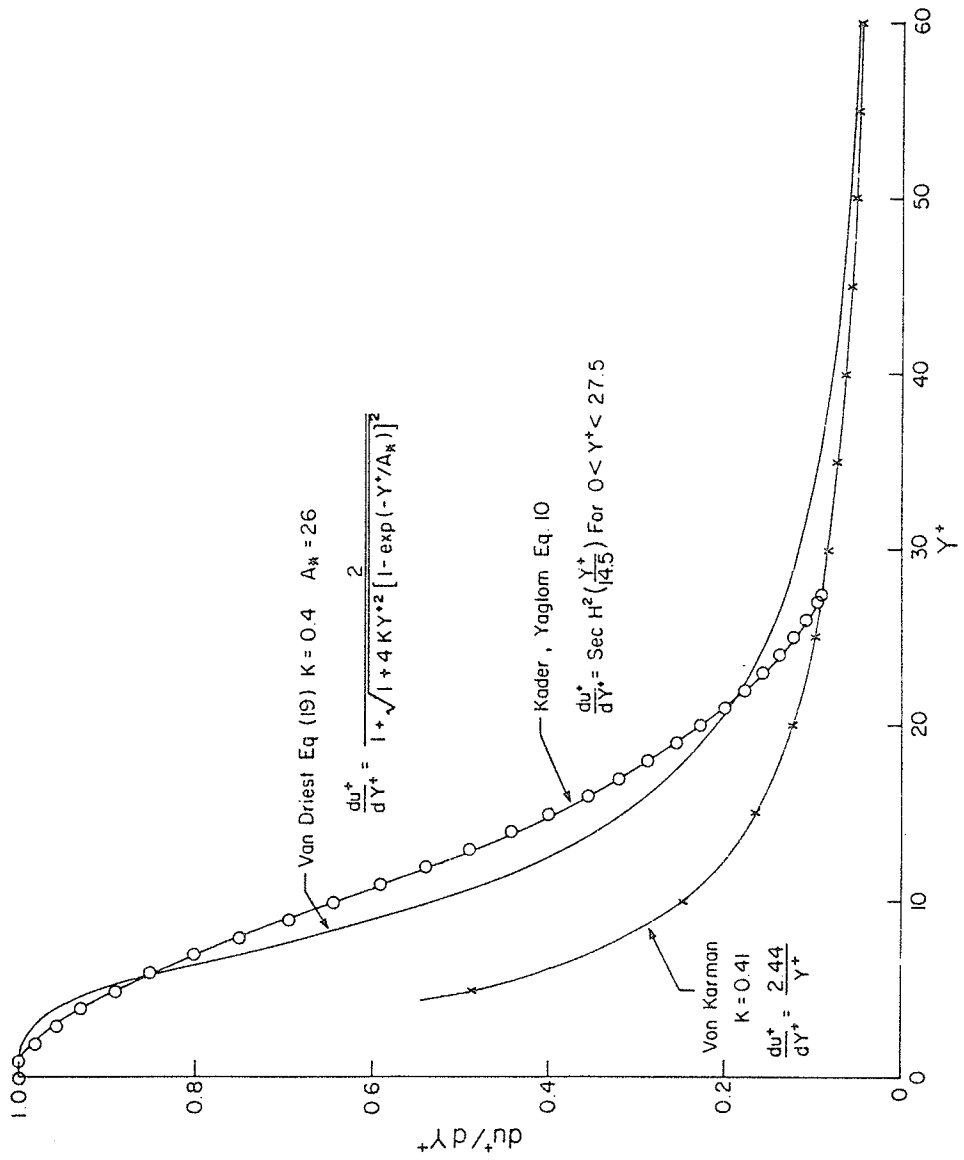

Figure 13: Non-dimensional Mean Velocity Gradients Near The Wall.

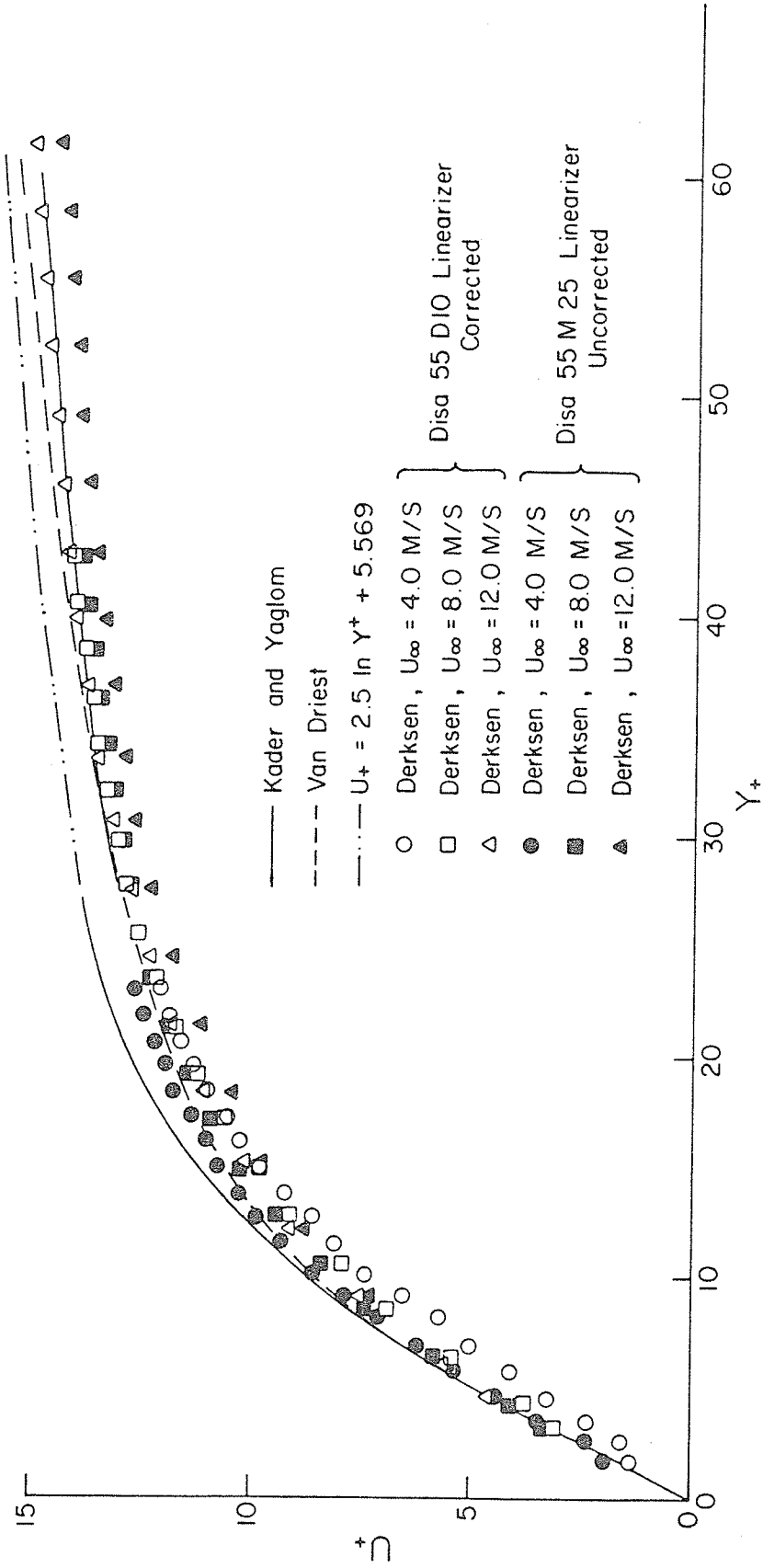

Figure 14: U_+ Versus Y_+ Linear Plot.

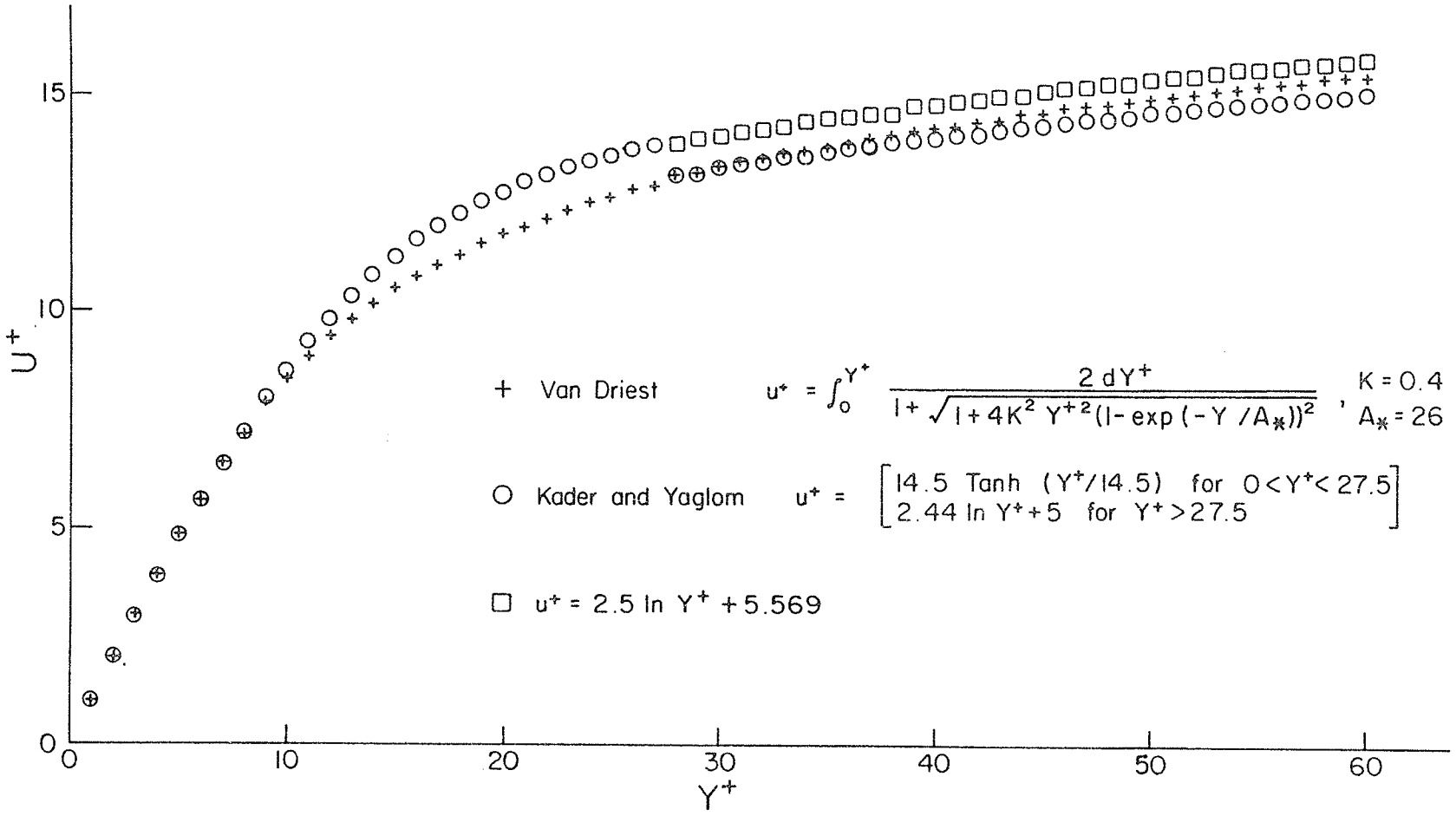

Figure 15: Plot of Viscous Sublayer-Buffer Layer Laws.

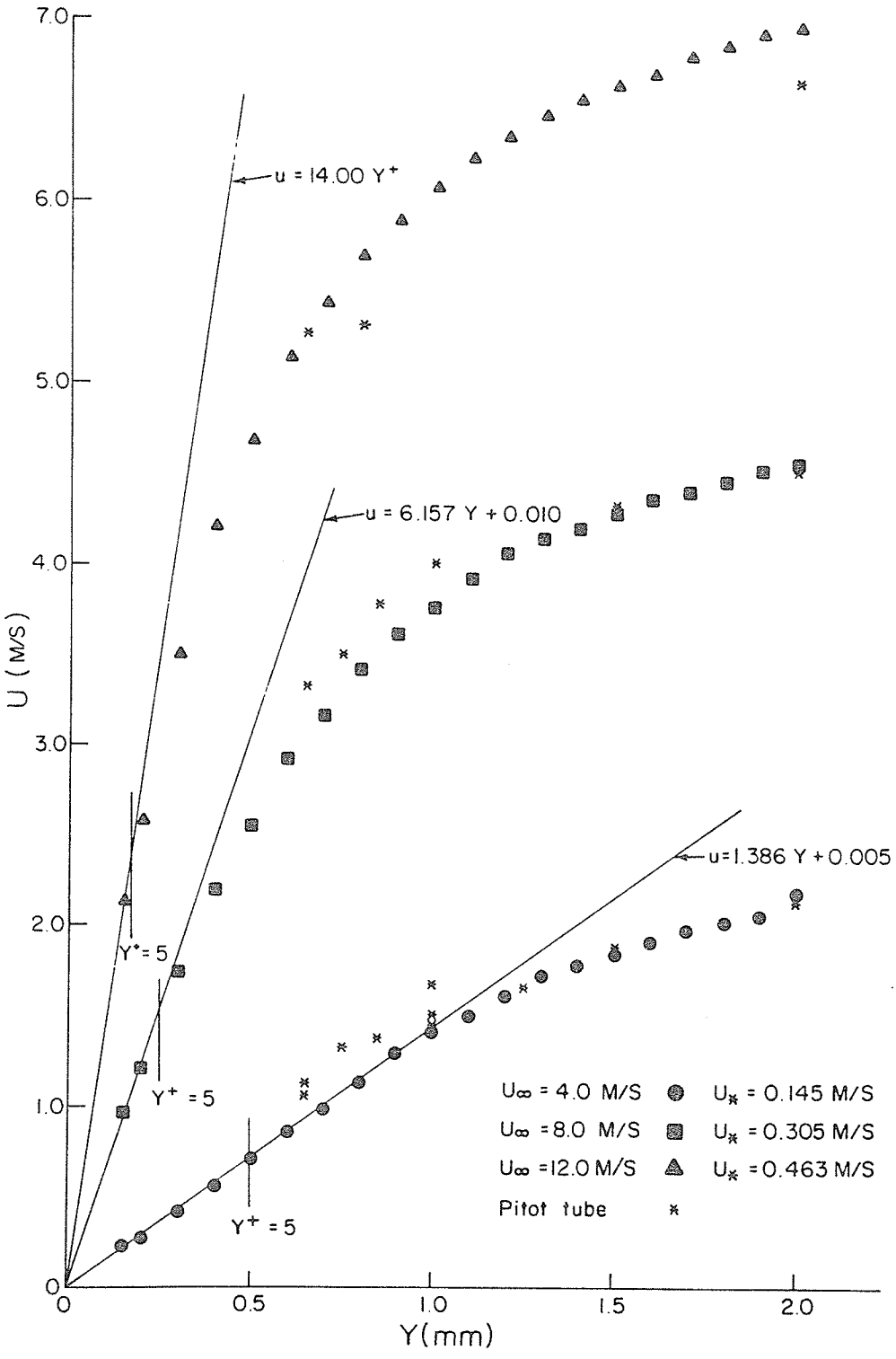

Figure 16: Mean Velocity Versus the Distance from the Wall (0 to 2 mm).

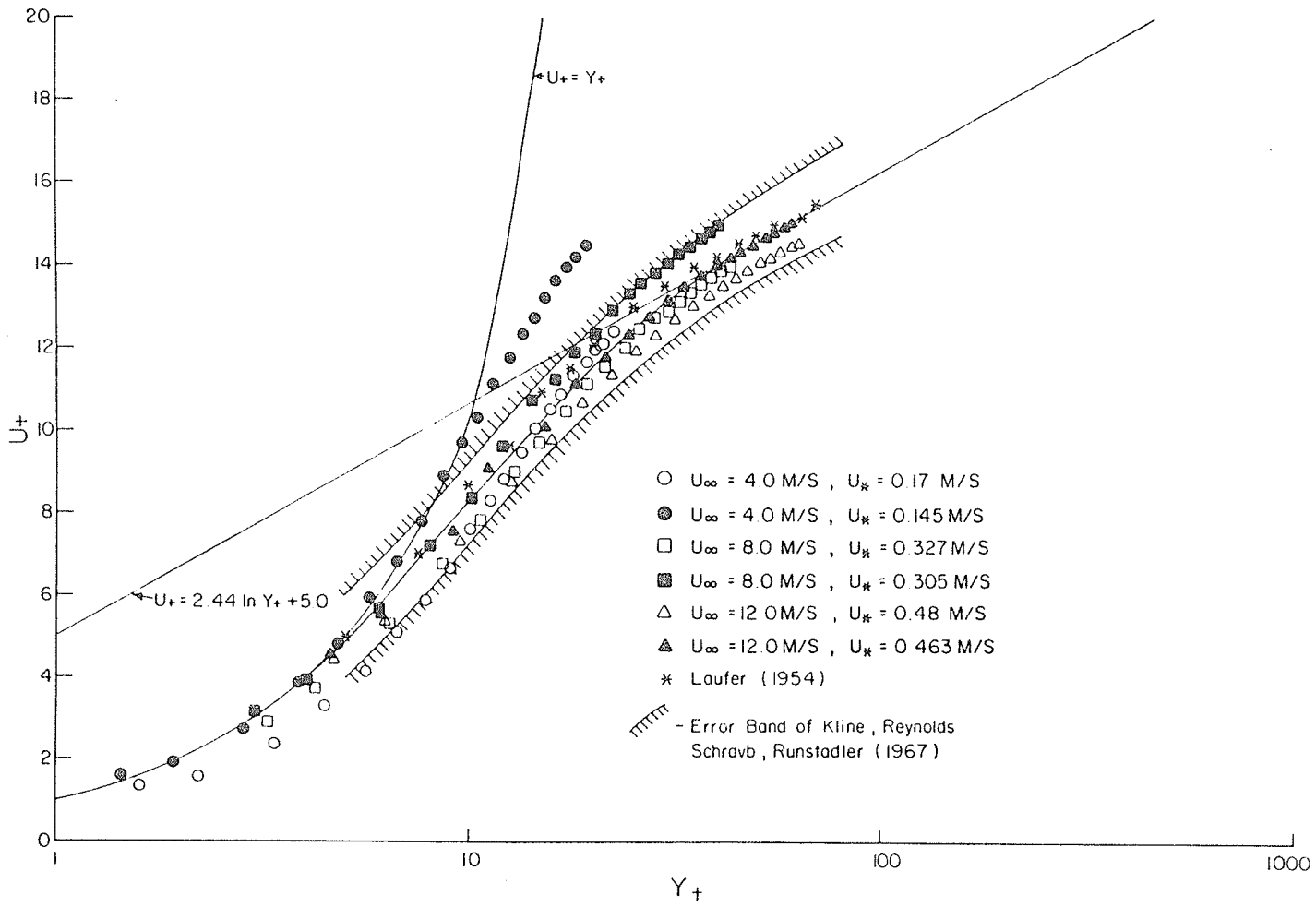

Figure 17: Uncorrected U_+ Distribution. Open symbols u_* calculated from wall derivative, closed symbols calculated from cross-log plots.

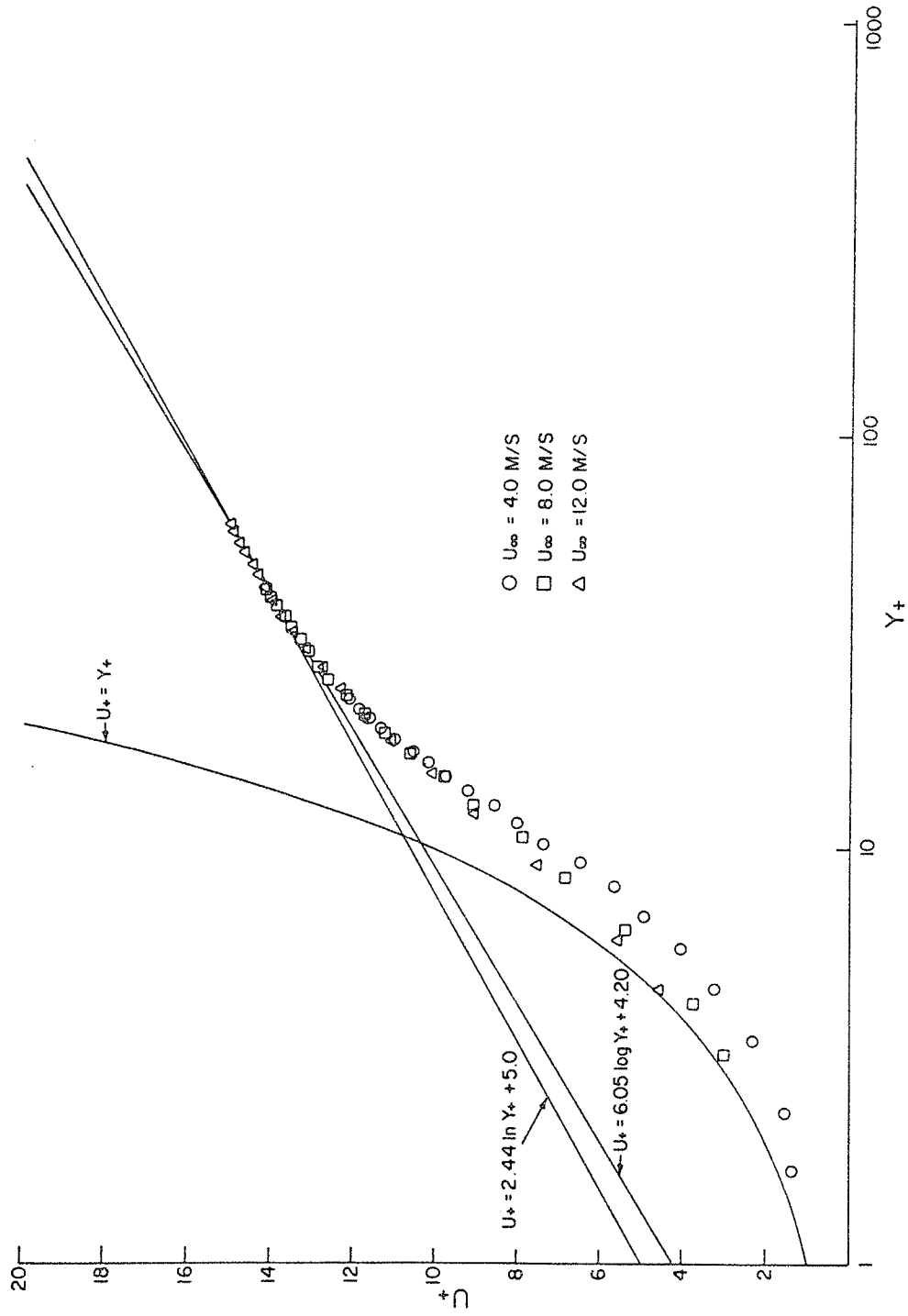

Figure 18: U_+ Distribution Corrected to Fit in Logarithmic Region.

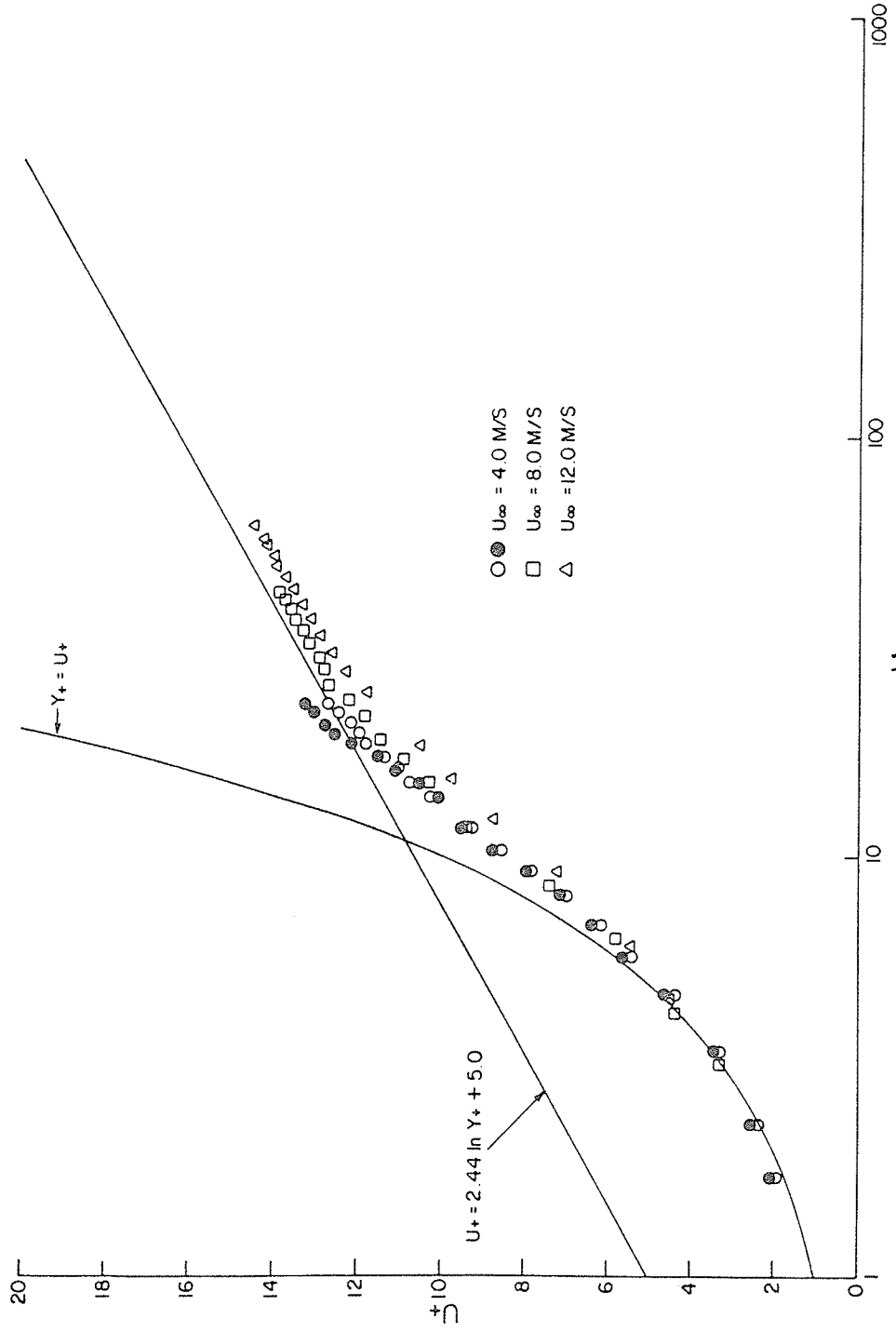

Figure 19: U_+ Distribution Corrected to Fit in Linear Region.

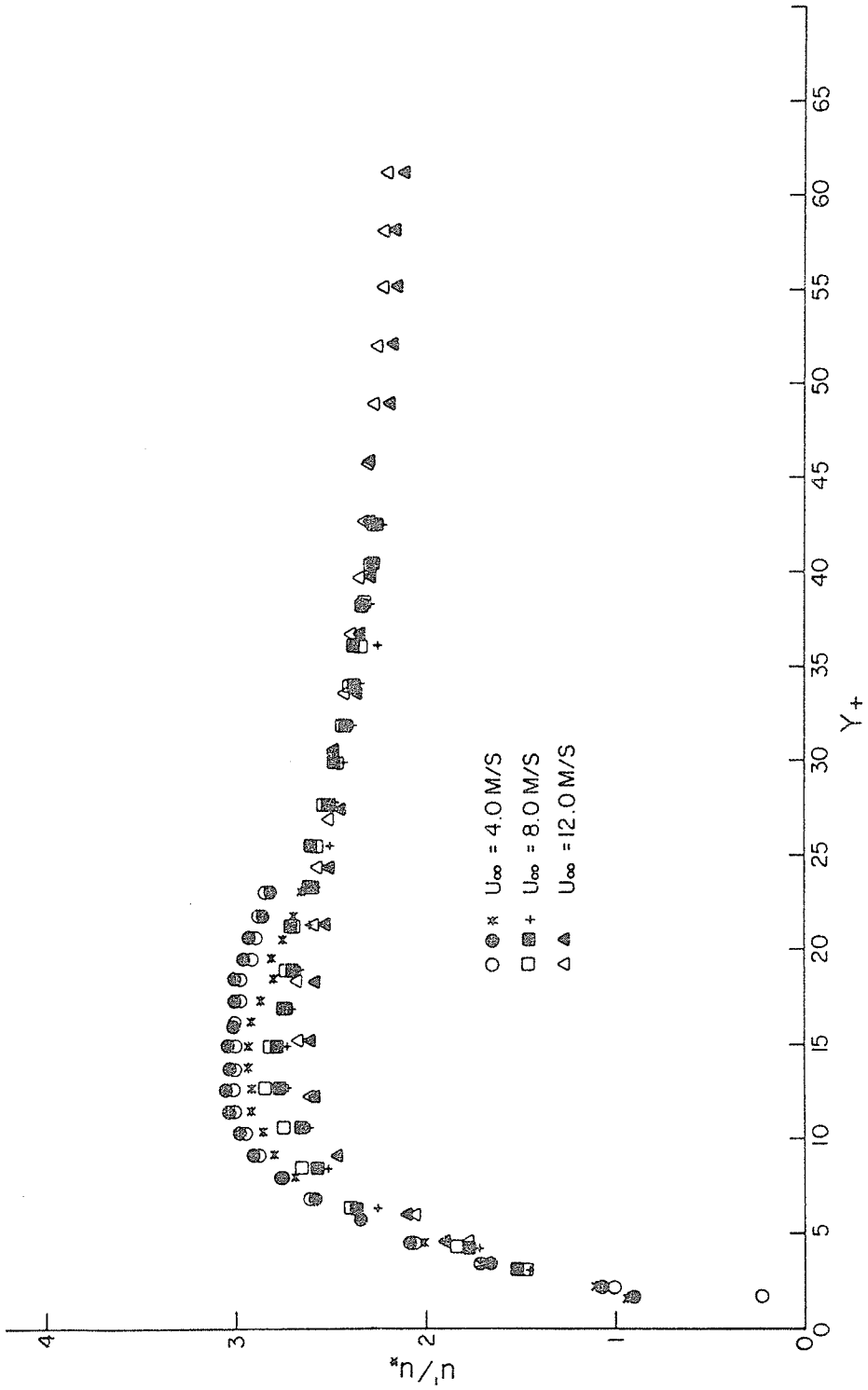

Figure 20: u'/u^* versus Y_+.

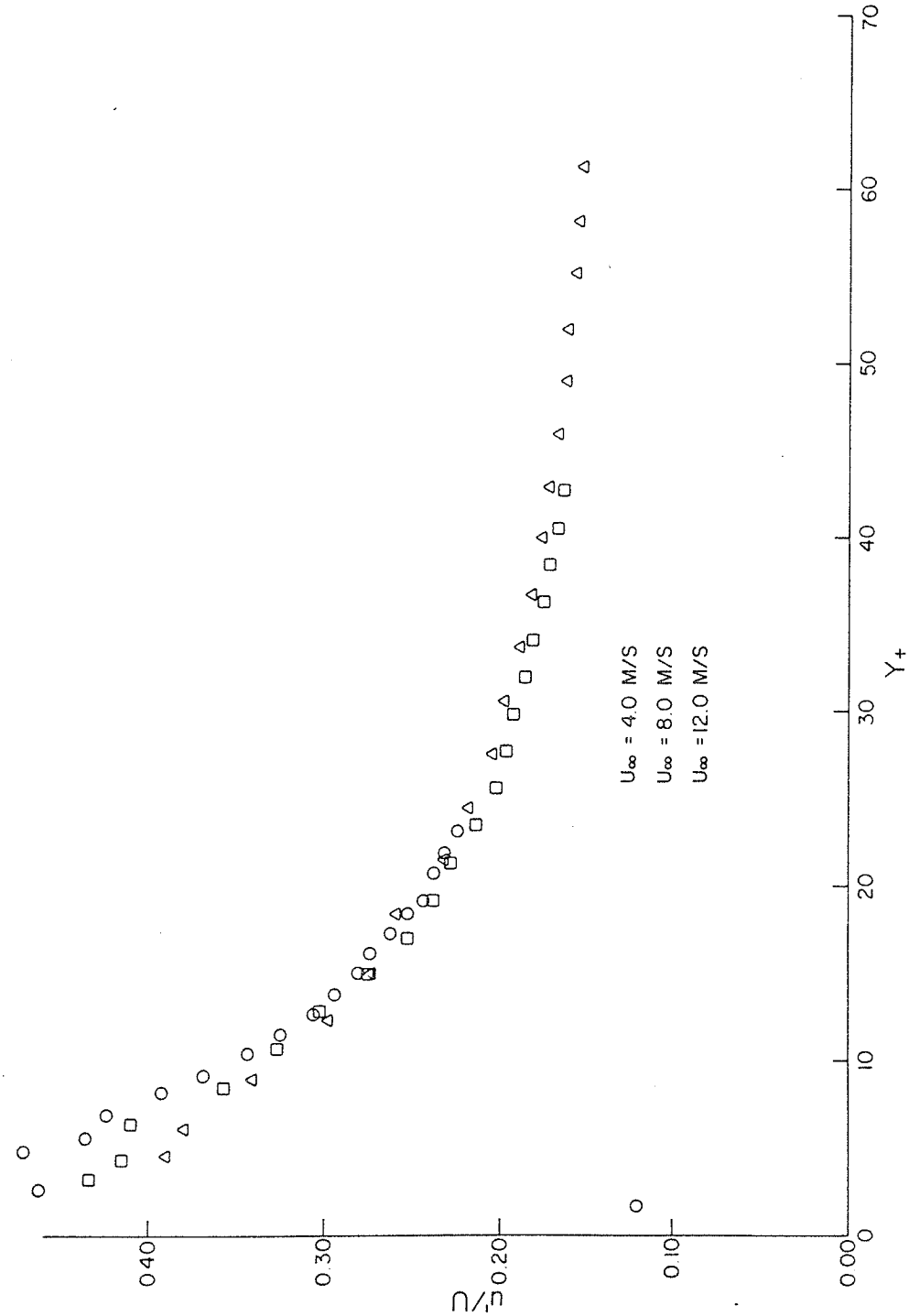

Figure 21: u'/U versus Y_+.

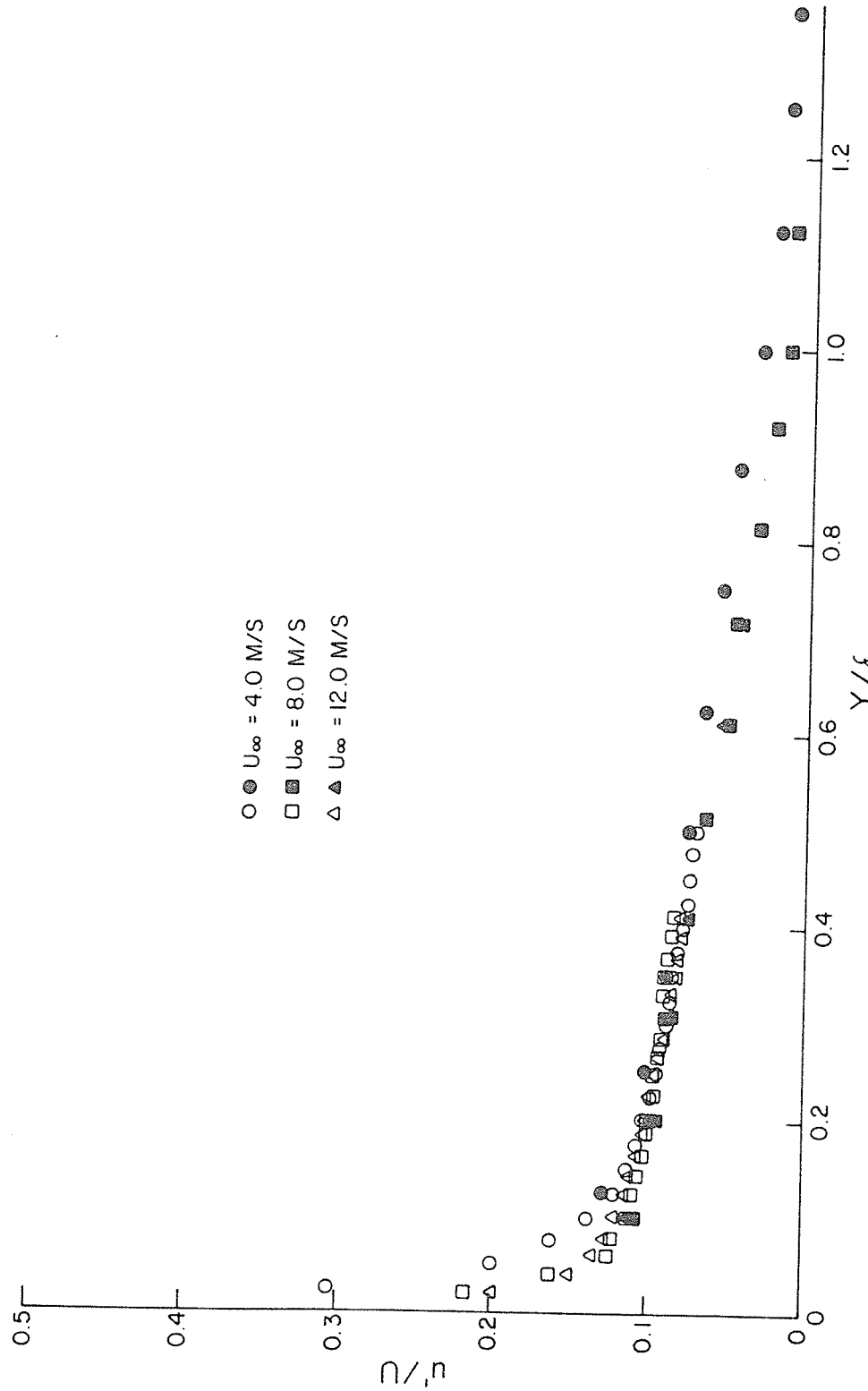

Figure 22: u'/U versus Y/δ_{99}.

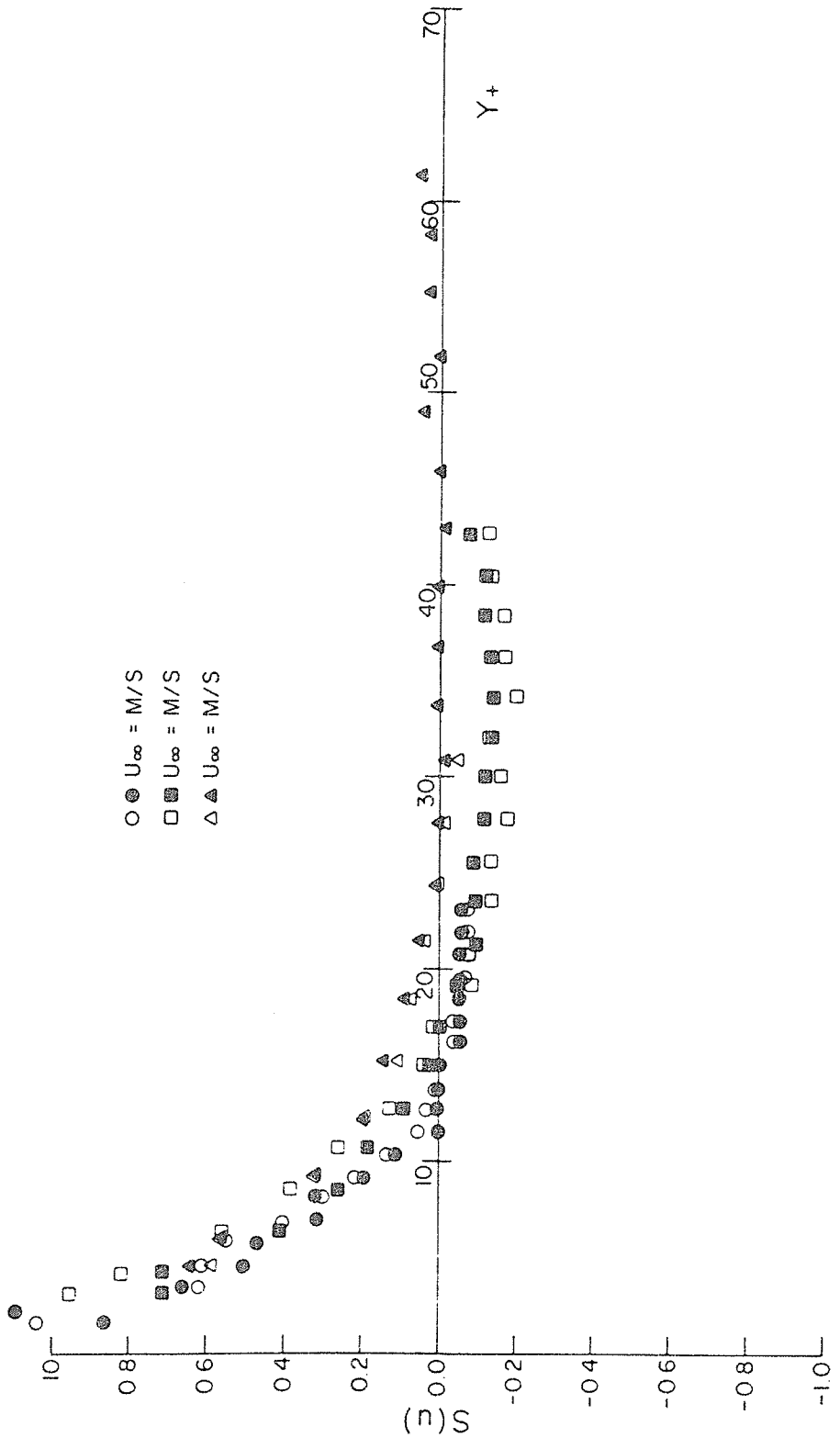

Figure 23: S(u) versus Y_+.

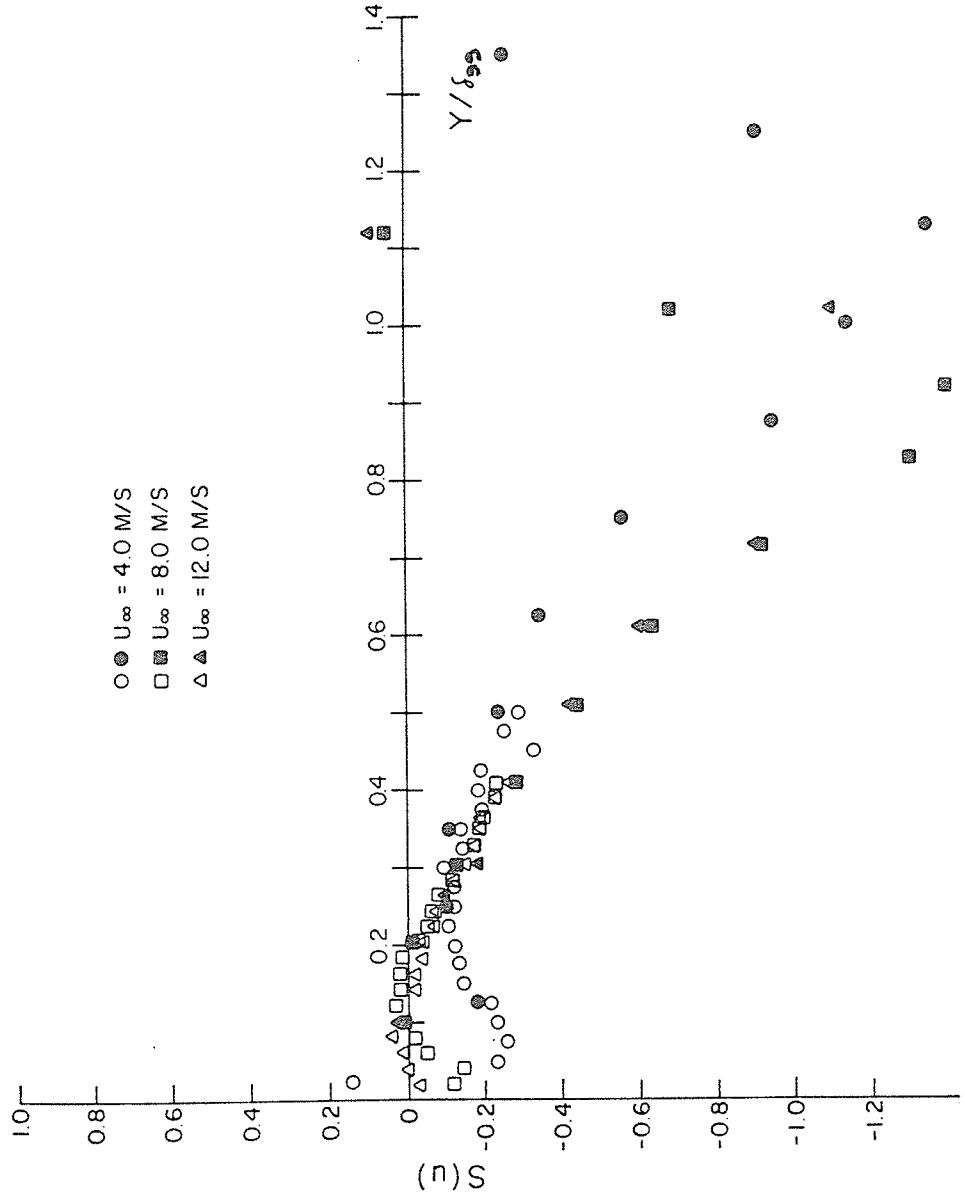

Figure 24: S(u) versus Y/δ_{99}.

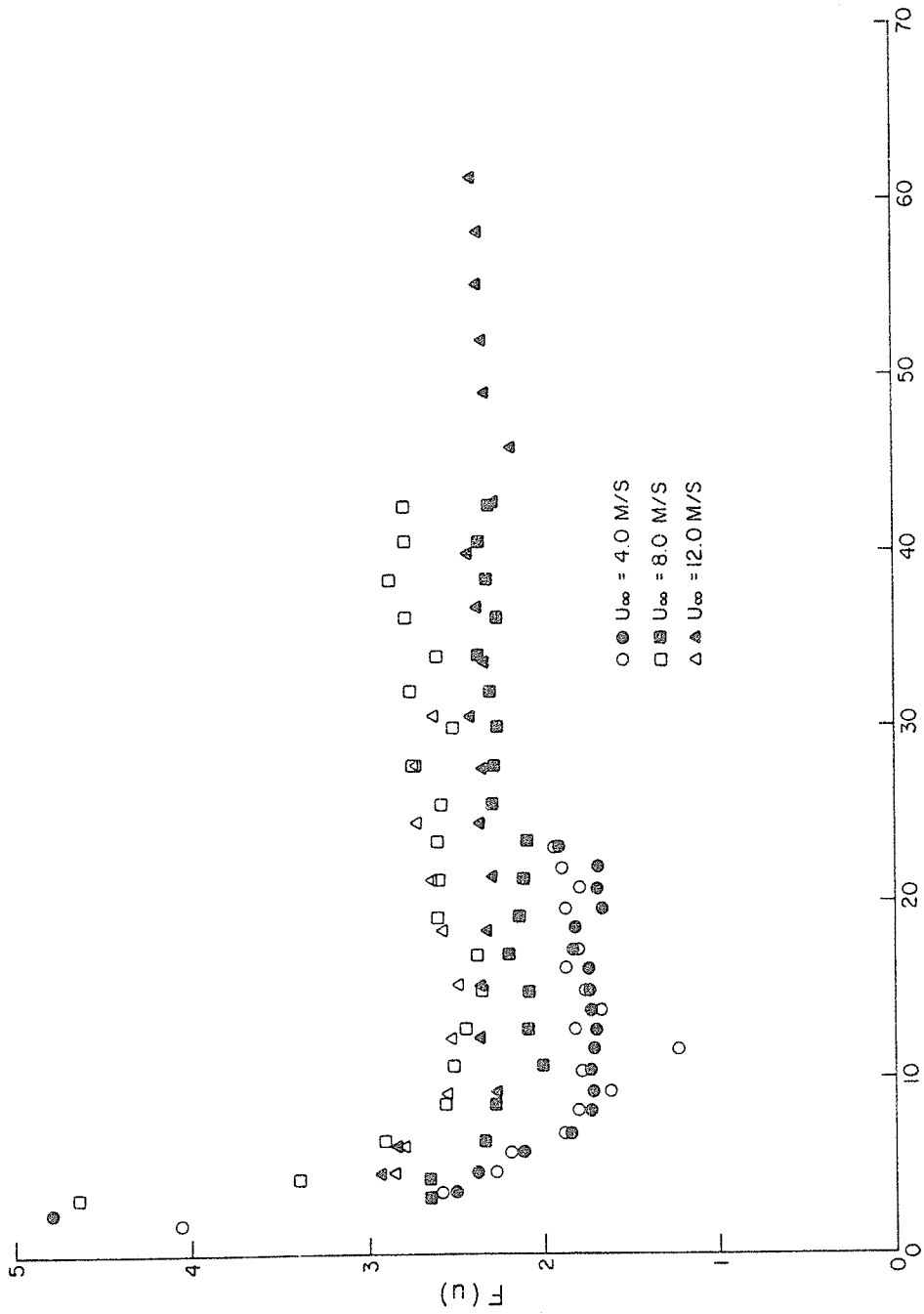

Figure 25: F(u) versus Y_+.

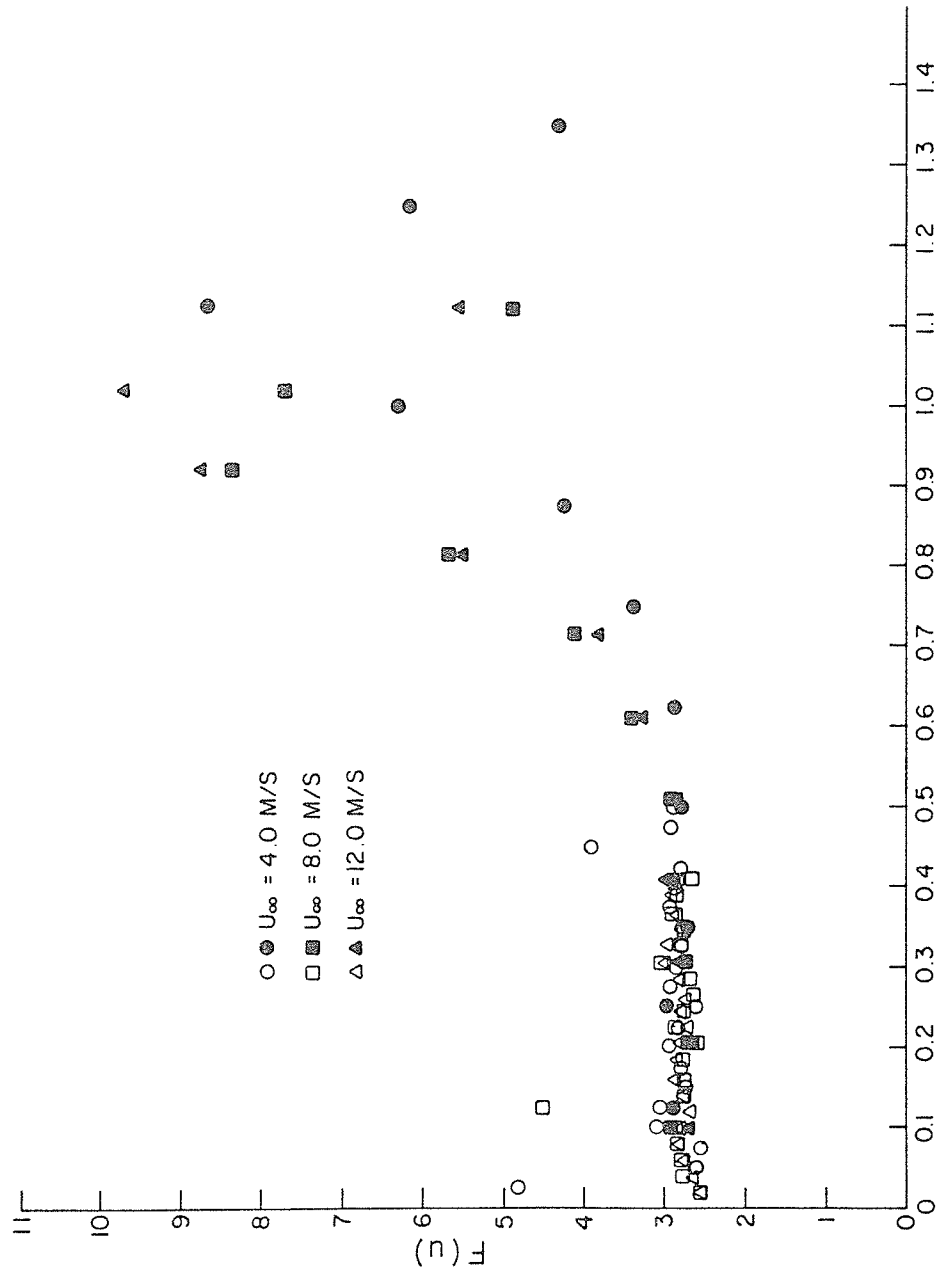

Figure 26: F(u) versus Y/δ_{99}.

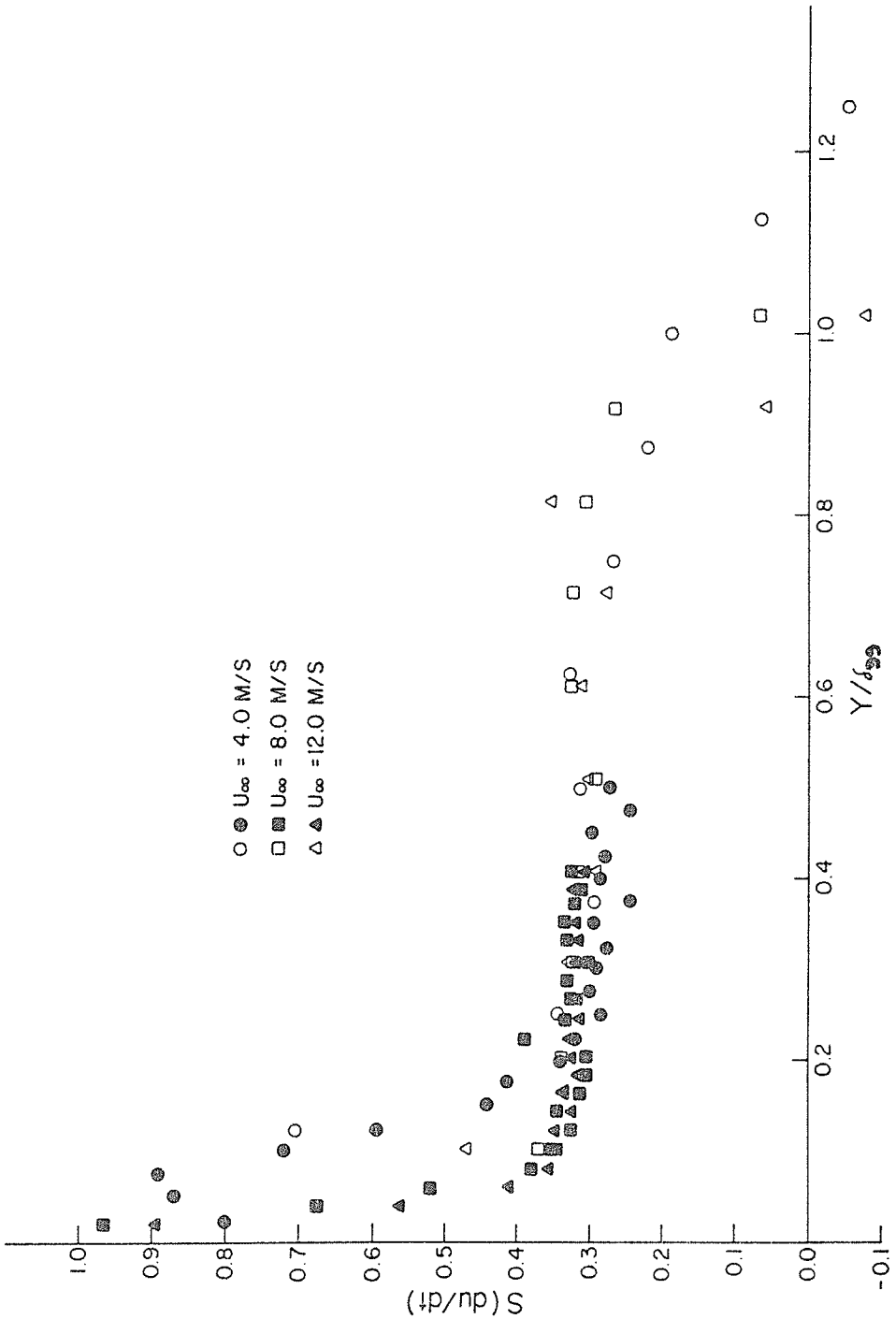

Figure 27: S(∂u/∂t) versus Y/δ_{99}.

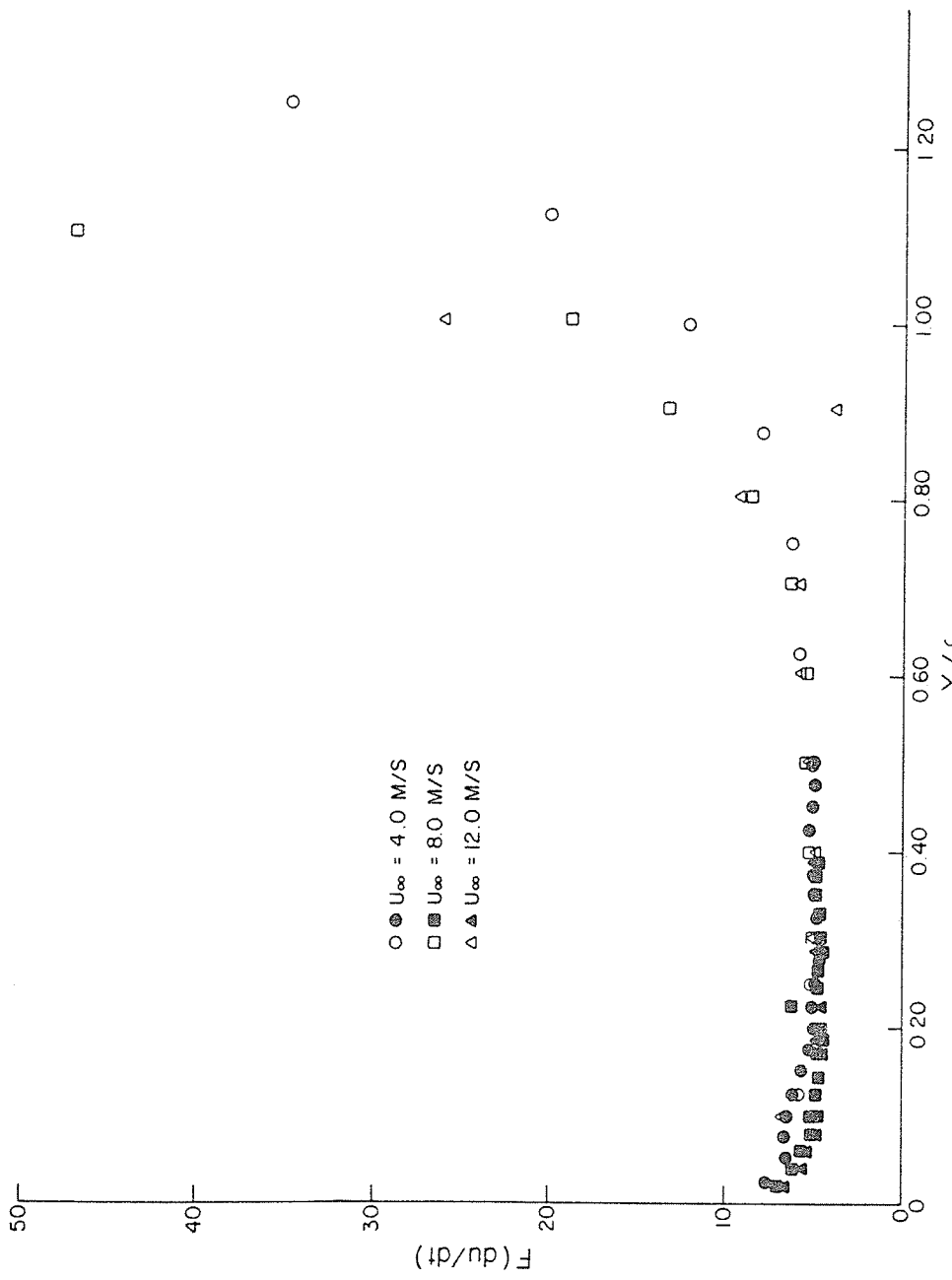

Figure 28: $F(\partial u/\partial t)$ versus Y/δ_{99}.

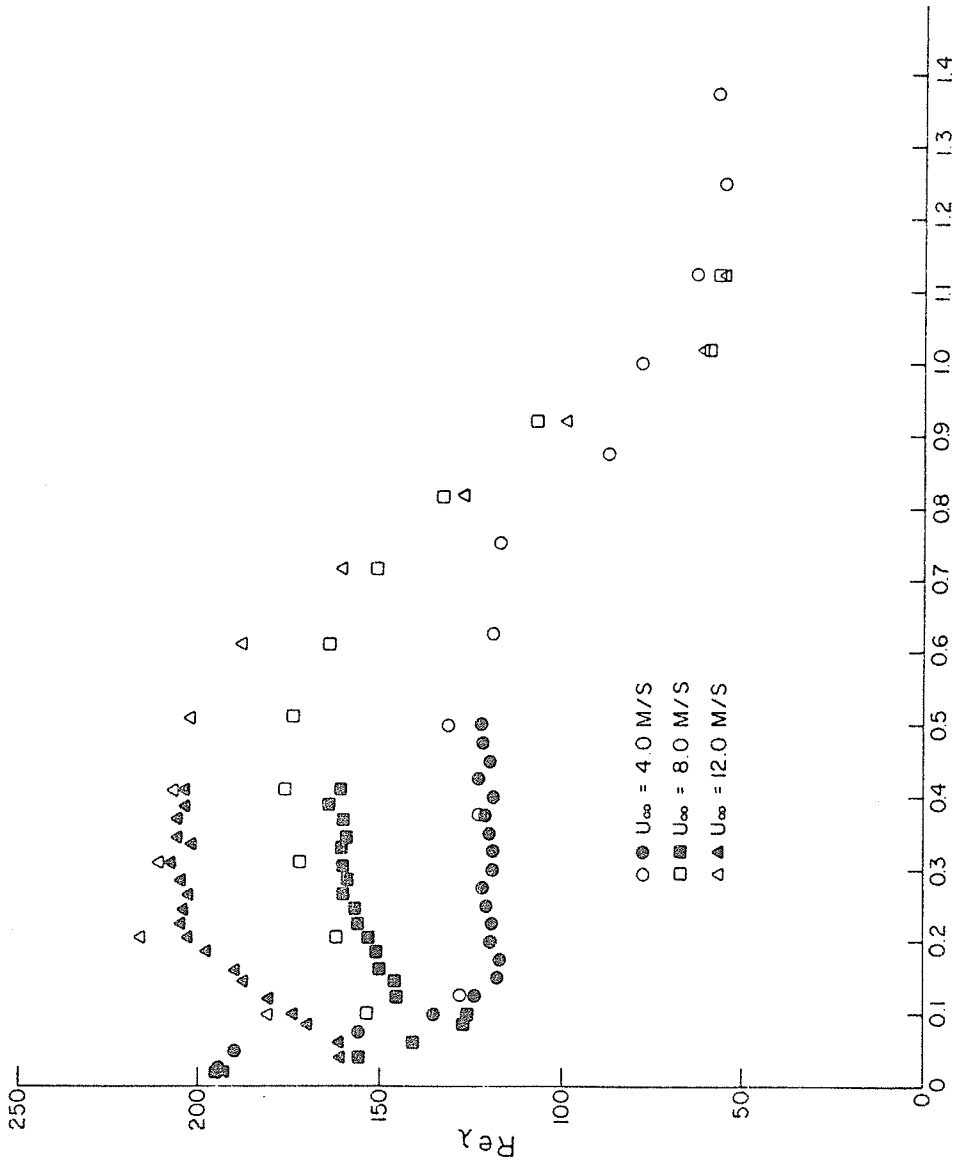

Figure 29: Re_λ versus Y/δ_{99}.

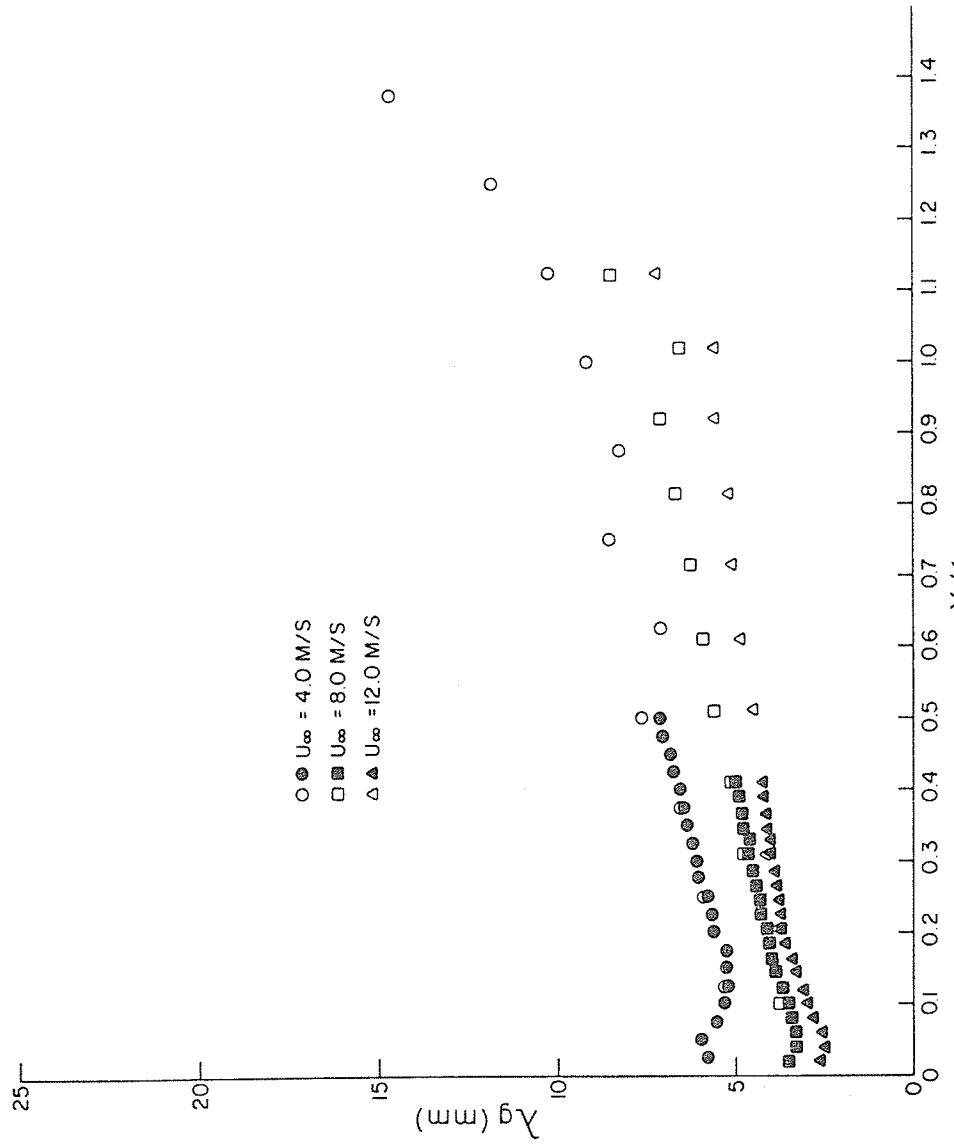

Figure 20: λ_g versus Y/δ_{gg}.

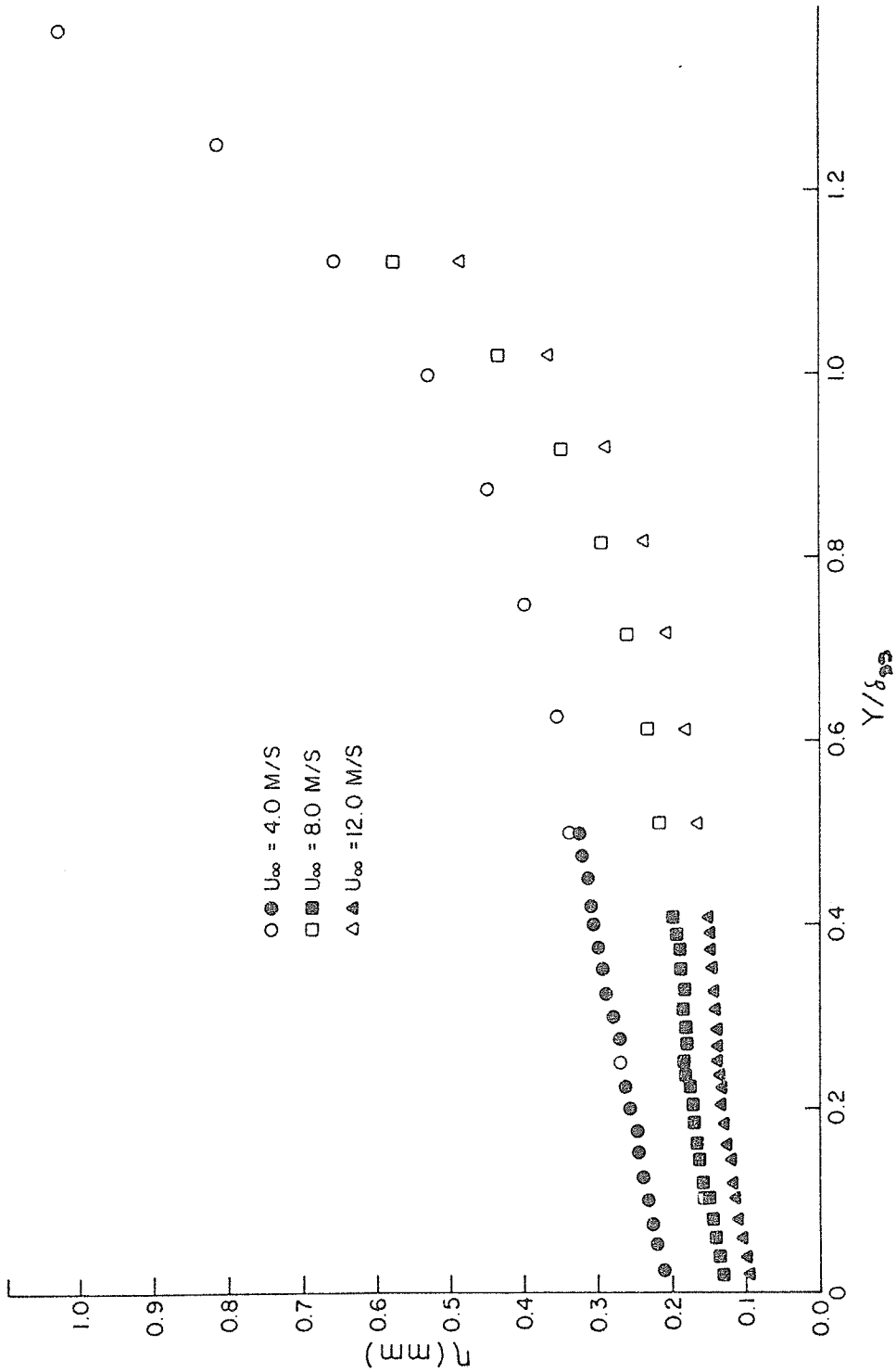

Figure 31: η versus Y/δ_{99}.

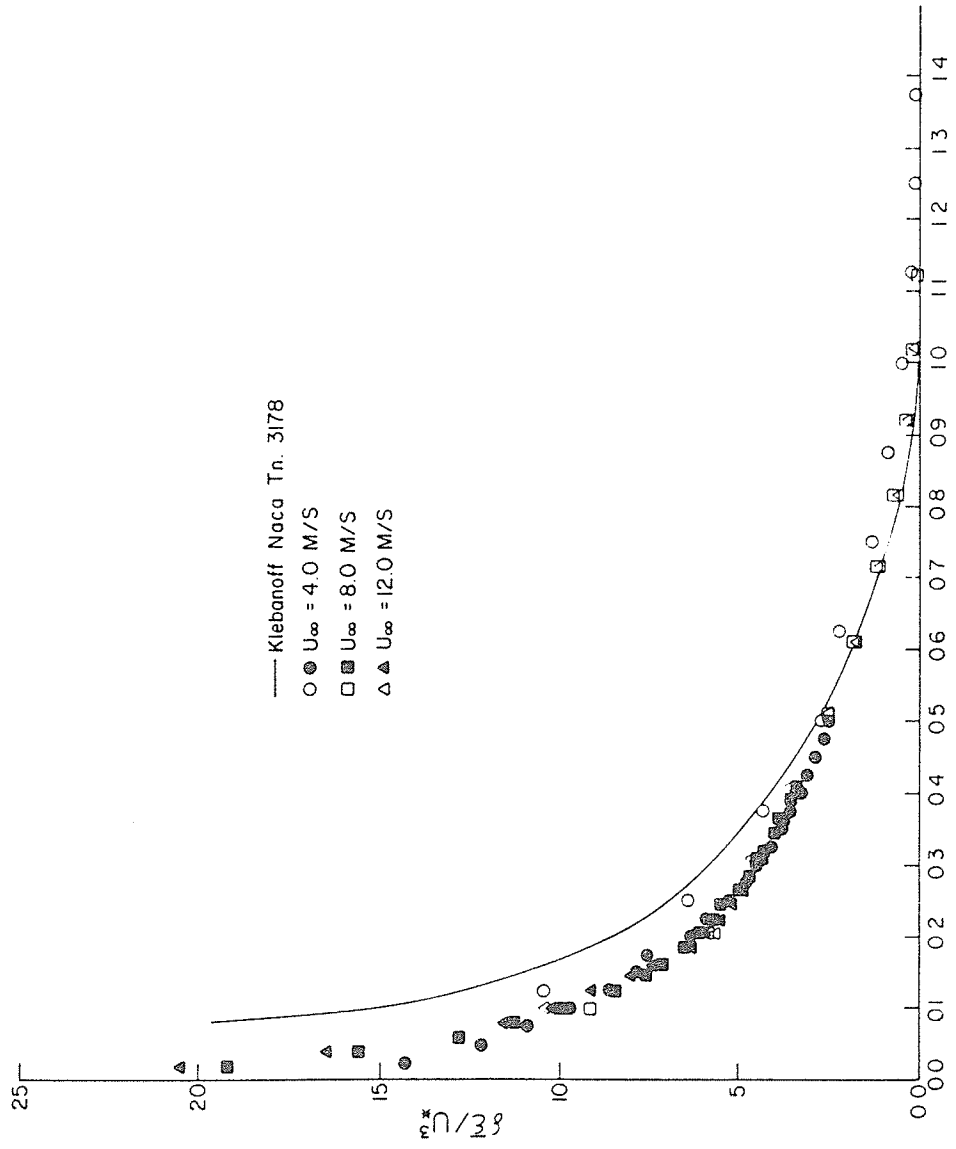

Figure 32: $\delta\tilde{\varepsilon}/u_*$ versus Y/δ_{99}.

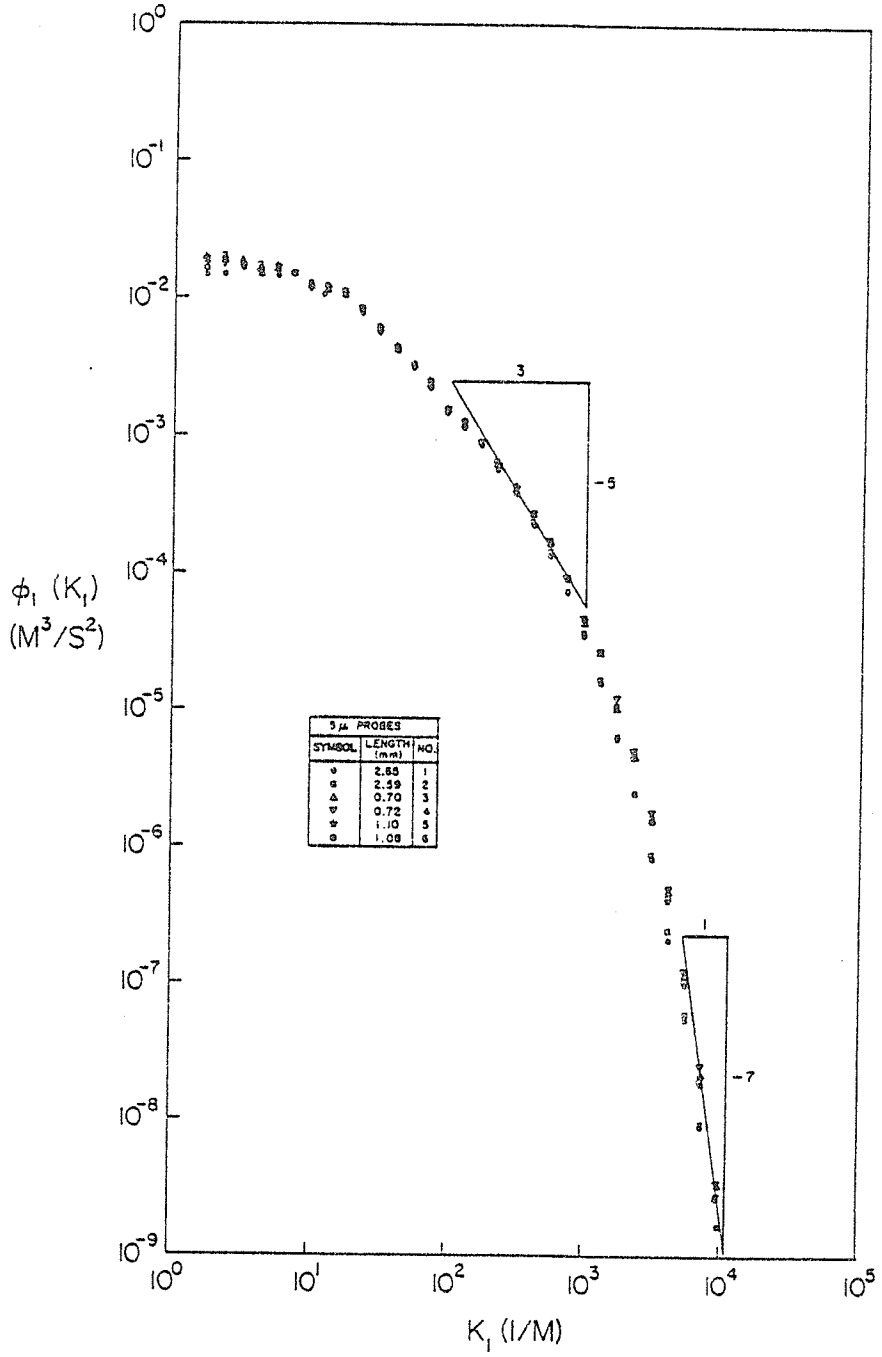

Figure 33: ϕ_1 Spectra for 5 μm Probes.

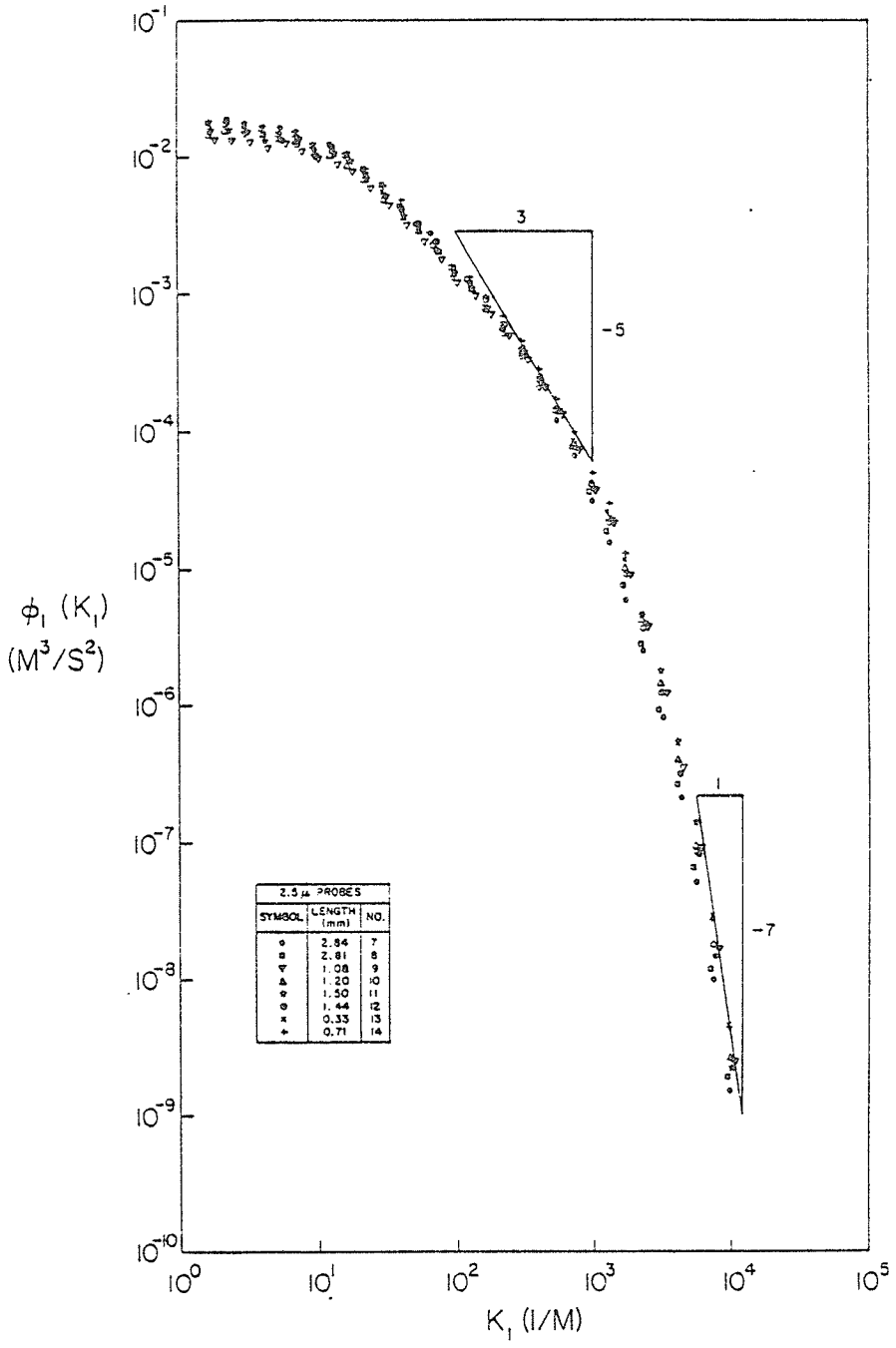

Figure 34: ϕ_1 Spectra for 2.5 μm Probes.

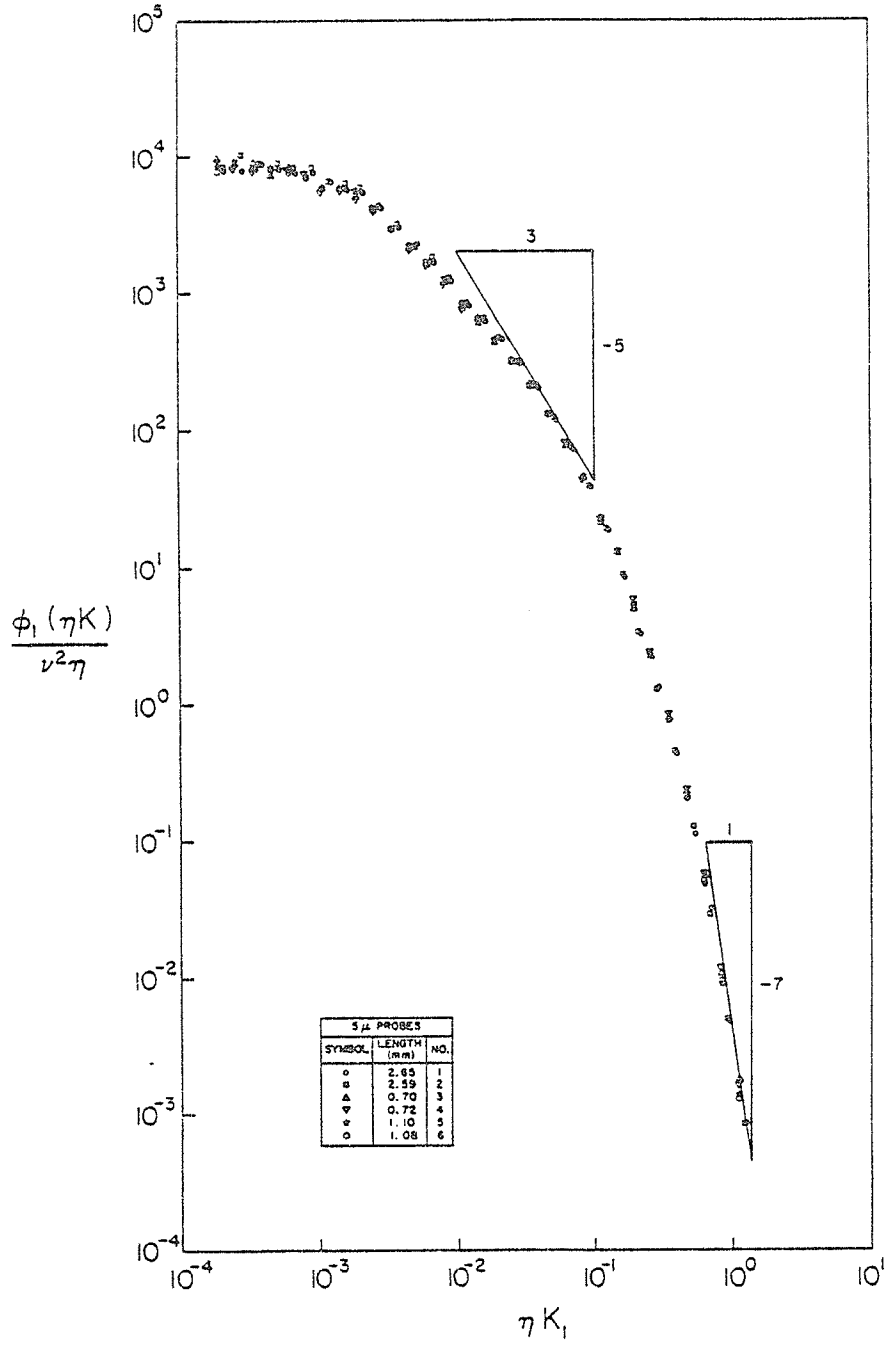

Figure 35: Non-dimensional ϕ_1 Spectra for 5 μm Probes.

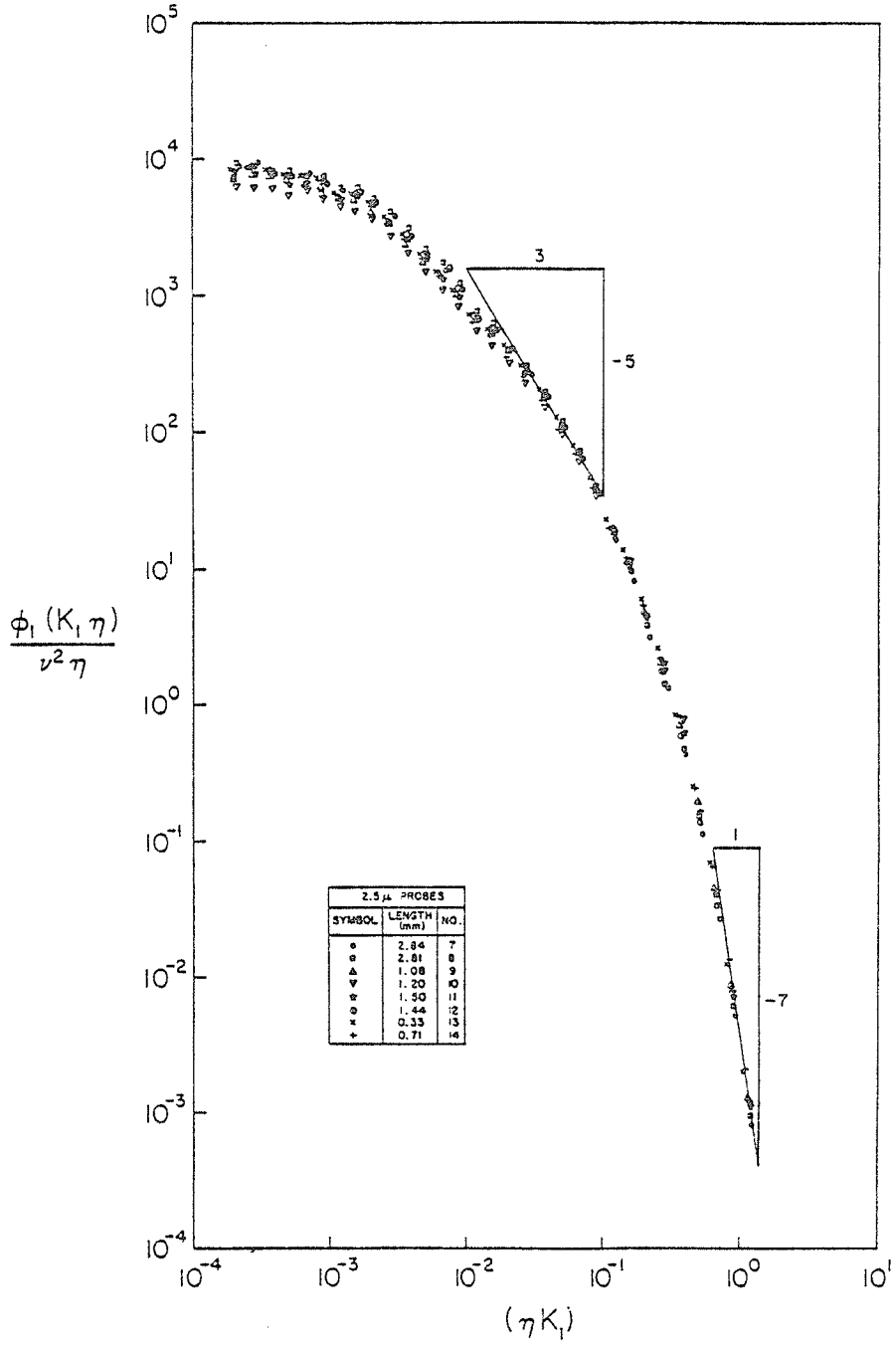

Figure 36: Non-dimensional ϕ_1 Spectra for 2.5 μm Probes.

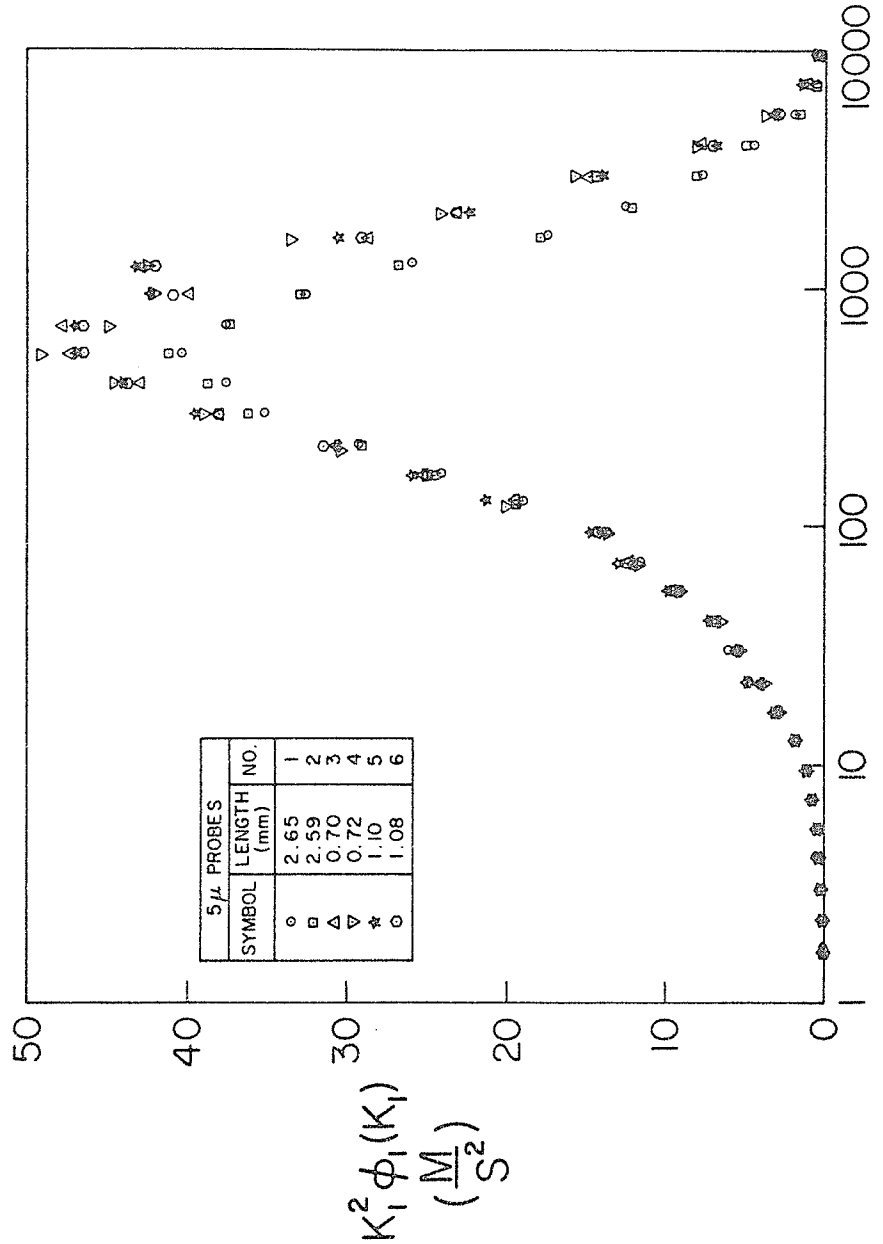

Figure 37: Dimensional Second Moment Spectra for 5 μm Probes, Semilog Plot.

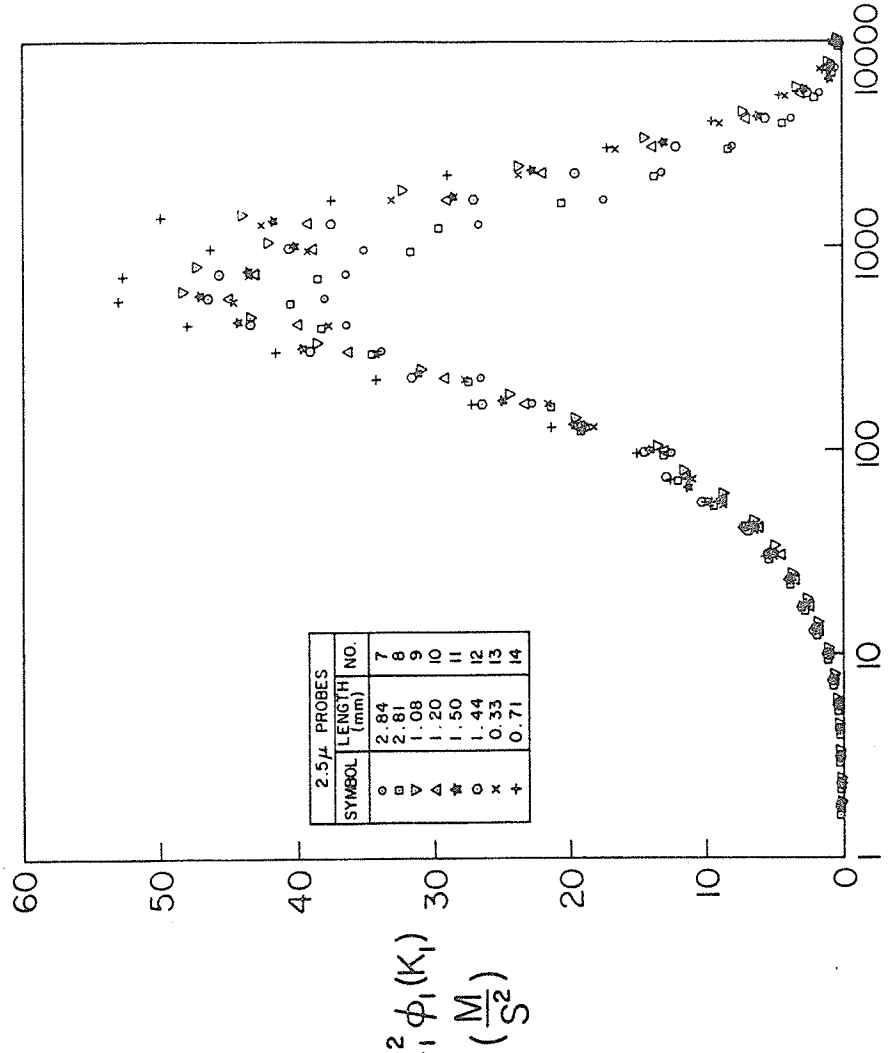

Figure 38: Dimensional Second Moment Spectra for 2.5 μm Probes, Semilog Plot.

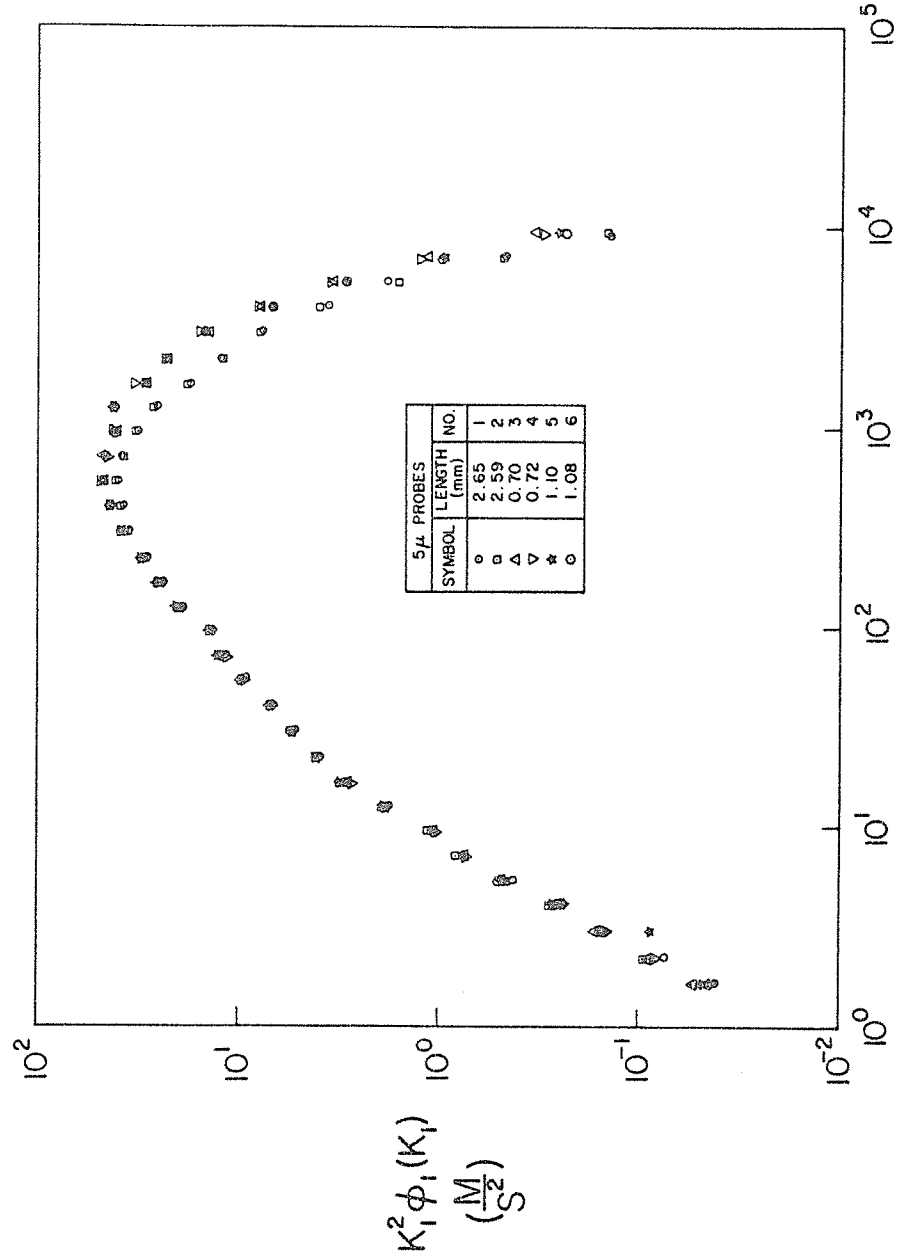

Figure 39: Dimensional Second Moment Spectra for 5 μm Probes, Fully Logarithmic Plot.

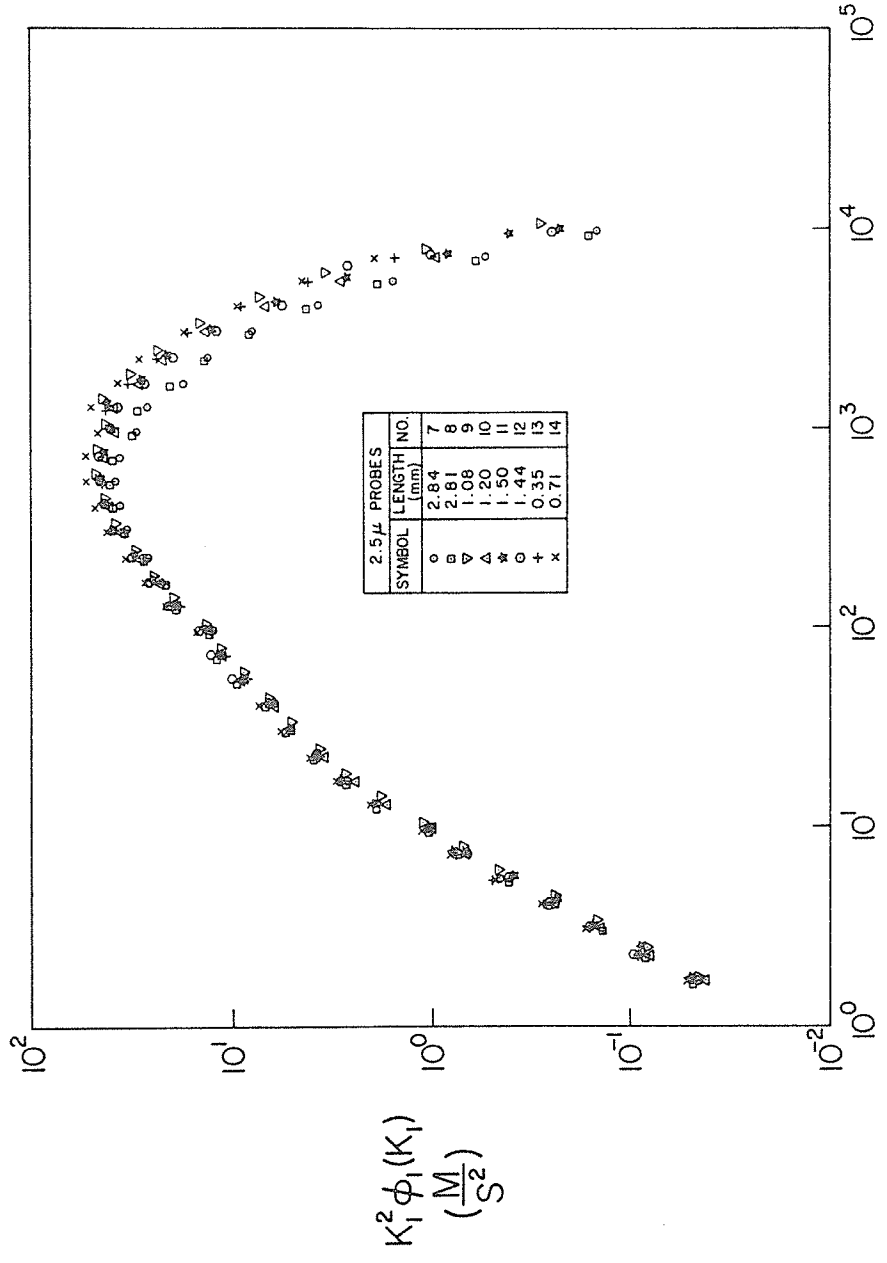

Figure 40: Dimensional Second Moment Spectra for 2.5 μm Probes, Fully Logarithmic Plot.

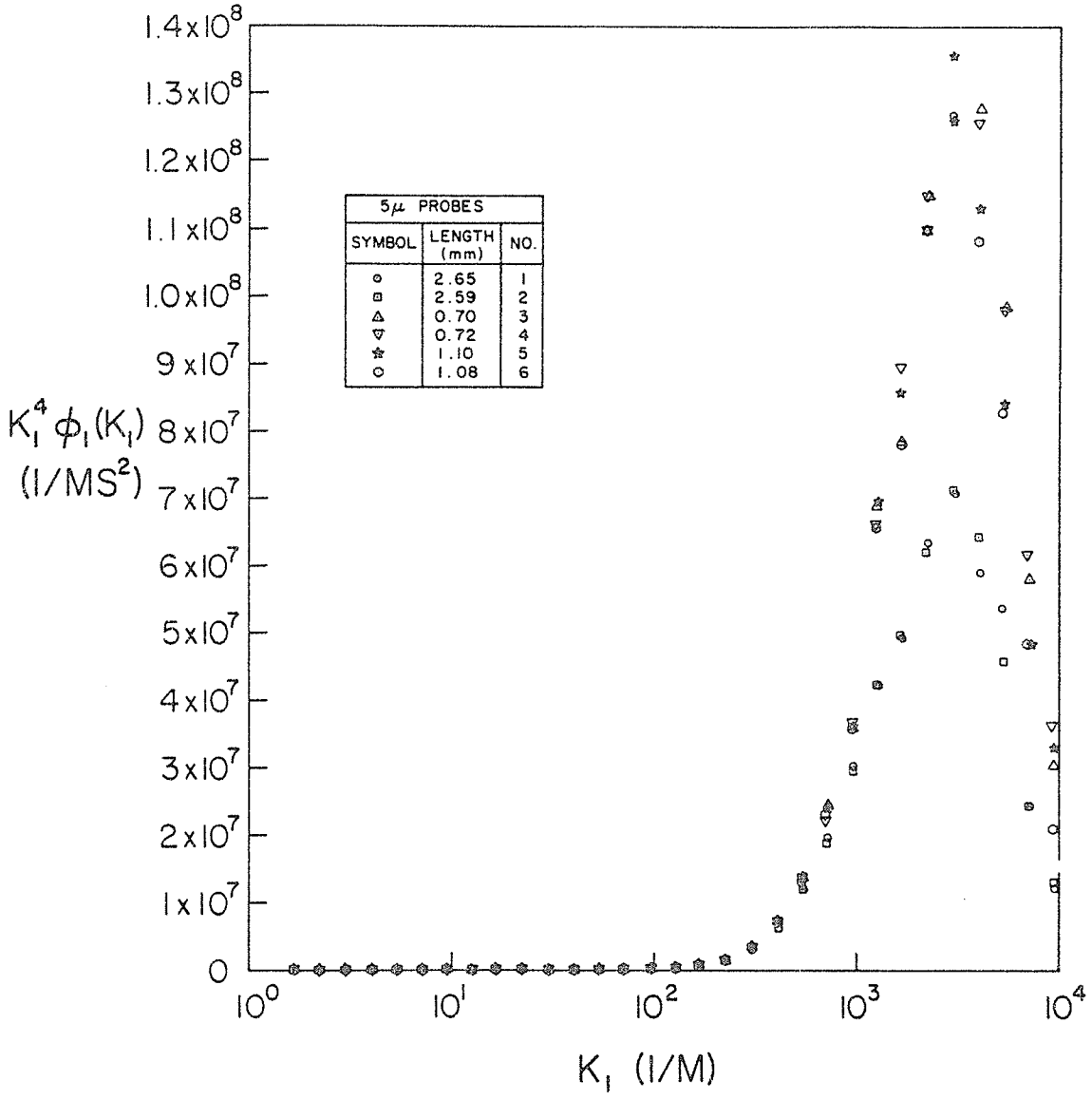

Figure 41: Dimensional Fourth Moment Spectra for 5 μm Probes, Semilog Plot.

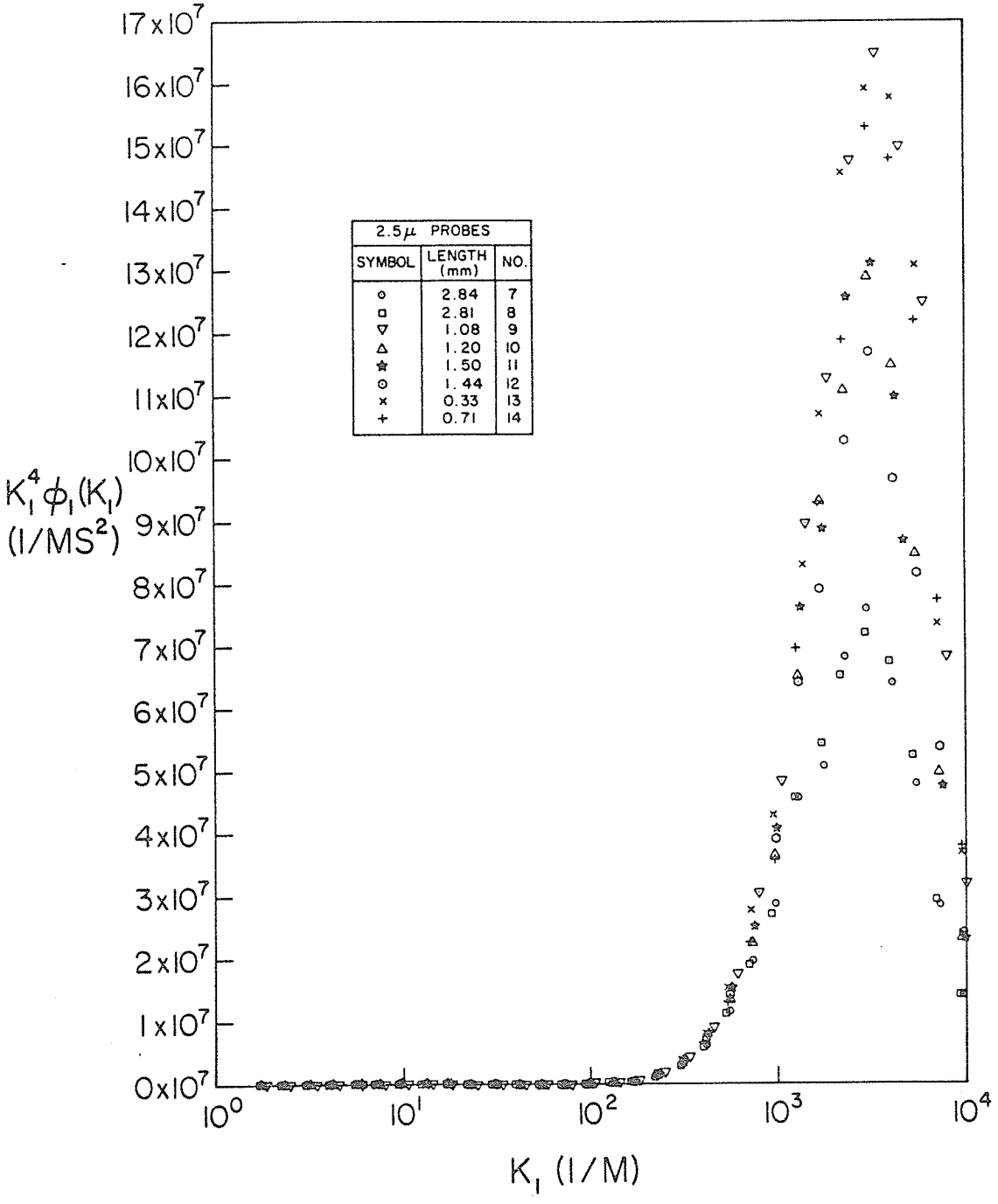

Figure 42: Dimensional Fourth Moment Spectra for 2.5 μm Probes, Semilog Plot.

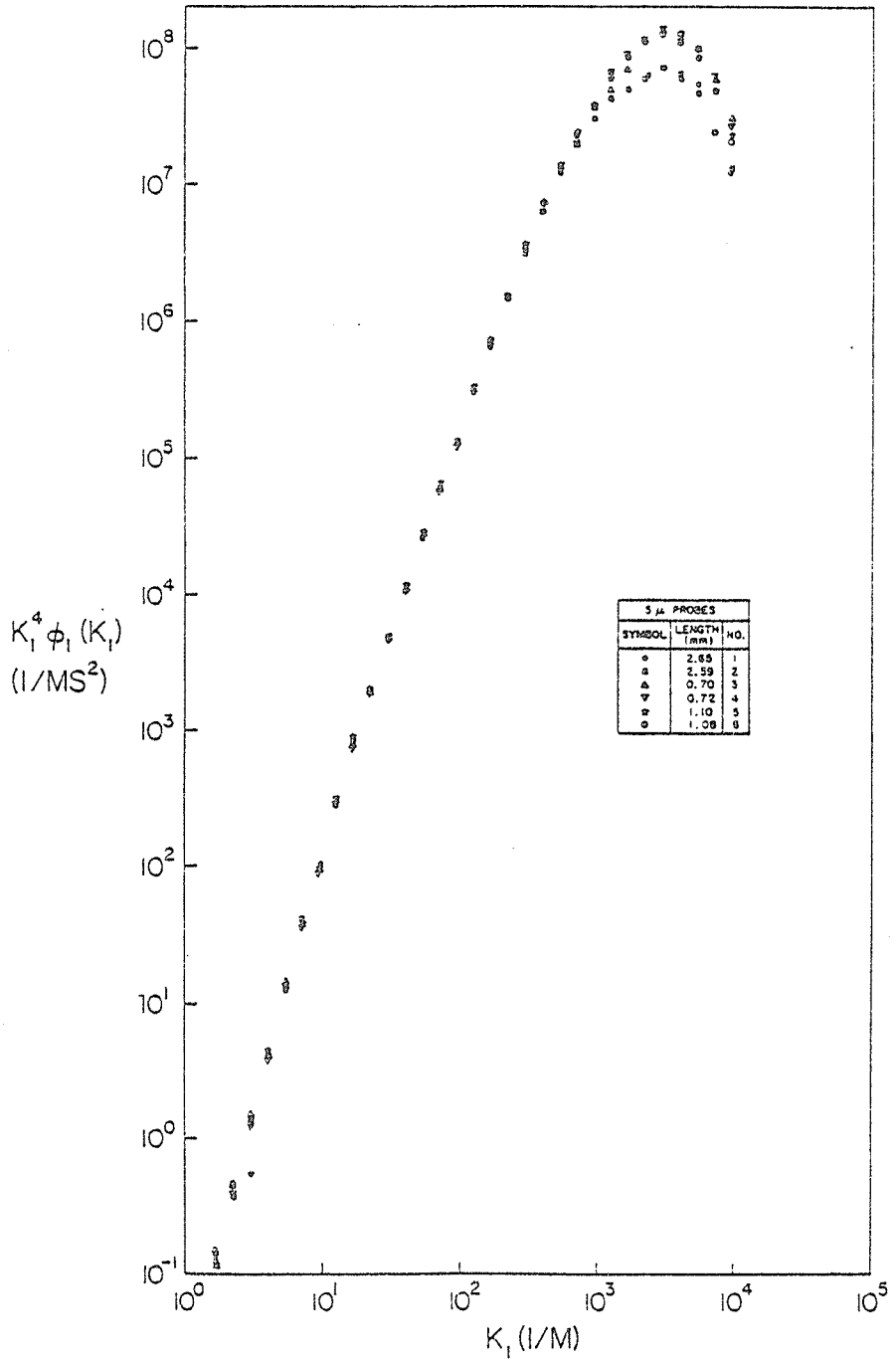

Figure 43: Dimensional Fourth Moment Spectra for 5 μm Probes, Fully Logarithmic Plot.

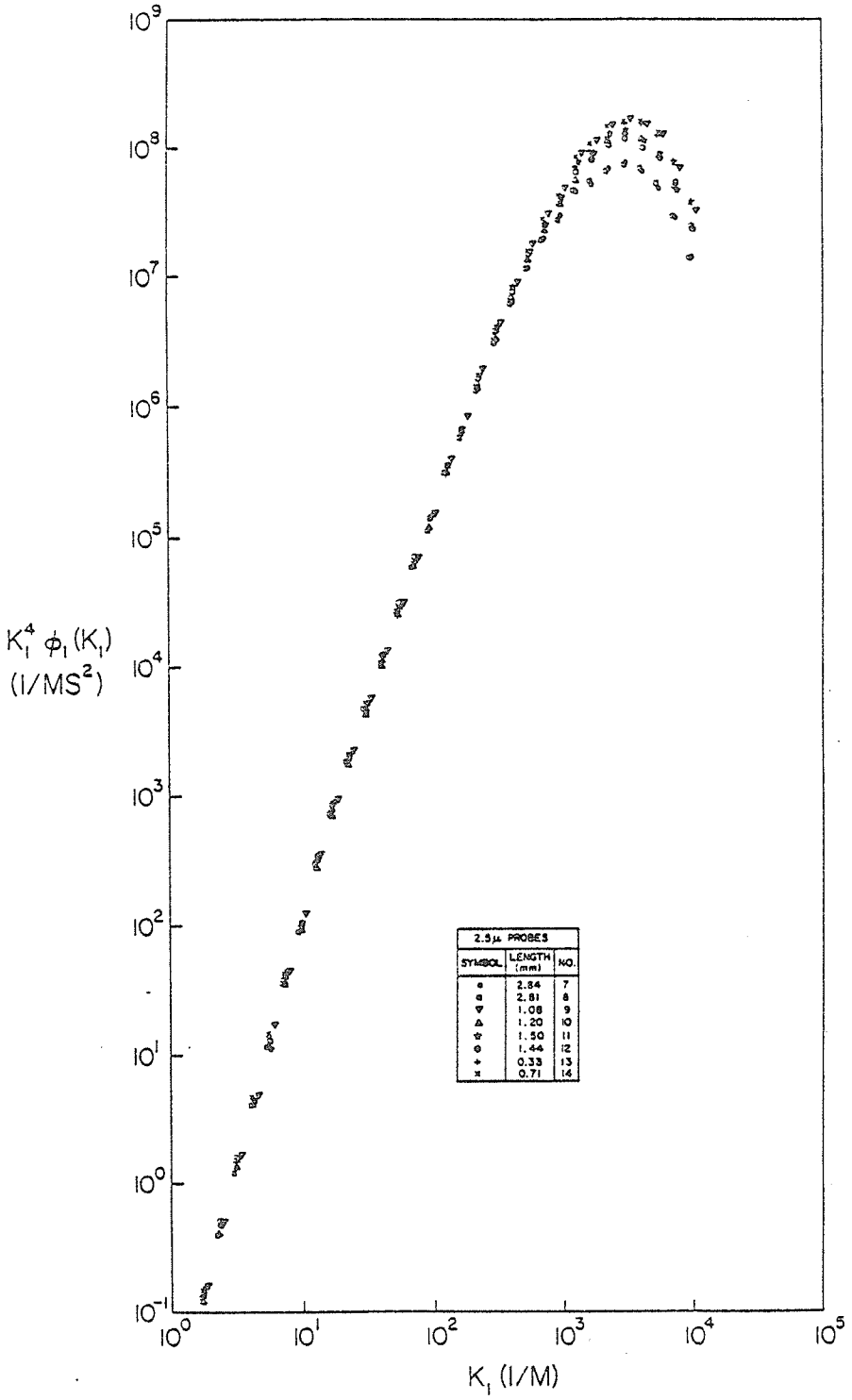

Figure 44: Dimensional Fourth Moment Spectra for 2.5 μm Probes, Fully Logarithmic Plot.

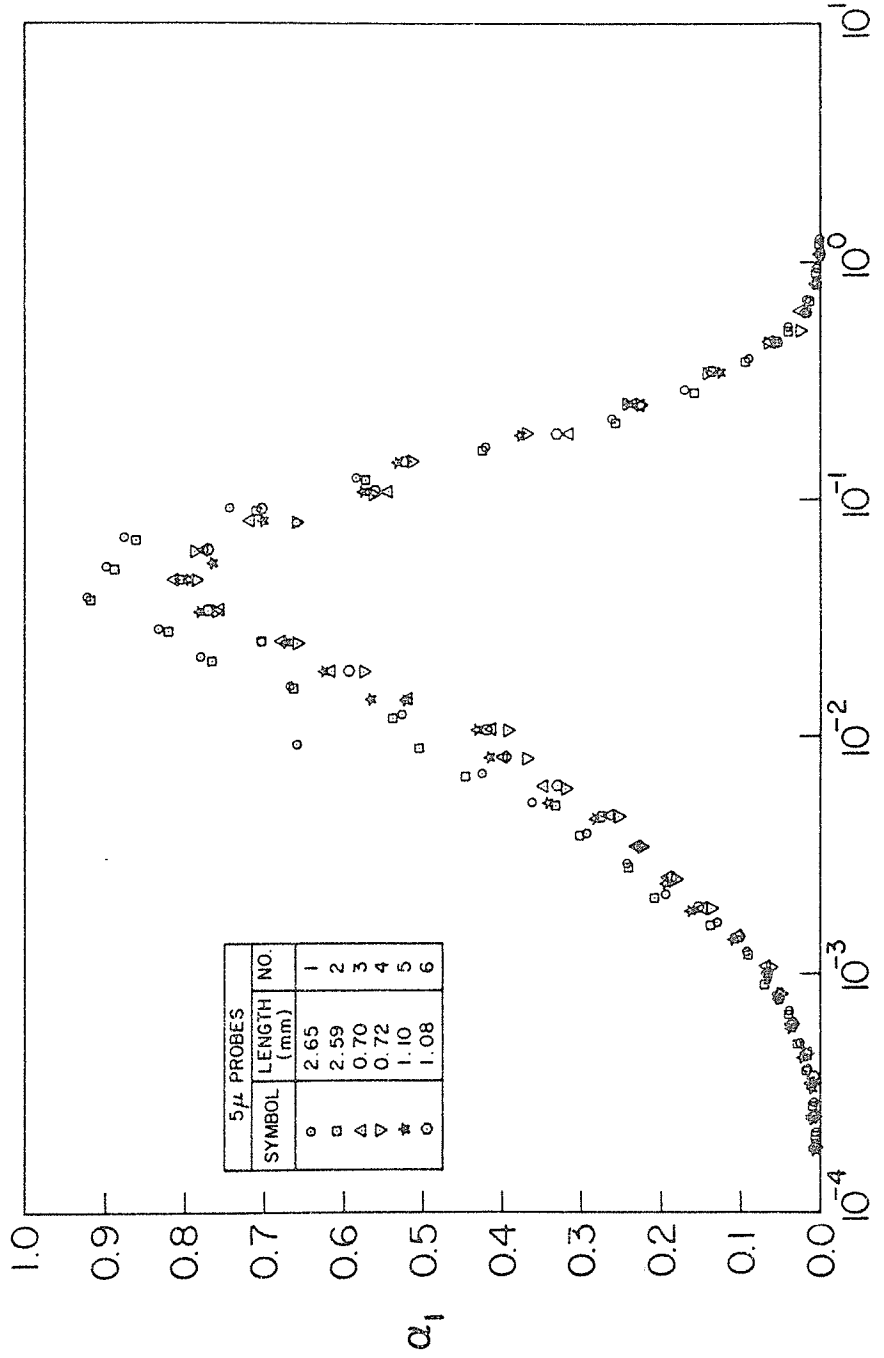

Figure 45: α_1 Versus ηK_1 5 μm Probes.

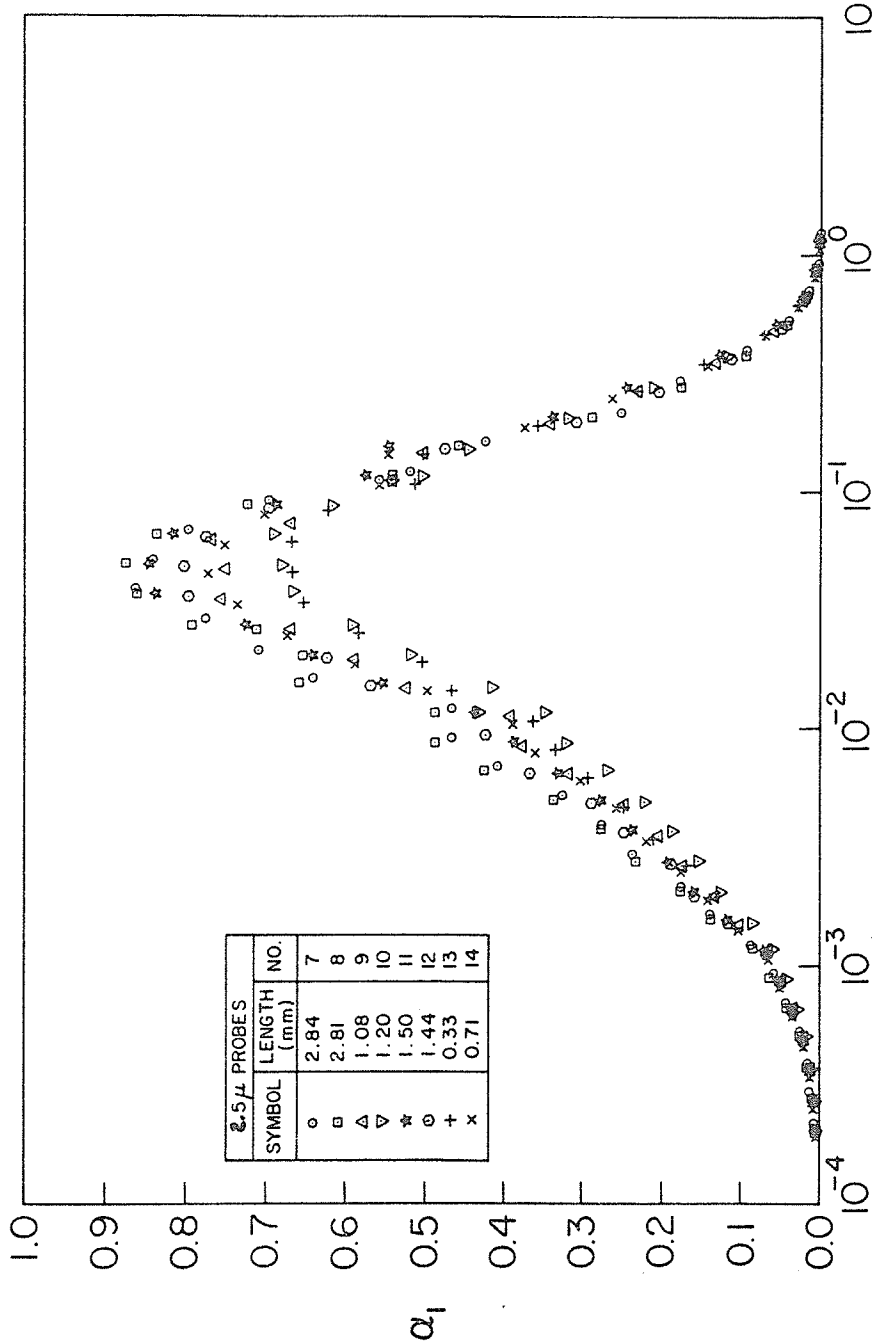

Figure 46: α_1 versus ηK_1 2.5 μm Probes.

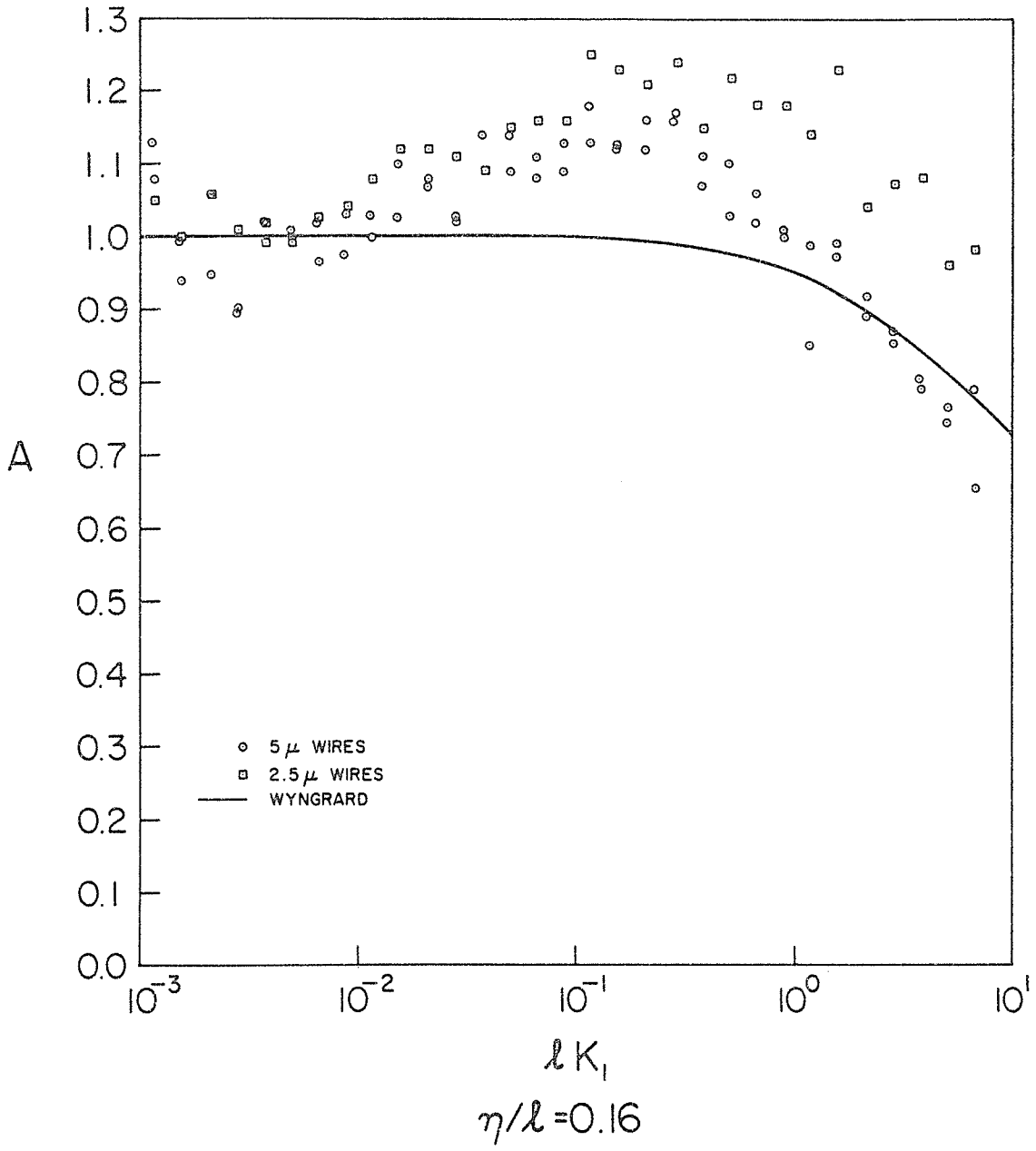

Figure 47: Attenuation A versus $\ell\kappa_1$, η/ℓ = 0.16.

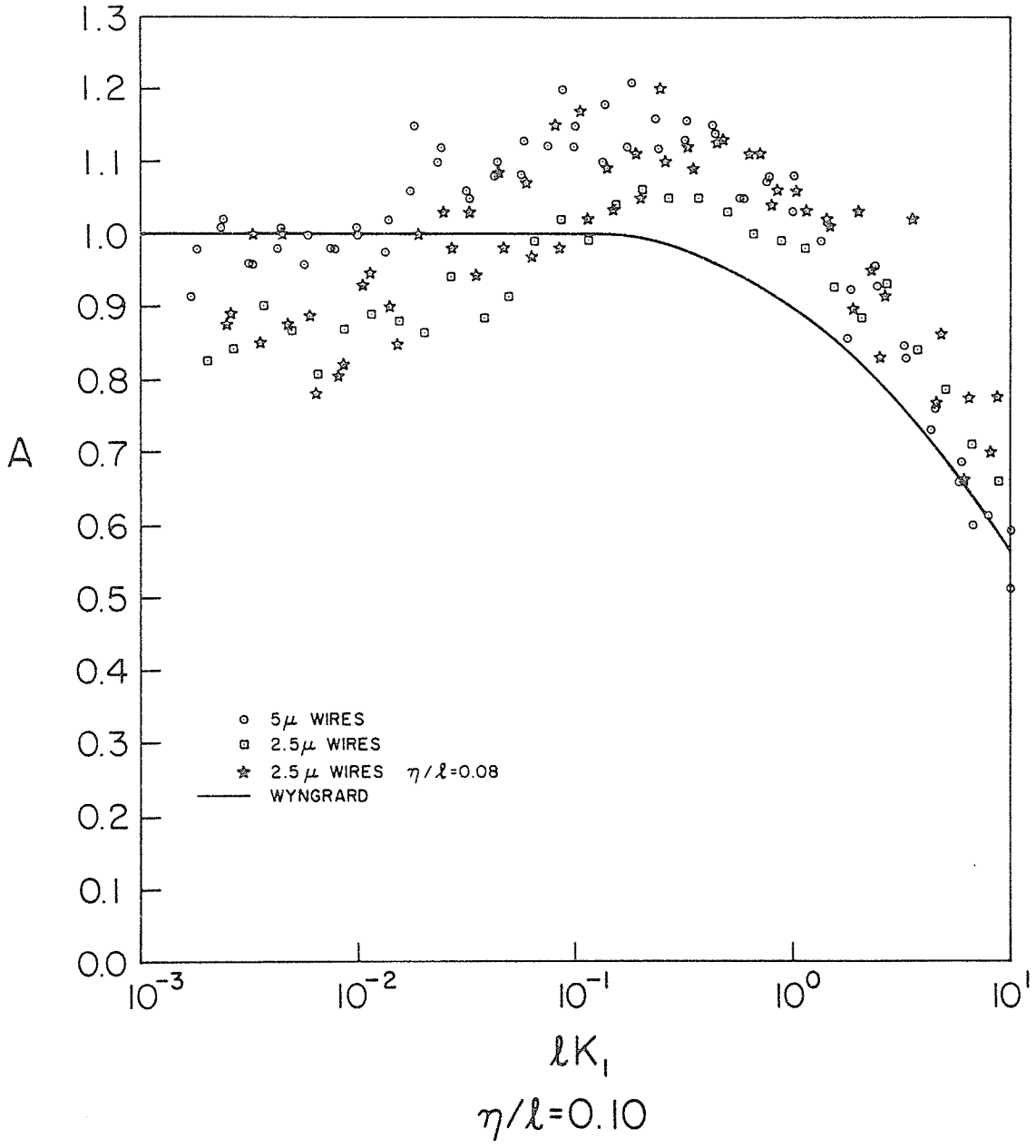

Figure 48: Attenuation A versus $\ell\kappa_1$, η/ℓ = 0.10.

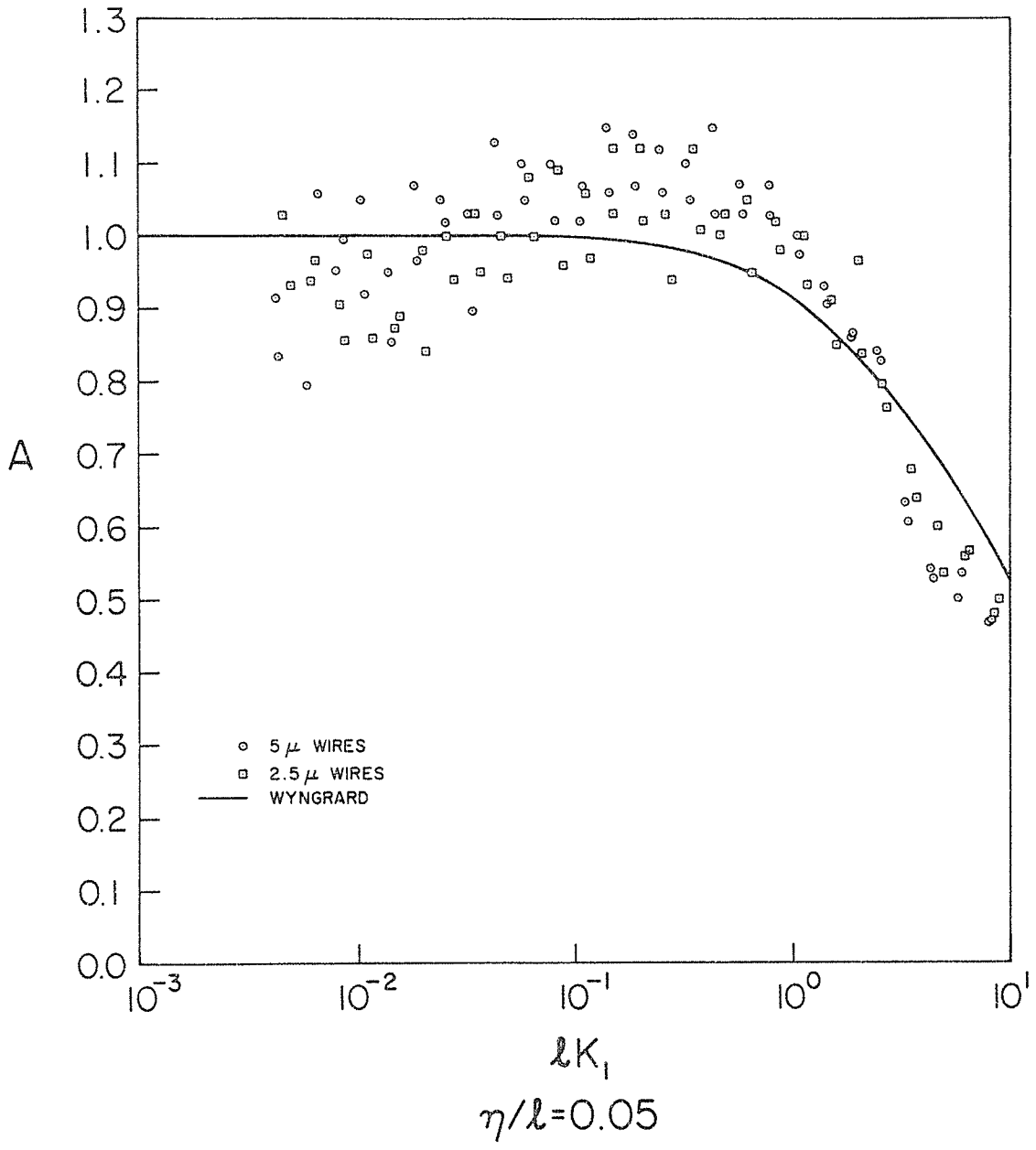

Figure 49: Attenuation A versus $\ell\kappa_1$, η/ℓ = 0.05.

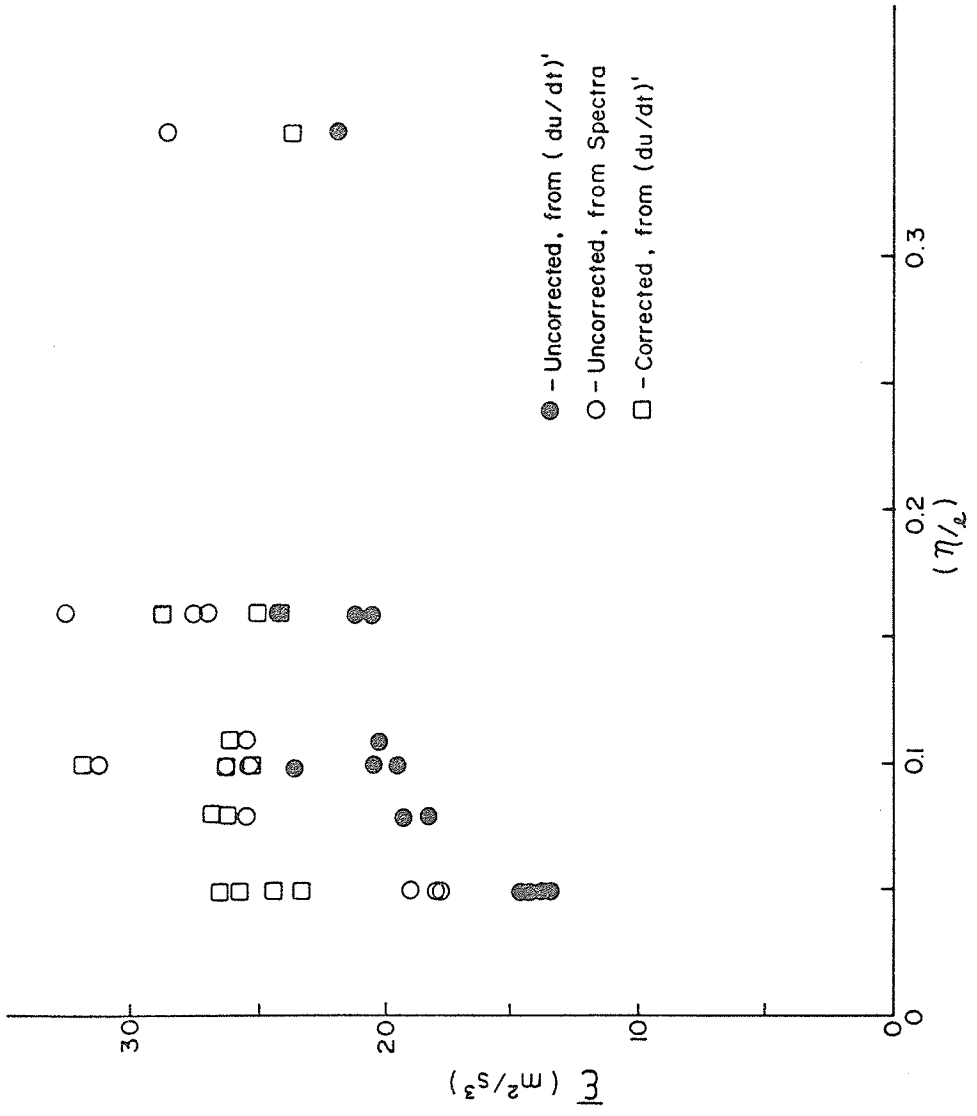

Figure 50: Dissipation versus η/ℓ.

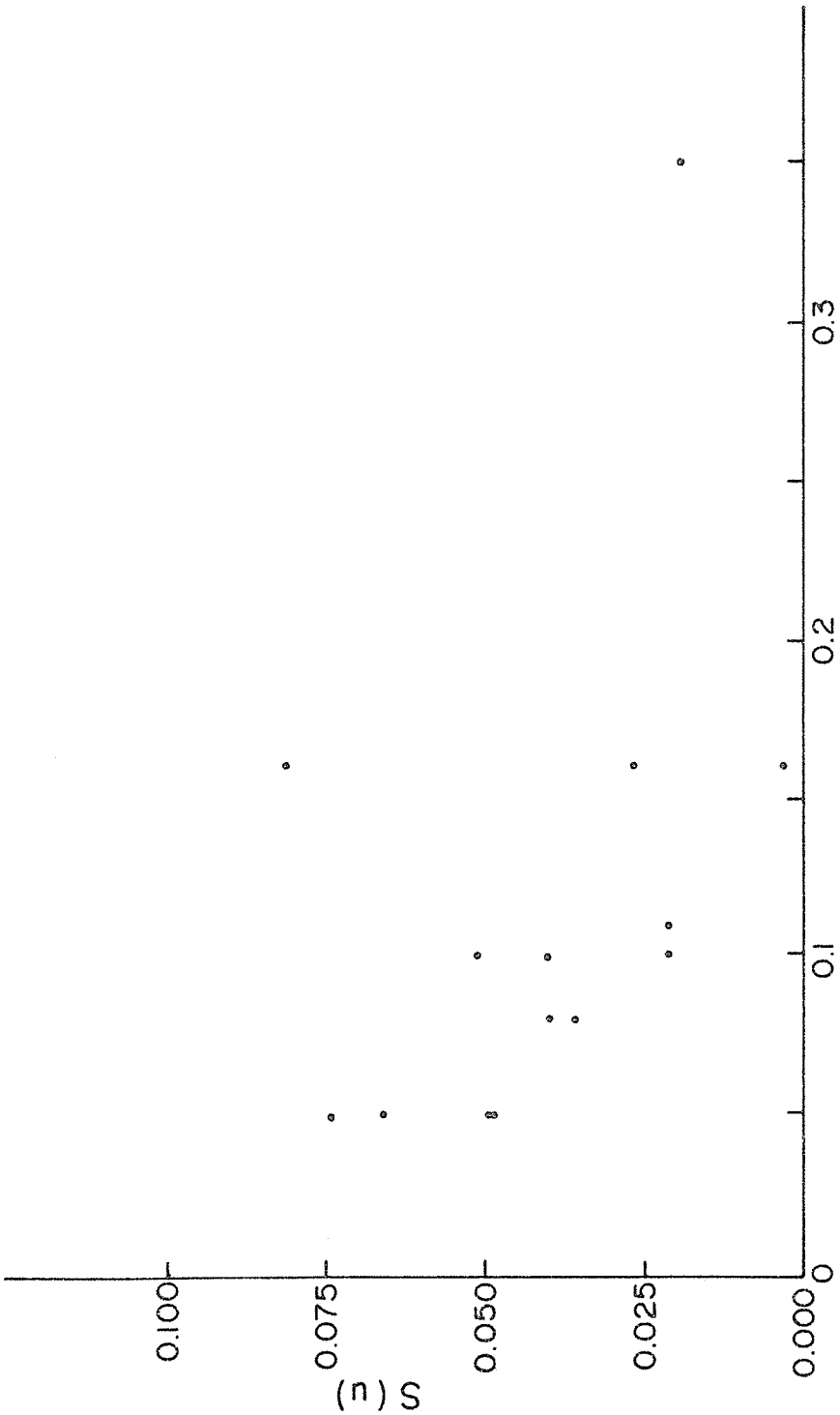

Figure 51: Skewness of u versus η/ℓ.

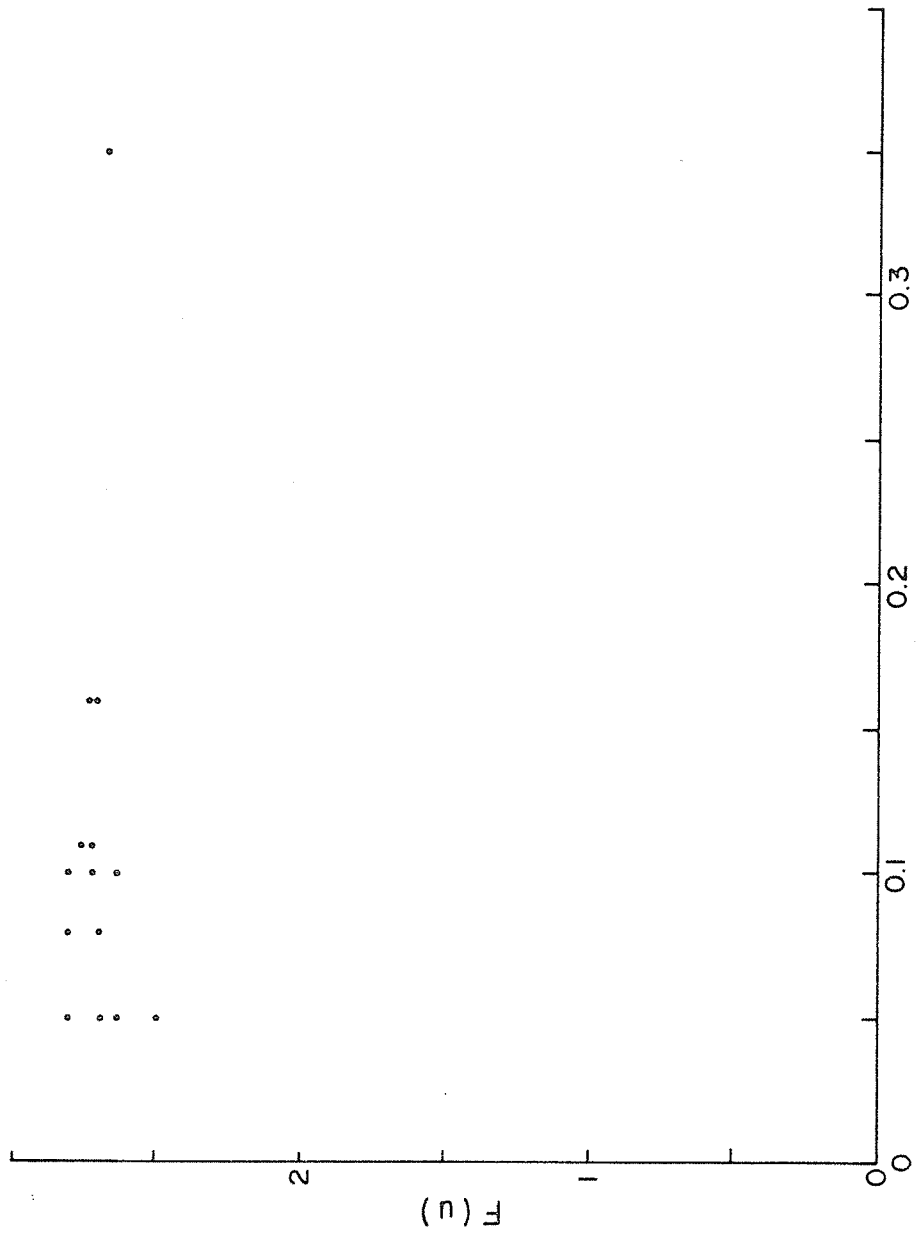

Figure 52: Flatness of u versus η/ℓ.

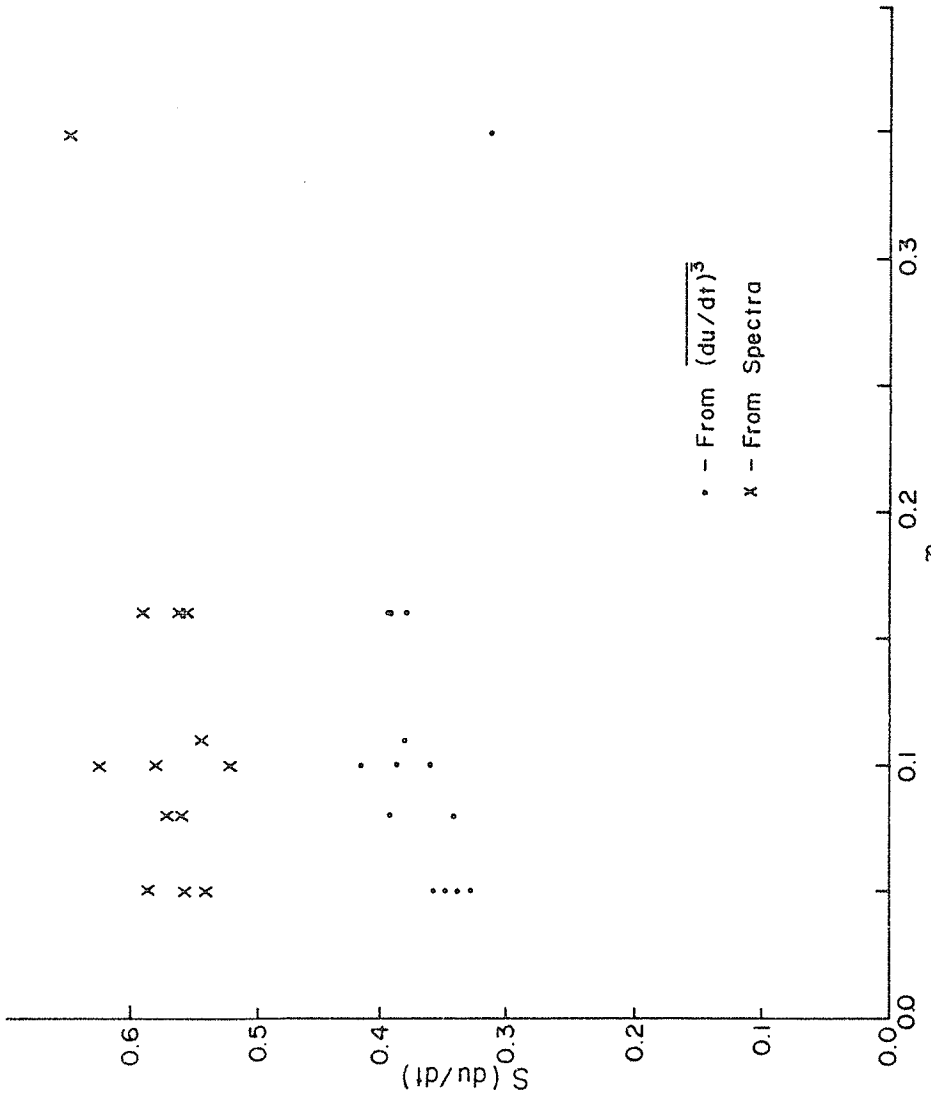

Figure 53: Skewness of $\partial u/\partial t$ versus η/ℓ.

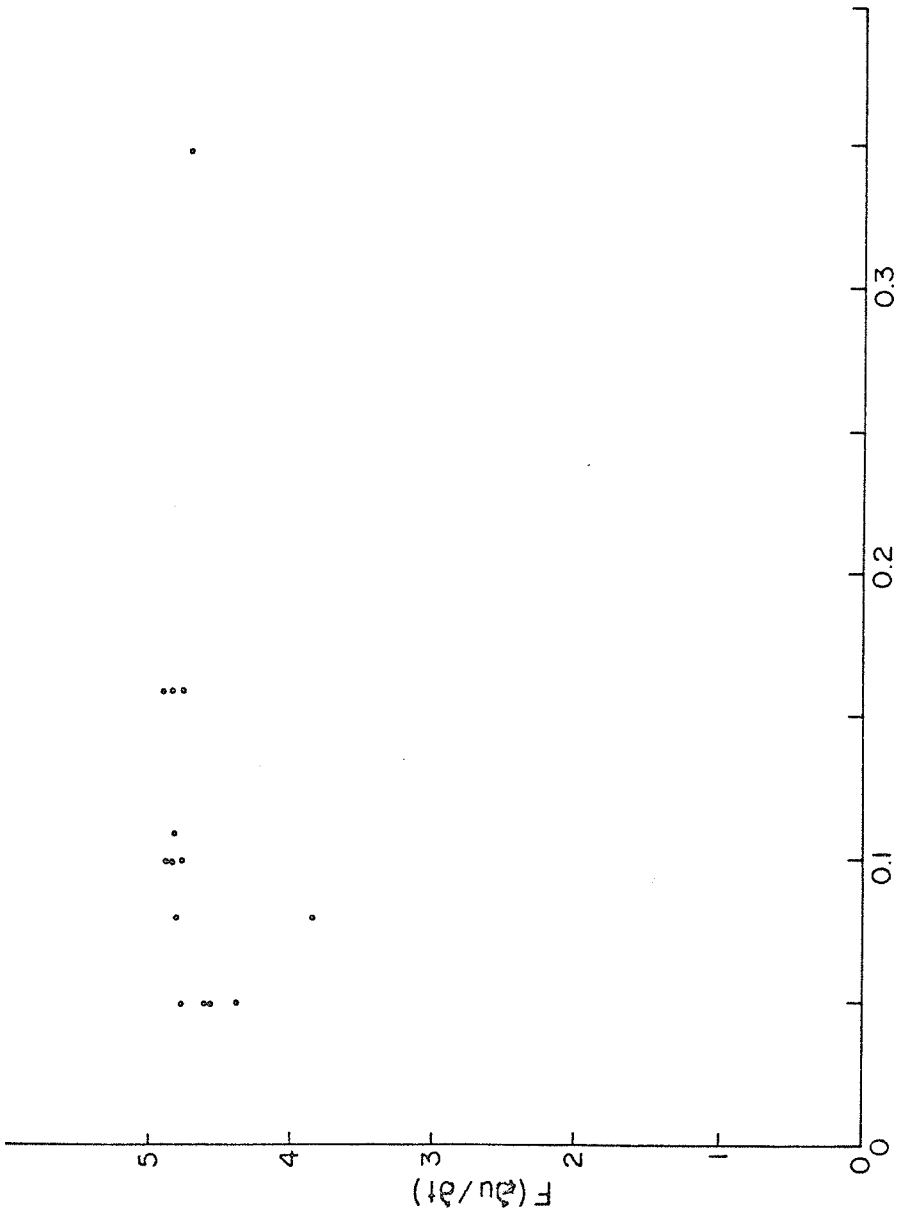

Figure 54: Flatness of $\partial u/\partial t$ versus η/ℓ.

APPENDIX A

DERIVATION OF S(∂u/∂t) RELATION (6)

The Navier Stokes equations and the equation of continuity for the fluctuating velocity field may be written in the following forms:

$$\frac{\partial u_i}{\partial t} + u_k \frac{\partial u_i}{\partial x_k} = - \frac{1}{\rho} \frac{\partial p}{\partial x_i} + \nu \Delta u_i \quad (i=1,2,3) \tag{A1}$$

$$\frac{\partial u_k}{\partial x_k} = 0 \tag{A2}$$

Where u_α are components of velocity, ρ is the density, p the pressure, and ν the kinematic viscosity. Taking the curl of equation A1 one obtains

$$\frac{\partial \omega_i}{\partial t} + u_k \frac{\partial \omega_i}{\partial x_i} - \omega_k \frac{\partial u_i}{\partial x_k} = \nu \Delta \omega_i \tag{A3}$$

where $\omega_k = \text{curl } \{\underline{u}(\underline{x})\} = \nabla x \, \underline{u}(\underline{x}) = \varepsilon_{k\ell m} \frac{\partial u_m(\underline{x})}{\partial x_\ell}$. Multiplying equation A3 by $2\omega_i$ and averaging yields.

$$\frac{d \overline{\omega^2}}{dt} = 2 \overline{\omega_i \, \omega_k \frac{\partial u_i}{\partial x_k}} + 2\nu \overline{\omega_i \, \Delta \omega_i} \quad . \tag{A4}$$

The first term on the right side represents the production of vorticity due to random, diffusive extension of vortex lines while the

second terms on the same side represents the dissipation of turbulent vorticity. The effect of stretching the vortex lines is to tend to make the vorticity distribution "spotty" with small regions of high vorticity; on the other hand, the effect of viscosity is strongest in regions of high vorticity, and tends to diffuse it evenly throughout the fluid. Equation A4 represents the balance between these two effects.

The vorticity equation for steady flows of sufficiently high Reynolds numbers can be approximated by (see Tennekes and Lumley 1972, p. 91).

$$\overline{\omega_i \omega_j \frac{\partial u_i}{\partial x_j}} = \nu \overline{\frac{\partial \omega_i}{\partial x_j} \frac{\partial \omega_i}{\partial x_j}}$$

$$\nu \overline{\frac{\partial \omega_i}{\partial x_j} \frac{\partial \omega_i}{\partial x_j}} = 35 \nu \overline{\left(\frac{\partial^2 u_i}{\partial x_1^2}\right)^2} = 35 \nu \int_0^\infty \kappa_1^4 \phi_1(\kappa_1) \, d\kappa_1$$

$$\overline{\omega_i \omega_j \frac{\partial u_i}{\partial x_j}} = -\frac{35}{2} \overline{\left(\frac{\partial u_1}{\partial x_1}\right)^3}$$

$$\overline{\left(\frac{\partial u_1}{\partial x_1}\right)^3} = -\frac{2}{35} \overline{\omega_i \omega_j \frac{\partial u_i}{\partial x_j}}$$

$$= -2 \nu \int_0^\infty \kappa_1^4 \phi_1(\kappa_1) \, d\kappa_1$$

$$\bar{\varepsilon} = 15 \nu \overline{\left(\frac{\partial u_1}{\partial x_1}\right)^2}$$

$$\overline{\left(\frac{\partial u_1}{\partial x_1}\right)^2} = \frac{\bar{\varepsilon}}{\nu} \frac{1}{15} \quad .$$

The skewness of $(\partial u_1/\partial x_1)$ or $(\partial u/\partial t)$ denoted by S is given by

$$\frac{\overline{(\partial u_1/\partial x_1)^3}}{[\overline{(\partial u_1/\partial x_1)^2}]^{3/2}} = -\frac{2\,(15)^{3/2}\,\nu^{5/2}}{\bar{\varepsilon}^{3/2}} \int^{\infty} \kappa_1^4 \phi_1(\kappa_1)\, d\kappa_1$$

$$= -116 \int^{\infty} (\eta\kappa_1)^4\, \phi_1(\eta\kappa_1) d(\eta\kappa_1) \quad .$$